An Investigation into *Toxoplasma gondii* Infection and the Expression of Arginase-1 and iNOS in Human Lung Tissue

Hannah Soothill

University of Salford MANCHESTER

School of Science, Engineering, and Environment

University of Salford, Greater Manchester, UK

Submitted in fulfilment of the Requirements of the Degree of Master of Science (By Research)

March 2021

Acknowledgements

A huge thank you to Professor Geoff Hide for recruiting me onto this fascinating project- I feel so incredibly privileged to have been involved. Thank you for your continued support throughout and for being the inspirational role model I need.

Thank you Dr Muyassar Tarabulsi for your patience and dedication in teaching me the techniques- you are a brilliant teacher! Although I never met you, thank you Jaro Bajnok for your previous research- you paved the way and without you, this project would likely not have existed.

Thank you, Dr Lucy Smyth, Cath Hide, and Manisha (Mo) Patel for your technical help in preparing the slides, optimising the IHC protocols, and for helping me identify specific lung tissues.

Another thank you to Cath Hide, as well as to my friends and family for all of your emotional support and encouragement- could not have done it without you!

Lastly I would like to thank the University of Salford, I have thoroughly enjoyed my time here as a student.

Abstract

This study aimed to investigate the relationship between *Toxoplasma gondii* infection and the expression of the immune modulating proteins Arginase-1 and iNOS in human lung biopsy samples. Previously, a 100% toxoplasmosis infection rate was found in 72 lung biopsy samples acquired from patients. This compared with 10% in healthy controls. Little is known of immune mechanisms acting on *T. gondii* infected lung tissue. Research on rat and mouse models found an association between resistance to the parasite and the expression of iNOS, whereas Arginase-1 expression was associated with susceptibility. The objectives of this study were to investigate the spatial distribution of iNOS and Arginase-1 expression in relation to *T. gondii* infection. Fifty-one of the samples, used in the Bajnok *et al* (2019) study, were sectioned onto slides and stained separately for the presence of *T. gondii*, Arginase-1, and iNOS using immunohistochemical specific staining. Analysis was performed on section images taken from randomised and specified fields of view. All samples were confirmed positive for toxoplasmosis. iNOS expression was consistently high throughout, whereas Arginase-1 was expressed minimally. No correlation was found in overall spatial distribution of *T. gondii* and Arginase-1 or iNOS expression. However, once the data was categorised into infection intensity grades, moderate positive spatial correlation could be seen between *T. gondii* and iNOS. Colocalisation analysis, using grid coordinates overlayed on the matched images, found a significant positive association in regions with high Arginase-1 and high *T. gondii* staining. Also, a negative association between iNOS and *T. gondii* high intensity staining was approaching significance. No tissue specific preferential staining could be determined for *T. gondii*, Arginase-1 and iNOS. In conclusion, interactions between *Toxoplasma gondii,* Arginase-1, and iNOS in these lung samples appear to be much more complicated than has been found in mice and rat models

Table of Contents

Acknowledgements.....ii

Abstract.....iii

List of Figures.....vi

List of Tables.....viii

Chapter 1 Introduction.....1

1.1 Introduction.....1

1.1.1 Biology and pathophysiology of *Toxoplasma gondii*.....1

1.1.2 Immunity, Arginase-1, and iNOS in the lungs.....6

1.1.3 *Toxoplasma gondii* adaptations for immune evasion.....13

1.2 Aims and Objectives.....22

Chapter 2 Methods & Materials.....25

2.1 Ethics.....25

2.2 Sample collection & sample details.....25

2.3 Slide preparation.....28

2.4 Staining for the presence of *T. gondii.*.....28

2.5 Staining for the presence of Arginase-1 and iNOS.....30

2.6 Protocol for image collection.....32

2.7 Data collection & statistical analysis……32

Chapter 3 Results……35

3.1 Development and optimisation of Immunohistochemical detection and quantitative analysis approaches for the quantification and spatial analysis of *Toxoplasma gondii*, iNOS, and Arginase-1……35

3.1.1 Development and optimisation of Immunohistochemistry protocols……35

3.1.2 Development of approaches for quantitative analysis of *T. gondii* infection using a pilot study……38

3.1.3 Quantification of the intensity of *T. gondii,* iNOS, and Arginase-1 staining with an approach used in Bajnok *et al*. (2019)……44

3.1.4 Development of an improved quantification of *T. gondii,* iNOS, and Arginase-1 specific staining……46

3.1.5 Development and use of scales for categorising spatial distribution and intensity of *T. gondii* infection and iNOS and Arginase-1 expression……50

3.2 Analysis of colocalization and coexpression of *T. gondii* with iNOS and Arginase-1……60

3.2.1 Measurement of spatial overlap of *T. gondii* infection with iNOS and Arginase-1 expression……60

3.2.2 Investigating the relationship between iNOS/Arginase-1 expression ratios and *T. gondii*……71

3.3 Investigation of tissue specific distribution of *T. gondii* infection and expression of iNOS and Arginase-1……80

3.4 Summary of conclusions……84

Chapter 4 Discussion……86

Appendix……113

References……119

List of Figures

Figure 1.1 Overview of the typical life cycle of *Toxoplasma gondii*.....3

Figure 2.1 Photographs taken at 400x magnification of five, 5µm thick, sections of the same lung tissue sample, in the same field of view.....34

Figure 3.1 Comparison of the use of a PT module with the microwave protocol for preparing slides.....37

Figure 3.2 Overlayered 4 x 5 grid on a 400x magnified lung tissue biopsy sample immunohistochemically stained for the presence of *Toxoplasma gondii*.....41

Figure 3.3 A box and whisker plot showing the distribution of *Toxoplasma* infection, iNOS and Arginase-1 expression in human lung samples.....45

Figure 3.4 A correlation between Dataset G and Dataset I of lung tissue specifically stained for the presence of *Toxoplasma gondii*.....47

Figure 3.5 A correlation between Dataset G and Dataset I of lung tissue specifically stained for the presence of Arginase-1.....48

Figure 3.6 A correlation between Dataset G and Dataset I of lung tissue specifically stained for the presence of iNOS.....49

Figure 3.7 A comparison of the number of samples from Dataset J and those of Bajnok *et al* (2019) when categorised into their infection grades as defined by Bajnok *et al* (2019).....52

Figure 3.8 A scattergram of *Toxoplasma gondii* and Arginase-1 percentage coverage of staining for samples in Dataset J that were categorised as having a Grade 1 (low) infection 53

Figure 3.9 A scattergram of *Toxoplasma gondii* and Arginase-1 percentage coverage of staining for samples in Dataset J that were categorised as having a Grade 2 (moderate) infection.....54

Figure 3.10 A scattergram of *Toxoplasma gondii* and Arginase-1 percentage coverage of staining for samples in Dataset J that were categorised as having a Grade 3 (High) infection.55

Figure 3.11 A scatterplot of the stain coverage of lung biopsy tissue specifically stained for the presence of *Toxoplasma gondii* and Arginase-1 with omission of 1 outlier reading (grade 3).....56

Figure 3.12 A scattergram of *Toxoplasma gondii* and iNOS percentage coverage of staining for samples in Dataset J that were categorised as having a Grade 1 (low) infection.....57

Figure 3.13 A scatterplot of *Toxoplasma gondii* and iNOS percentage coverage of staining for samples in Dataset J that were categorised as having a Grade 2 (moderate) infection……58
Figure 3.14 A scatterplot of *Toxoplasma gondii* and iNOS percentage coverage of staining for samples in Dataset J that were categorised as having a Grade 3 (high) infection……59
Figure 3.15 Summary of the range and median of Dataset D……60
Figure 3.16 A scatterplot of the stain coverage of lung biopsy tissue specifically stained for the presence of *Toxoplasma gondii* and Arginase-1 (Dataset J)……62
Figure 3.17 A scatterplot of the stain coverage of lung biopsy tissue specifically stained for the presence of *Toxoplasma gondii* and Arginase-1 (Dataset D)……63
Figure 3.18 A scatterplot of the stain coverage of lung biopsy tissue specifically stained for the presence of *Toxoplasma gondii* and Arginase-1 with omission of 6 outlier readings……64
Figure 3.19 A comparison of *T. gondii* and Arginase-1 intensity of staining in paired images taken at the same field of view (3 groups)……65
Figure 3.20 A comparison of *T. gondii* and Arginase-1 intensity of staining in paired images taken at the same field of view (2 groups)……66
Figure 3.21 A scatterplot of the staining coverage of lung biopsy tissue specifically stained for the presence of *Toxoplasma gondii* and iNOS (Dataset J)……67
Figure 3.22 A scatterplot of the staining coverage of lung biopsy tissue specifically stained for the presence of *Toxoplasma gondii* and iNOS (Dataset D)……68
Figure 3.23 A comparison of *T. gondii* and the intensity of staining of iNOS in paired images taken at the same field of view (3 groups)……69
Figure 3.24 A comparison of *T. gondii* and iNOS intensity of staining in paired images taken at the same field of view (2 groups)……70
Figure 3.25 The intensity of Arginase-1 specific staining in coordinates with high, low, and nil iNOS specific staining……72
Figure 3.26 A comparison of Arginase-1 and iNOS intensity of staining in paired images taken at the same field of view……73
Figure 3.27 A scattergram of the stain coverage of lung biopsy tissue specifically stained for the presence of *Toxoplasma gondii* and the iNOS/Arginase-1 staining ratio (Dataset J)……75
Figure 3.28 A scatterplot of the stain coverage of lung biopsy tissue specifically stained for the presence of *Toxoplasma gondii* and the ratio of iNOS/Arginase-1 specific staining (Dataset J, omission of outlier readings)……77

Figure 3.29 A scattergram of the stain coverage of lung biopsy tissue specifically stained for the presence of *Toxoplasma gondii* and the iNOS/Arginase-1 stain ratio (Dataset D)……78

Figure 3.30 A scatterplot of the stain coverage of lung biopsy tissue specifically stained for the presence of *Toxoplasma gondii* and the ratio of iNOS/Arginase-1 specific staining (Dataset D, omission of outlier readings)……79

Figure 3.31 Microphotograph (100x magnification) of a section of lung tissue immunohistochemically stained for the presence of iNOS with identified cell/tissue types and their positive/negative status……81

Figure 3.32 The tissue or cell type and the quantity that were found to be positive or negative for *Toxoplasma gondii* specific staining within 51 lung biopsy samples……82

Figure 3.33 The amount of smooth muscle and alveolar macrophages positive and negative for the presence of *Toxoplasma gondii*, Arginase-1, and iNOS……83

List of Tables

Table 2.1 Basic information and medical history from the patients of which the lung biopsy tissue samples were obtained……26

Table 3.1 Summary of the different categories of images and how they were analysed……42

Table 3.2 Each lung tissue biopsy sample and its inclusion in the 12 different datasets for the data generated from the sections stained for the presence of *Toxoplasma gondii*, Arginase-1, and iNOS……43

Table 3.3 The iNOS/Arginase-1 ratio of Dataset J and Dataset D……75

Chapter 1 Introduction

1.1 Introduction

The overall aim of this research is to investigate the distribution of the parasite *Toxoplasma gondii* in infected human lung tissue and the relationship of distribution to expression of the important human immune regulatory genes, Inducible Nitric Oxide Synthase (iNOS) and Arginase-1.

1.1.1 Biology and pathophysiology of *Toxoplasma gondii*

Toxoplasma gondii is a highly prevalent protozoan parasite, found in all warm-blooded animals, and arguably one of the most successful parasites in existence (Liu, Singla & Zhou, 2012). It is currently thought to infect 30% of the global population, and about 10% of UK residents (Flatt & Shetty, 2013; Flegr *et al*, 2014; Villena *et al,* 2010). Causative agent of toxoplasmosis that can lead to birth defects and miscarriage for pregnant women as well as being fatal to immunocompromised individuals if left untreated (Holliman, 1988; Rabaud, 1996). Although much is still unknown about its interactions with its human hosts, *T. gondii* has a myriad of different mechanisms to evade detection from the immune system whilst optimising its distribution around the body (Hunter & Sibley, 2012; Wong *et al,* 2020).

It is an obligate intracellular parasite, with a specialised apical complex that enables it to invade many different cell types in a wide range of hosts. It has a complex lifecycle where sexual reproduction only takes place in the gut of its definitive host, the cat. Other felids can act as the definitive host for *T. gondii,* but it is the domesticated cat that is the most significant

(Must *et al,* 2017). *T. gondii* has three main life stages and forms: the active stage termed the tachyzoite, the latent encysted bradyzoite stage, and the infective egg stage, the oocyst. All three of these stages are relevant to human infection, although humans and some other warm-blooded animals are considered dead-end hosts where typically no transmission occurs after being infected with the parasite (Dubey, 2010). See Figure 1.1.

Oocysts develop after sexual reproduction through fusion of gametocytes, of which are tachyzoite derived. Within each of these oocysts are two sporoblasts encasing four sporozoites that once ingested and ruptured, differentiate into tachyzoites (Dubey, 2009). Cats tend to be infected quite early in life, owing to the ubiquity of the parasite, before developing immunity (Tenter, Heckeroth & Weiss, 2000). However, this one instance of illness leads to the expulsion of up to a billion oocysts into the environment over the two-week course of infection (Dubey, 1995; Dubey & Frenkel, 1972; Fritz *et al*, 2012a), where they will become infectious to all mammals once sporulated after 1-5 days in the environment (Elmore *et al,* 2010). Oocysts are very environmentally resistant and can withstand mechanical damage as well as exposure to acids, household bleach, chlorination, ultraviolet radiation, and variations in temperature (Dumètre *et al,* 2013; Fritz *et al,* 2012b; Jones & Dubey, 2010). If another cat gets infected from oocysts, the sexual reproduction cycle will repeat, after first completing an asexual reproduction cycle within the cat. If a different mammalian species ingests an oocyst, successive tachyzoites can infect various cell types for rapid asexual (clonal) reproduction (Dubey, 2009). This cycle is repeated until the tachyzoites are triggered to develop into the slower proliferating bradyzoites which form a cyst structure and remain dormant almost indefinitely, evading attack from immune cells. This was found to start after 6 days in mice *in vivo* experiments (Dubey, 1997a). Should the immune system fail, or spontaneous rupture of the cyst occurs, tachyzoites can re-emerge, and there is resumption

of the rapid asexual proliferation cycle (Dubey, 1997a). Ingestion of these cysts by carnivory is a common transmission route of this parasite by humans and other animals alike (Dubey, 2009).

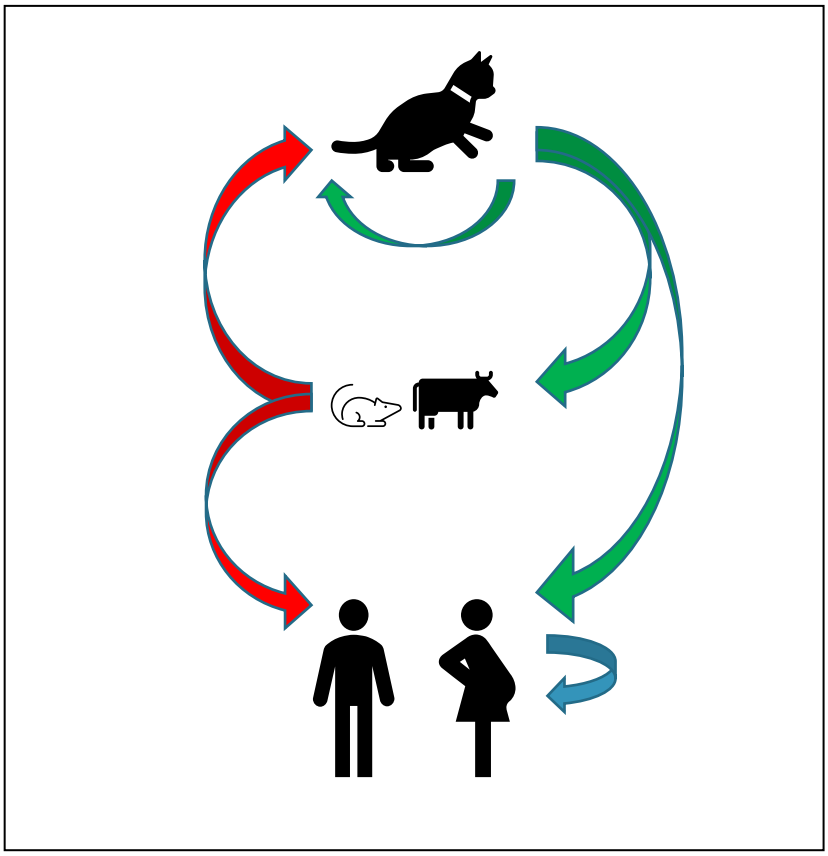

Figure 1.1: Overview of the typical life cycle of Toxoplasma gondii. The definitive host is the cat, and all other warm-blooded animals are intermediate hosts. Humans are considered dead-end or incidental hosts as there is typically no further transmission. However, congenital transmission can occur from mother to foetus if infection is acquired whilst pregnant, as indicated by the blue arrow. The green arrows represent the transmission of infective T. gondii oocysts, after being excreted from a cat. The red arrows represent transmission via ingestion of tissue encysted T. gondii, i.e., by carnivory.

Tachyzoites in an active infection can cross the maternal-foetal blood barrier and infect the developing foetus, termed vertical transmission. Vertical transmission has also been implicated in the loss of preterm lambs, causing financial hardships for farmers (Hide *et al,* 2009). More devastating is the damage *T. gondii* can have on the human foetus, where congenital toxoplasmosis causes severe birth defects such as hydrocephalus, as well as

spontaneous abortion of the pregnancy. *T. gondii* chorioretinitis or ocular toxoplasmosis, a disorder of the eye that can lead to blindness, also arises from vertical transmission of *T. gondii* although more recent research is implicating this condition as a rare complication of a generalised toxoplasmosis infection (Delair *et al,* 2008). The ability to cross barriers such as the blood-brain, and the maternal-foetus barrier likely aids the parasite in avoiding immune attack.

T. gondii is the causative agent of a more generalised infection, toxoplasmosis, in humans. Most often this pathogenicity is limited to an acute mild flu-like illness followed by a chronic asymptomatic period whereby the parasite preferentially encysts in neural and muscle tissue (Flegr, 2007; Weiss & Kim, 2000). Globally, rates of chronic or latent infection differ greatly, with up to 90% of French nationals found to carry the parasite in the 1980's and now thought to be around 44%; contrasting with the roughly 1 in 10 UK residents chronically infected (Flatt & Shetty, 2013; Flegr *et al*, 2014; Villena *et al,* 2010). This variation in infection rate possibly arises due to differences in infectivity of the predominant *T. gondii* strains or host genetics (Maubon *et al,* 2008) as well as differing diets, particularly those that involve consuming cured or undercooked meats. A European multicentre case-study control found 6-17% of primary toxoplasmosis infections were oocyst originated via the ingestion of vegetables, while 30-60% were bradyzoite derived via the consumption of meat (Cook *et al,* 2000). Very rarely, infection is acquired by organ transplantation or blood transfusion (Campbell *et al,* 2006; Guy & Joynson, 1995).

Untreated toxoplasmosis is almost always fatal to immunocompromised people. Most commonly, fatality is brought about by the parasite crossing the blood-brain barrier, creating a severe encephalitic infection termed cerebral toxoplasmosis; the second commonest killer

being by the development of pulmonary toxoplasmosis (Holliman, 1988; Rabaud, 1996). Of great concern for immunocompromised patients is for acute toxoplasmosis to reactivate from a latent infection that may have been contracted when the individual was immunocompetent. The explosion of the AIDS epidemic in the 1980s brought toxoplasmosis into the forefront of opportunistic pathogen research, and today it still remains a concern for AIDS patients, in addition to those on immunosuppressant treatment after transplant or for autoimmune diseases (Baddley *et al,* 2014). The immunosuppressive effect of chemotherapy treatments for cancer is one of the most significant causes of an increase in susceptibility to active *T. gondii* infection (Abdel Malek *et al,* 2018). Concern surrounding *T. gondii* in cancer patients is warranted as those affected by cancer are on the rise and looks only set to increase globally (Cannon *et al,* 2012).

Little is understood of the dynamics of *T. gondii* infection in localised regions of immunosuppression or deficiency, specifically like that of the tumour microenvironment that make individuals more vulnerable to toxoplasmosis (Guerrouahen *et al,* 2020). Moreover, repeated surveillance screening has found a higher rate of *T. gondii* infection in cancer patients than the respective regional average, even in untreated patients (Anvari *et al,* 2019; Cong *et al*, 2015; Jiang, Li, Chen & Chen, 2015). It was also found that out of a range of different cancer types, those with a cancer of the lung had the highest rates of infection with *T. gondii* (Cong *et al,* 2015). This discrepancy could not be explained with age or sociodemographic factors of the lung cancer patients, and so there does appear to be a heightened susceptibility in lung cancer patients to *T. gondii* or perhaps even an association between the development of lung cancer after infection with *T. gondii* (Cong *et al,* 2015).

Surveillance methods are not without controversy, with the efficacy of serology-based tests such as ELISAs being brought into question when applied to immunosuppressed people as opposed to genetic probe-based PCR screens. This is because an immunocompromised individual would produce few anti-*T. gondii* antibodies as compared with an immunocompetent person, perhaps leading to an underrepresentation of the true rate of infection (Machala *et al,* 2015). PCR based tests screen for the presence of a specific sequence of DNA only present in that organism, and so the competence of a person's immune system would have little impact in the outcome of a positive or negative result.

1.1.2 Immunity, Arginase-1, and iNOS in the lungs

With alveolar tissue having such a large surface area to volume ratio in its interaction with the external environment, it makes sense that the lungs are protected effectively as a first line of defence against infection (Martin & Frevert, 2005). Immunity in the lungs is primarily supported cellularly by alveolar macrophages, lymphocytes, and neutrophils. However, lung tissue does not proficiently heal from damage, with the development of scar tissue that lacks elasticity and cannot function in the way healthy lung tissue can. As such, a delicate balance must be achieved between attacking foreign intruders and the self-injury that comes with the fallout (Newton, Cardani & Braciale, 2016).

In healthy lungs, mature alveolar macrophages ingest all manner of particles that enter the alveolus, many of which are inert, to keep the airways clear. Although there is eagerness to phagocytose, these cells will only trigger an immune response to a detected pathogen, and even so make poor antigen-presenting cells (Martin & Frevert, 2005; Martin *et al,* 1992; Martin *et al,* 1997). Alveolar macrophages, like other macrophages, can be in classically activated or alternatively activated. When classically activated, macrophages are referred to

as M1 and when alternatively activated, they are referred to as M2. M1 macrophages are pro-inflammatory, typically activated by Lipopolysaccharides (LPS) or IFNγ, in response to bacterial or viral infection. In this M1 conformation, macrophages will initiate an immune response, release pro-inflammatory cytokines, and will undertake phagocytosis of microbe invaders. This conformation also activates the production of nitric oxide, to aid in the destruction of pathogens. There are three identified M2 subtypes, dependent on the mechanism of activation (*i.e* helminth infection, glucocorticoids, IL-10). These are termed M2a, M2b, and M2c. All have little or no inflammatory affect, and alongside alternatively activated tissue dwelling macrophages, are orientated towards repair and growth (Rőszer, 2015; Walton *et al,* 2019).

This variation in how macrophages can be activated helps regulate the balance between immune defence and self-injury.

Arginase-1 expression is associated with the reduction and/or cessation of an inflammatory response, and as such, expression is stimulated by anti-inflammation mediators IL-10 and transforming growth factor- beta (TGF-β). Two isoforms of Arginase exist in the human body, namely Arginase-1 and Arginase-2. Arginase-1 is the most common type to be expressed and is found widespread throughout the body (Caldwell *et al,* 2018; Grody, Dizikes, & Cederbaum, 1987; Iyer *et al,* 1998; Vockley *et al,* 1996). Although there is differentiation, both isoforms have been found to share 60-100% homology (Vockley *et al,* 1996). Therefore, of the Arginases, Arginase-1 is the focus of this study.

Arginase-1 has two major functions in the somatic cells of the human body; being the final enzyme involved in the catabolism of ammonia in the urea cycle for nitrogen disposal, as well as being responsible for ornithine production in the synthesis of proline and polyamine

(Caldwell *et al,* 2018; Wu & Morris, 1998). Both these functions are vital for cellular housekeeping and maintenance, along with growth and repair.

Ammonia is very toxic to cells and occurs because of surplus nitrogen in the body. Therefore, it must be broken down or neutralised before being allowed to build up. In the latter stages of the urea cycle Arginase-1 cleaves L-arginine to form L-ornithine and the less toxic nitrogen compound, urea. Ornithine aminotransferase (OAT) is involved with the synthesis of proline, vital for collagen formation, an important component of connective tissue (Morris, 2009; Pegg, 2014). Polyamines can be synthesised by either ornithine decarboxylase, followed by spermidine and spermine synthases, or via arginine decarboxylase and agmatine (Caldwell *et al,* 2018; Wu & Morris, 1998). These proteins are essential in cell proliferation and growth, as well as in inflammatory responses, wound healing, tissue healing and neuronal development (Caldwell *et al,* 2018). As such, a repair phase is triggered after 3-5 days into an inflammatory response, involving myeloid lineage cells increasing Arginase-1 expression (Kämpfer, Pfeilschifter, & Frank, 2003). As discussed earlier, this also has a downregulation effect on iNOS activity, and so goes some way to reduce inflammation along with its effect of suppressing $CD4^+$ and $CD8^+$ T-cells (Czystowska-Kuzmicz *et al,* 2019).

In the context of the lungs, Arginase-1 has a vital role in modulating nitric oxide synthase (NOS) for a variety of different functions. One such function, as previously discussed, is through downregulation of iNOS in alveolar macrophages. This action reduces the inflammatory response of the cell (Redente *et al,* 2010). Also, within the lower portion regions of the lung, Arginase-1 mediates the permeability of the capillaries surrounding the alveoli (Lucas *et al,* 2013). It does this through downregulation of endothelial NOS (eNOS), of which increases the permeability of the capillary. This decreases efficiency of gas exchange but

allows cells and macromolecules to pass through (Lucas *et al,* 2009). Data is lacking on what is considered a normal, healthy baseline of Arginase-1 expression in the lungs in humans, but research was conducted on mice models to gain an understanding on the typical distribution of Arginase-1 in the lungs and other tissues. Here Hochstedler *et al* (2013) found distribution of Arginase-1 expression throughout the mouse lung- although expression was noticeably higher in the upper airways as compared with the smaller airways. Notably, Arginase-1 expression was higher in the alveolar macrophages of mice incidentally found to be diseased than those that were healthy.

Although tissue destruction is usually associated with direct parasite damage or self-injury from the inflammatory response, the repair response can go awry with hyperactivity of the arginase-ornithine pathway leading to fibrosis, thickening, and stiffening of the airways and blood vessels (Durante, 2013; Lucas *et al,* 2014; Popovic *et al,* 2007; Yang & Ming, 2014). Arginase-1 has also been associated with the suppression of the immune system in malignant mouse models as well as ovarian cancer patients (Czystowska-Kuzmicz *et al,* 2019). In these studies, extracellular vesicles containing Arginase-1 were isolated from the malignant mice and were associated with localised immunosuppression. When fluid samples of blood plasma and ascites were taken from ovarian cancer patients, they were also found to have Arginase-1 containing extracellular vesicles. Thus, it comes to no surprise that the immune suppressive qualities of Arginase-1 create the perfect environment for parasites to exploit.

iNOS, shortened from inducible nitric oxide synthase and also referred to as NOS2, is a pro-inflammatory enzyme responsible for the synthesis of reactive nitrogen species (RNS) or nitric oxide (NO). NO can also be produced by two other NO synthase isoforms, namely endothelial NO synthase (eNOS) and neuronal NO synthase (nNOS) (Hickey, 2001). eNOS or NOS3 is vital

for the maintenance of the blood vessels and can induce dilation to cope with increasing demand for blood from different organs and tissues of the body (Heiss, Rodriguez-Mateos, & Kelm, 2015). Likewise, nNOS is essential for every-day functioning whereby the induced NO acts as a type of neurotransmitter that can aid long-term memory formation, the relaxation of muscle tissue and regulation of systemic blood pressure (Böhme *et al,* 1993; Hölscher, & Rose, 1992; Zhou & Zhu, 2009). nNOS may even be utilized if there is failure of eNOS (Förstermann & Sessa, 2012). All three NO synthase isoforms originate from different genes and employ L-arginine for utilization of oxygen and cofactors NADPH, FMN, FAD, and BH_4 (Förstermann *et al,* 1994). However, eNOS and nNOS are calcium dependent in their formation of NO, whereas iNOS is inducible and calcium independent (Vannini, Kashfi, K., & Nath, 2015). RNS or NO compounds are highly reactive and are synthesised in macrophages, other phagocytic cells, as well as cells that are not directly part of the immune system but encounter parasitic invaders, such as endothelia and hepatic cells (James, 1995). RNS combine with reactive oxygen species (ROS) and this is utilized for causing rapid death or severe damage to microbes. There are different pathways for an oxidative burst to take place, but one such important method involving RNS is thought to involve the reaction of nitric oxide with superoxide anions to create peroxynitrate ions (Fang, 2004). So rapid is this reaction, that the mechanism is not yet fully understood (Slauch, 2011). However, peroxynitrate is a strong oxidising agent and reacts with lipids as well as the nitrogen groups, and possibly specific amino acid groups as well as transition metals, within proteins; ultimately interfering with functionality and microbial structure (Fang, 2004). Oxidative bursts occur in the phagolysosome of phagocytic immune cells such as macrophages. This works to protect the other organelles and proteins within the cell.

Phagocytosis is a fundamental part of innate immunity and the activation of the adaptive immune system. As such, it can be initiated in several ways. Two major pathways involve the use of opsonins that bind to the pathogen, such as complement or antibodies; or cell surface pattern recognition receptors (PRRs) that recognise specific structures on pathogens that are evolutionary conserved on microbes, termed pathogen-associated molecular patterns (PAMPS). Examples of such receptors on macrophages include toll-like receptors (TLRs), and lectins such as the mannose receptor (Mogensen, 2009). Once a receptor has been stimulated in this way, it triggers the cell membrane to invaginate and create pseudopods that envelope the foreign body and bud off intracellularly to form a phagosome. A lysosome, containing proteases and hydrolases, then fuses with the phagosome (to form a phagolysosome), to create an inhospitable environment where an oxidative burst can take place.

Pro-inflammatory cytokines such as TNF-α, IL-1β, and IFNγ also stimulate the synthesis of iNOS, whereas resting or inactive immune cells lack iNOS (Darnell*,* Kerr, & Stark, 1994). Signal cascades occurring from activation of a receptor, such as that of the LPS pathway, lead to switching on of the NOS2 gene and the transcription of the iNOS proteins. Thus, there are multiple pathways in which iNOS may be expressed. Similarly, there several pathways in which synthesis of iNOS can be inhibited. Expression can be inhibited post-translationally through the binding of NOS-associated protein 110KDA (NAP110) with the iNOS homodimers to form NOS2-NAP110 heterodimers, meaning that iNOS can no longer be produced (Ratovitski *et al*, 1999). TGF-β inhibits iNOS expression through transcriptional, post-transcriptional, and post-translational mechanisms. Transcriptionally, TGF-β inhibits the synthesis of iNOS by blocking the expression of scaffolding protein HMG-I(γ) (Vodovotz *et al,* 1993).

In addition to direct pathogen destruction, iNOS is also thought to play a role in immune system regulation by means of the downregulation of Th17 cells in addition to regulation of the macrophage immune response and the Th1 response (Calabrese *et al,* 2007; Giordano *et al,* 2011). Th17 cells have been implicated as causative of inflammatory disorders such as inflammatory bowel disorder (IBD) (Obermajer *et al,* 2013; Yang *et al,* 2013). Conversely, elevated iNOS levels have been found in and have long been associated in patients with a wide range of autoimmune and chronic inflammatory disorders such as asthma, multiple sclerosis, type 1 diabetes, and rheumatoid arthritis (Bagasra *et al,* 1995; Eizirik *et al,* 1996; Grabowski *et al,* 1997; Hamid *et al,* 1993; Kröncke *et al*, 1991; McInnes *et al,* 1996).

In a similar contradiction, iNOS has a confusing relationship with cancer with it thought to have both anti-tumour immunity actions in addition to NO being the driving force of immunosuppression within the cancer microenvironment (Ekmekcioglu, Grimm, & Roszik, 2017; Jayaraman *et al,* 2014). iNOS and NO activity have been indicated as carcinogenic by means of direct DNA damage, inhibition of tumour suppresser genes and DNA repair enzymes, as well as the activation of oncogenes, and metastasis and apoptosis modulation (Lala & Orucevic, 1998; Wink *et al,* 2008; Wink *et al,* 1998a; Wink *et al,* 1998b). Oesophageal adenocarcinoma has specifically been linked with the actions of iNOS being a causal factor (McAdam *et al,* 2012). Additionally, high levels of iNOS have also been found in lung, breast, prostate, and colon cancers (Aaltoma, Lipponen, & Kosma, 2001; Kojima *et al,* 1999; Marrogi *et al,* 2000; Vakkala *et al,* 2000). Animal studies suggest that whether iNOS behaves in a pro-tumour or anti-tumour capacity, may differ depending on the type of cancer (Lala & Chakraborty, 2001; Xie *et al,* 1995; Zhang, Urbanski, & McCafferty, 2007). Research on cancer cell line cultures have shown the opposite, with high iNOS expression being associated with inhibition of cell division and consequently cessation of tumour growth (Lelchuk *et al,* 1992;

Thomsen *et al,* 1994; Thomsen *et al,* 1995). Therefore, it is likely that iNOS and NO being pro-tumour or anti-tumour is largely dependent on the level of expression, the cell type and microenvironment, genetic factors, and the timing as well as the duration of NO delivery (Vannini, Kashfi, & Nath, 2015).

In regard to healthy human lung tissue, no information could be found quantifying a baseline expression of iNOS. However, a study on inbred rat lines sought to investigate iNOS expression in lungs in health and with a simulated infection (Ermert *et al,* 2002). In the control rats, they had found high iNOS expression in the epithelial tissue of the first two generations of the bronchi. Moderate iNOS expression was found in smooth muscle cells surrounding the bronchi as well as those surrounding the blood vessels. Likewise, alveolar macrophages, alveolar septum cells, as well as bronchus associated lymphoid tissue (BALT), were also confirmed positive for iNOS expression. However, mast cells and leukocytes within the connective tissue, in addition to endothelial cells were found not to be actively expressing iNOS in the control rat lungs. Once administered endotoxin Lipopolysaccharide (LPS), expression of iNOS was increased in all lung tissues that were confirmed to express iNOS in the control screening. Up-regulation of iNOS was detected in the leukocytes, and endothelia were found to be expressing the protein. This increase in iNOS expression in response to inhaled endotoxins was also found in a study undertaken on 8 healthy volunteers. This study had found an overall 30% increase in iNOS expression after the exposure to the endotoxins (Huang *et al,* 2015).

1.1.3 *Toxoplasma gondii* adaptations for immune evasion

T. gondii and some other pathogens have evolved mechanisms in which they can avoid destruction by the oxidative burst within a macrophage. Recent research is also highlighting

the ability of *T. gondii* to prevent the expression of iNOS within the host cell (Cabral *et al,* 2018). In mice, a reduction or absence of iNOS has been associated with an increased proliferation of the parasite (Alexander *et al,* 1997; Scharton-Kersten *et al,* 1997) and so this is likely to be an evolutionary driving factor to develop tools to suppress host iNOS expression.

Innate immune recognition of *T. gondii* is not fully understood in humans but is thought to differ from that of mice. *In vitro* Human macrophages appear to not respond to dead *T. gondii* cells or to invasion by tachyzoites, but an inflammatory response is triggered if these live tachyzoites are instead phagocytosed by the macrophage. This suggests that it may be intracellular free-floating *T. gondii* RNA that may trigger intracellular receptors in the cytoplasm of a myeloid cell (Sher, Tosh, & Jankovic, 2017). *T. gondii*-host cell immunity in mice has been studied more extensively. It was found in these mice models that pro-inflammatory cytokine IFNγ plays a crucial role in the recognition and immune response against *T. gondii*. IFNγ is largely produced by $CD4^+$ T-cells and natural killer cells, and activates mobile cells such as macrophages, dendritic cells, and even fibroblasts (Suzuki *et al,* 1988).

IFNγ activates the STAT1 transcription factor, of which has the effect of stimulating the expression of hundreds of genes (Platanias, 2005). Consequently, this induces expression of GTPase genes and iNOS, inhibiting parasite growth and aiding in the clearance of *T. gondii* (Zhou *et al,* 2009). Uncertainty exists as to whether this mechanism is fully utilised in the human immune response to *T. gondii* (Bekpen *et al*, 2005; Murray & Teitelbaum, 1992; Ohshima *et al,* 2014). There is evidence to suggest IFNγ has some anti-*T. gondii* role in humans, possibly through the degradation of intracellular tryptophan by indoleamine 2,3-dioxygenase (IDO). Tryptophan is an amino acid that is essential for tachyzoite growth in human host cells. Thus, the impact from the actions of IDO is inhibition of tachyzoite growth

and proliferation, ultimately starving the intracellular tachyzoites (Bando *et al,* 2008; Pfefferkorn, Eckel, & Rebhun, 1986a; Pfefferkorn, Eckel, & Rebhun, 1986b).

The apical complex, a collection of specialist organelles within the *T. gondii* tachyzoite allow it to not only invade a host cell but also manipulate its behaviour to benefit the parasite's proliferation and spread (Hunter & Sibley, 2012; Wong *et al,* 2020). The apical complex consists of polar rings, a conoid, and secretory organelles micronemes and rhoptries (Bradley *et al,* 2005; Carruthers & Tomley, 2008). Many virulence factor proteins have been identified that are secreted from the rhoptries that aid in these functions, some of which act as immunomodulaters (Bando *et al,* 2018a). Within the mouse host, proteins: GRA7, ROP5, ROP16, ROP17, ROP18, and TgIST have been implicated as effectors for the evasion of the immune system, the more of which that are secreted from the rhoptries or dense granules, the more virulent the strain of *T. gondii* is (Alaganan *et al,* 2014; Behnke *et al,* 2011; Etheridge *et al,* 2014; Fentress *et al,* 2010; Gay *et al,* 2016; Jensen *et al,* 2013; Olias *et al,* 2016; Reese *et al,* 2011; Rosowski *et al,* 2014; Rosowski & Saeij, 2012; Steinfeldt *et al,* 2010). *Toxoplasma gondii* also has some resistance to complement (Fuhrman & Joiner, 1989).

It is perhaps this capacity for host manipulation, in addition to the myriad of mechanisms *Toxoplasma gondii* utilizes to evade the immune system that makes it such a successful parasite. Tachyzoites are not as resilient as other *T. gondii* life stages and can only replicate within a host cell and so seek to become intracellular, of which they can enter nearly every type of cell (Weiss & Kim, 2014). *T. gondii* may also manipulate cells in which it does not go on to invade (Koshy *et al,* 2012). Although they preferentially target macrophages and other cells of dendritic lineage for invasion, in so evading the immune system and using them as trojan horses to infect other areas of the body (Bierly *et al*, 2008; Chtanova *et al*, 2008;

Courret *et al*, 2006). A tachyzoite's ability to manipulate the infected leukocyte to adhere to capillary endothelia tissue is thought to assist the exiting process without evoking attack from the immune cell and aid the infection of the peripheral organs (Baba *et al,* 2017). This may also explain why the parasite prefers to encyst in vascular heavy tissue such as the brain, heart, and the lungs.

Dense granule protein GRA6 can activate NFAT4, a host transcription factor to switch on genes for the expression of chemokines, in so, recruiting nearby neutrophils to the area which the parasite can utilise to invade and be transported throughout the body (Ma *et al,* 2014). Similarly, a different dense granule protein, GRA15, once secreted into the cell triggers a host immune response via activation of inflammasome NLRP3 that then goes on to mediate IL-1 (Gov *et al,* 2013). However, this action seems to have a negative impact on the parasite, as studies on mice have shown that strains without GRA15 secretion are more virulent and have more intracellular proliferation (Rosowski *et al,* 2011). A theory has been put forward that this may in fact act as a control measure on tachyzoite reproduction, and so to limit the population to a size that is not detrimental to the host or the parasite itself (Jensen *et al,* 2013; Rosowski *et al,* 2011). It is important to also recognise that these mice studies are performed in specialist research mice and not wild-type mice that would represent the normal or average behaviour within a given natural mouse population.

Release of dense granules and other proteins from the micronemes into the apical tip appears to be calcium dependent, a process that is triggered once *T. gondii* has made contact with a potential host cell (Carruthers, Moreno, & Sibley, 1999). *T. gondii* is also likely able to manipulate host cell functioning through the secretion of microRNAs that can interfere with normal gene expression (Cakir & Allmer, 2010; Wang *et al,* 2012).

This ability of *T. gondii* to modulate the host cell genome using microRNAs likely implicates the parasite in the development of brain cancer, possibly interfering with the host microRNAome as the causing factor (Thirugnanam, Rout & Gnanasekar, 2013; Thomas *et al,* 2012). Conversely, a study by Mohamadi *et al* (2019) in mice found anti-*T. gondii* antibodies will attach to cancer cells and not to healthy, non-malignant cells, and so is being looked at as a form of immunotherapy treatment. This reinforces the how complex the dynamics are between host and *T. gondii* and may offer explanation to the higher incidence of *T. gondii* infection in cancer patients. Little is known also on the impact an active *T. gondii* infection in the lungs has on the longer-term prognosis of a lung cancer patient, although some studies have found a correlation between toxoplasmosis and an increased fatality rate in patients with a collection of different cancers (Carey *et al,* 1973; Israelski & Remington, 1993; Scerra *et al,* 2013; Vietzke *et al,* 1968; Zhou *et al,* 2011).

Lung cancer, although on the decline, is still a significant cause of death globally. Worldwide, it is the leading cause of cancer deaths in both women and men after breast cancer and prostate cancer, respectively (Alberg, Brock, & Samet, 2005; Jemal *et al,* 2004; Jemal *et al,* 2003; Siegel, Miller, & Jemal, 2018). Lung cancer can be broadly categorised into two main types: small cell lung carcinomas or non-small cell lung carcinomas. The latter are the most diagnosed and comprise squamous cell carcinomas, adenocarcinomas, and large cell carcinomas. Whereas small cell carcinomas tend to be less common, but more aggressive and quicker to metastasize (Travis *et al,* 2015; Wahbah *et al,* 2007). By far, smoking is the primary cause factor in the development of lung cancer, although air pollution and inhalation of other airborne carcinogens are important aetiologies as well (Alberg *et al,* 2013; Field & Withers, 2012). Chronic interstitial lung disease (ILD) may also play a role in the development of lung cancer (Archontogeorgis *et al,* 2012).

There are hundreds of identified ILDs, with or without confirmed aetiologies, although about two thirds are classified as idiopathic (Raghu, Nyberg, & Morgan, 2004). An overlap between idiopathic pulmonary fibrosis (IPF) and the development of lung cancer, particularly squamous cell carcinoma, has been documented (Aubry *et al,* 2002; Mizushima & Kobayashi, 1995; Park *et al,* 2001). It is theorised that the pathological repair process of idiopathic pulmonary fibrosis imitates that of a cancer, with the rapid unlimited cell proliferation of fibroblasts, a marked resistance to apoptosis, and the ability to quickly migrate (Drakopanagiotakis *et al,* 2008). The chronic damage inflicted by this disorder likely has a harmful effect on the DNA of lung tissue cells, possibly leading to atypia, metaplasia, dysplasia, and then perhaps the development of cancer (Kuwano *et al,* 1996; Takahashi *et al,* 1985).

Chronic obstructive pulmonary disease (COPD) is a progressive disease of the lungs that ultimately leads to loss of lung function and death (Vestbo *et al,* 2013). COPD is the third leading cause of worldwide deaths and a major preventable disease burden affecting up to 50% of all smokers (Burney *et al,* 2015; Lundbäck *et al,* 2003; Vestbo *et al,* 2013). Although COPD is markedly different from idiopathic pulmonary fibrosis and other ILDs, it is suspected that COPD may also instigate the development of lung cancer like IPF, independent of the risk factor of smoking (Bozzetti *et al,* 2016; Young *et al,* 2015; Young & Hopkins, 2010).

It is becoming increasingly apparent that *T. gondii* infection of the lungs drives a more severe outcome and illness with complications in those with pneumonia and other pre-existing lung conditions (Guo *et al,* 2015; Leal *et al,* 2007). Plus, those with chronic lung conditions such as COPD have been found to be more likely to be seropositive for *T. gondii* than the general,

healthy population (Li *et al*, 2020; Zhang *et al,* 2015), although much is not known or understood about this dynamic.

Similarly, Bajnok *et al* (2019) had found a much higher *T. gondii* positivity rate in lung cancer patients. Of the 72 samples, taken by fine needle aspiration of lung tissue surrounding a lung carcinoma, 100% were confirmed positive by both PCR amplification of *T. gondii* specific genetic markers as well as specific immunohistochemistry staining analysis. When they screened lung lavage samples from healthy volunteers (n = 10), the infection rate was much lower, and closer to the national average at 10%. As the patients were not yet receiving cancer treatment, the generalised immunosuppression associated with chemotherapy can not be considered a causative agent for this high rate of *T. gondii* infection.

However, it is important to note that some of the patients had comorbid lung disease, and so may have been receiving corticosteroid treatments for associated inflammation. Wang *et al* (2014) had found that the class of anti-inflammatory drugs, the glucocorticoids, once administered to rats, reduced iNOS expression and increased vulnerability to *T. gondii* infection.

Mice are extremely susceptible to *T. gondii*. Rats, on the contrary, are markedly resistant to infection with *T. gondii* (Benedetto *et al,* 1996; Evans *et al,* 2014; Fujii, Kamiyama, & Hagiwara, 1983; Lewis & Markell, 1958; Li *et al,* 2012; Nakayama & Hoshiai, 1960). This stark difference has driven investigations into what might be causative agent in this dynamic. Some studies on the divergence have highlighted the increasing importance of the role of Arginase-1 and iNOS in determining this sensitivity and resistance to infection by *T. gondii* (Gao *et al,* 2015; Li *et al,* 2012; Zhao *et al,* 2013). Moreover, the difference in susceptibility between these two

rodent species may offer answers as to why the samples obtained by Bajnok *et al* (2019), and that are focal to this study, have such a high rate of infection.

Li *et al* (2012) analysed the peritoneal macrophages of different inbred model rat strains. These macrophages are noted for their strong resistance to *T. gondii* infection *in vitro.* Different rat strains had varying levels of intensity of iNOS expression, but iNOS was found to be expressed in the peritoneal macrophages of all the analysed rat strains. This contrasted with the peritoneal macrophages of four model inbred mouse strains, where no expression of iNOS was detected until they were activated. Mouse peritoneal macrophages are notably sensitive to infection with *T. gondii* in *in vitro* studies (Lüder *et al,* 2003; Seabra, de Souza, & DaMatta, 2002). Further supporting these findings is that lower iNOS synthesis relative to Arginase-1 expression in mouse macrophages has been cited as a potential causal factor in their distinctive proneness to toxoplasmosis (Adams *et al*, 1990; Davis *et al*, 2007; EI Kasmi *et al*, 2008; James, 1995; Von Bargen *et al*, 2011). Similarly, the role of the Arginase-1 and iNOS balance in sensitivity and resistance to infection from other parasites has been investigated and appears to follow this finding (Duleu *et al,* 2004; Meireles *et al,* 2017; Stadelmann *et al*, 2013).

Zhao *et al* (2013) further expanded on the work of Li *et al* (2012), by investigating epigenetic factors that may also influence the Arginase-1 and iNOS, sensitivity and resistance dynamic. Zhao *et al* (2013) analysed alveolar macrophages in different strains of rats to assess their resistance to infection with *T. gondii*. Their findings illustrated a stark contrast to what was seen in the rat peritoneal macrophages. Rat alveolar macrophages were found to be very sensitive to infection, comparably so to the mouse peritoneal macrophages of the Li *et al* (2012) study. It was also concluded that the reduced iNOS and higher Arginase-1 expression

was likely the cause of this. Given that macrophages throughout an individual's body are genetically identical, these differing expression levels are being instigated through epigenetic factors.

Genetic factors as well as the condition of the immune system have previously been implicated as determining components on susceptibility to *T. gondii* (Kempf *et al,* 1999). Therefore, to expand on their previous work (Li *et al,* 2012), Gao *et al* (2015) investigated the Arginase-1 and iNOS relationship interaction with *T. gondii* alongside rats of different ages and strains. In their study, the extent of infection was ascertained by counting *T. gondii* cysts in a 10µl brain tissue sample, with a further 3 replicate samples for increased accuracy. The presence of bradyzoite cysts in the brain would be recorded as positive, and if no cysts were identified that would be considered a negative. For further confidence, PCR testing of the brain and other major organs for the negative rats was performed to limit false negatives. In addition to differing rat strains, the age was noted, with them being categorised as either adults or newborns of between 5-20 days of age.

The results of the Gao *et al* (2015) study corroborated with those of Li *et al* (2012), in that they both found a positive correlation between a higher ratio of iNOS to Arginase-1 and alongside stronger resistance to *T. gondii* infection. In the Gao *et al* (2015) study, all but one of the adult rat strains had no observed brain cysts, as well as testing negative for the presence of the parasite via a diagnostic PCR. The results for the neonates showed more variability, suggesting age as a susceptibility. The rat strains absent from *T. gondii* infection and brain cysts were strains, noted in the Li *et al* (2012) study, as being strains that typically express higher levels of iNOS in comparison to their relative Arginase-1 expression. Interestingly, the one rat strain, F344, that succumbed to infection with the mild Prugniaud

strain of *T. gondii* was the strain with a typical lower ratio of iNOS to Arginase-1 expression. Wang *et al* (2014) further supported these findings, with exception for the BN strain rats who were resistant to *T. gondii* infection regardless of their lower iNOS to Arginase-1 ratio.

Although this research surrounding the role of Arginase-1 and iNOS in determining susceptibility and resistance to *Toxoplasma gondii* in rodents is promising; this avenue of research is notably lacking for human *T. gondii* infections.

Utilizing the recent literature outlined above and acknowledging the large gap in the knowledge surrounding its potential role in humans, this study looks comparatively at the intensity and distribution of *T. gondii* infection alongside the expression of Arginase-1 and iNOS in these lung tissue biopsy samples.

Similarly, as far as could be determined, no such data was found for the typical distribution of *T. gondii* in pulmonary toxoplasmosis (in humans and or other mammals). Therefore, this study aims to investigate whether a tissue specific distribution of *T. gondii* is present in these lung biopsy samples. Parallel to this, expression of Arginase-1 and iNOS will also be looked at in these specific tissue types.

1.2 Aims and Objectives

Fifty-one lung cancer fine needle aspiration biopsy samples were previously requisitioned from The University Hospital of South Manchester NHS Foundation Trust as part of a previous study (Bajnok *et al* 2019). These samples were already embedded and fixed in paraffin blocks as per the norm in tissue sample storage. Prior to this investigation, scrapings were made from the tissue blocks and using diagnostic PCR, were tested for the presence of the parasite

Toxoplasma gondii. Surprisingly, all tested samples were found to be positive for *T. gondii* infection. This contrasting with the national average of 1 in 10 UK inhabitants carrying the pathogen. The same diagnostic PCR test was taken on lung lavage samples taken from 10 healthy volunteers to act as a control group. In these control samples, the rate of infection matched that of the UK average at 1/10 of the samples being positive for *T. gondii*. These findings, discussed in Bajnok *et al* (2019) naturally brought up questions about what may be causing this high rate of infection in these lung cancer patients, many of which also presented with comorbid lung disease. Much of this uncertainty brought about by the novel nature of this research.

One hypothesis, based on the recent research by Gao *et al* (2015) and similar research undertaken with other protozoan human pathogens (Duleu *et al,* 2004; Meireles *et al,* 2017; Stadelmann *et al*, 2013), was whether expression of immune system proteins Arginase-1 and iNOS has any influence on susceptibility to *T. gondii* infection. As discussed in the previous section, these proteins are in competition for the limited pool of cellular L-arginine and associations have been found for vulnerability to *T. gondii* infection and expression of Arginase-1 in macrophages. iNOS expression has been associated with resistance to infection with *T. gondii* in rats.

These findings raised questions on whether a similar dynamic maybe occurring in these lung cancer patients; whereby the presence of cancerous tissue may alter the typical Arginase-1/iNOS expression bias that may be seen in healthy lung tissue or lung tissue without malignancy.

Therefore, the broad aim of this study was to investigate the relationship between *T. gondii* infection and the expression of proteins Arginase-1 and iNOS in these lung tissue biopsy samples.

Outlined below are the objectives of this investigation:

1. Development and optimisation of Immunohistochemical detection and quantitative analysis approaches for the quantification and spatial analysis of *Toxoplasma gondii,* iNOS, and Arginase-1.
2. Analysis of colocalization and coexpression of *T. gondii* with iNOS and Arginase-1.
3. Investigation of tissue specific distribution of *T. gondii* infection and expression of iNOS and Arginase-1.

Chapter 2 Materials and Methods

2.1 Ethics

The original sample collection was made by the University of Manchester as described previously (Bajnok *et al* 2019). The study gained ethical approval by the local South Manchester research ethics committee (03/SM/396, lung tissue collection) and the NRES Committee North West – Greater Manchester South (06/Q1403/156, control sampling). All subjects provided written informed consent. Additional ethical approval was obtained for the work conducted at the University of Salford by the Research Governance and Ethics committee for the work covered by Bajnok *et al* (2019) (CST12/37) and associated work by Dr Muyassar Tarabulsi (ST16/124). Approval for the work specifically described in this thesis was granted by the University of Salford Research, Enterprise and Engagement Ethical Approval Panel (STR1819-17).

2.2 Sample collection and sample details

Fifty one of these 72 patient samples were included in the study here. The samples were taken as part of their normal clinical care and patients were not specifically recruited for this study. The samples used were taken for exploratory investigations into the possibility of lung cancer and were taken prior to any treatment or intervention. Subsequent diagnostic activity confirmed that all subjects had lung cancer. Table 2.1 lists basic information in addition to medical details from the 51 subjects of which the biopsy samples originated from.

Table 2.1: Basic information and medical history from the patients of which the lung biopsy tissue samples were obtained.

Sample No.	Age	Sex	Cancer Diagnosis	Comorbid Lung conditions	FEV1	FEV1%Pred	FVC	FEV1/FVC ratio	Current Drug Treatment	Smoking Status	Lobectomy position
664	75	M	Adenocarcinoma	COPD (moderate)	1.7	67.3	3.4	49.9	Nil	Smoker	Lower Left
757	75	M	Unconfirmed	COPD (moderate)	1.3	52.0	2.8	44.0	Veritol, Seretide, Spiriva	Ex-smoker	Upper Left
812	78	F	Squamous Cell Carcinoma	None	1.6	121.0	2.3	70.6	Nil	Smoker	Unknown
813	79	M	Small Cell Carcinoma	None	1.9	71.0	3.4	56.5	Nil	Ex-smoker	Unknown
818	78	M	Unconfirmed	COPD (mild)	2.7	85.0	4.7	58.2	Inhalers (unspecified)	Smoker	Upper Right
819	79	M	Unconfirmed	COPD (severe)	1.3	54.0	3.1	42.5	Salbutamol, Seretide, Spiriva	Ex-smoker	Lower Left
821	72	M	Unconfirmed	COPD (mild)	2.8	94.0	4.1	67.4	Salbutamol, Atrovent	Smoker	Lower Right
822	67	M	Small Cell Carcinoma	COPD (moderate)	2.0	66.0	3.0	67.4	Nil	Ex-smoker	Lower Left
823	84	M	Non-Squamous Cell Carcinoma	None	1.5	76.0	2.0	72.9	Unknown	Ex-smoker	Lower Left
827	68	M	Adenocarcinoma	COPD (mild)	2.4	90.0	3.5	69.3	Nil	Ex-smoker	Upper Right
828	50	F	Unconfirmed	None	3.3	130.0	4.0	82.5	Nil	Smoker	Upper Left
965	82	F	Unconfirmed	COPD (mild)	1.4	86.0			Nil	Smoker	Upper Right
968	82	F	Squamous Cell Carcinoma	None	2.0	99.7	2.5	78.5	Nil	Ex-smoker	Lower Right
972	75	F	Unconfirmed	None	1.2	83.0	1.8	65.7	Nil	Ex-smoker	Unknown
973	66	F	Unconfirmed	None	1.8	77.0	2.3	76.1	Salbutamol	Smoker	Upper Left
975	71	F	Unconfirmed	None	2.5	124.0			Nil	Smoker	Upper Right
976	69	F	Unconfirmed	COPD (moderate)	1.8	74.0	2.8	64.3	Nil	Smoker	Upper Right
979	75	F	Non-Squamous Cell Carcinoma	COPD (mild)	1.3	81.0	2.1	62.9	Salbutamol	Smoker	Upper Left
985	67	M	Unconfirmed	None	2.9	112.0	3.5	85.0	Nil	Ex-smoker	Lower Left
988	73	F	Unconfirmed	None	1.7	109.0	2.3	72.8	Nil	Ex-smoker	Lower Left
989	71	M	Squamous Cell Carcinoma	COPD (moderate)	1.9	62.0	3.5	52.6	Spiriva, Seretide	Ex-smoker	Unknown
997	80	M	Unconfirmed	COPD (moderate)	1.6	73.0	2.4	67.2	Spiriva, Salbutamol, Seretide	Ex-smoker	Unknown
999	60	M	Unconfirmed	COPD (mild)	3.5	92.0	5.4	64.8	Spiriva	Smoker	Upper Left
1004	67	M	Unconfirmed	COPD (moderate)	1.5	55.0	3.4	45.4	Prednisolone, Spiriva, Seretide, Salbutamol	Smoker	Lower Right

1005	78	M	Unconfirmed	COPD (moderate)	1.5	55.0	3.2	47.8	Spiriva, Salbutamol	Ex-smoker	Lower Right
1006	72	M	Unconfirmed	COPD (moderate)	1.7	63.0	3.3	50.0	Nil	Ex-smoker	Lower Left
1008	76	M	Non-Squamous Cell Carcinoma	None	3.2	127.0	3.7	85.8	Nil	Ex-smoker	Upper Left
1013	60	M	Adenocarcinoma	COPD (severe)	1.4	48.0	89.0	1.6	Spiriva, Seretide	Ex-smoker	Upper Right
1014	62	F	Unconfirmed	COPD (moderate)	1.8	76.0	2.7	66.7	Unknown	Ex-smoker	Upper Right
1017	70	M	Unconfirmed	COPD (severe)	1.7	58.0	3.7	45.7	Spiriva	Ex-smoker	Upper Right
1018	44	F	Non-Squamous Cell Carcinoma	None	3.1	125.0	3.6	86.1	Nil	Smoker	Upper Right
1025	68	F	Squamous Cell Carcinoma	None	1.9	113.0	2.7	70.7	Nil	Smoker	Upper Left
1026	77	M	Unconfirmed	COPD (moderate)	1.7	57.0	2.9	59.0	Spiriva, Seretide	Ex-smoker	Upper Right
1028	58	F	Unconfirmed	None	2.5	117.4	3.0	84.1	Nil	Ex-smoker	Upper Left
1029	66	M	Non-Squamous Cell Carcinoma	COPD (moderate)	1.9	69.0	3.7	51.4	Nil	Smoker	Upper Left
1030	61	M	Squamous Cell Carcinoma	COPD (severe)	1.5	45.0	2.6	56.0	Nil	Ex-smoker	Unknown
1032	59	M	Unconfirmed	None	2.4	70.0	3.2	74.8	Nil	Smoker	Upper Left
1033	62	F	Unconfirmed	None	1.8	81.0	2.8	64.9	Nil	Ex-smoker	Upper Right
1037	72	M	Squamous Cell Carcinoma	COPD (mild)	2.8	96.0	4.2	67.5	Nil	Smoker	Lower Right
1040	71	M	Unconfirmed	None	3.0	94.0	4.4	66.9	Nil	Smoker	Upper Left
1043	75	F	Adenocarcinoma	COPD (mild)	1.8	91.0	2.4	74.7	Salbutamol	Smoker	Upper Right
1045	59	M	Non-Squamous Cell Carcinoma	None	1.7	47.0	3.0	56.7	Nil	Ex-smoker	Unknown
1047	65	M	Unconfirmed	COPD (moderate)	2.0	59.0	3.8	52.8	Spiriva, Salbutamol	Smoker	Upper Left
1052	79	M	Unconfirmed	COPD (severe)	1.3	47.0	2.4	54.0	Seretide, Salbutamol	Ex-smoker	Upper Left
1054	67	F	Unconfirmed	None	1.9	131.0	2.6	74.0	Nil	Smoker	Upper Right
1064	75	M	Unconfirmed	COPD (moderate)	1.6	56.0	2.6	60.5	Spiriva, Salbutamol	Ex-smoker	Lower Right
1067	52	M	Unconfirmed	None	2.9	84.0	3.7	77.2	Nil	Ex-smoker	Upper Left
1068	66	M	Unconfirmed	COPD (severe)	1.1	40	3.36	33.9	Nil	Smoker	Upper Left
1069	57	F	Unconfirmed	None	1.4	68.0	1.9	71.1	Nil	Smoker	Unknown
1071	64	F	Unconfirmed	None	2.4	109.0	3.2	72.8	Nil	Ex-smoker	Upper Right
1072	74	M	Unconfirmed	Unknown	2.3	84.0	4.1	55.3	Nil	Ex-smoker	Upper Left

2.3 Slide Preparation

A total of five sections per sample were cut using a microtome (LEICA BIOSYSTEMS RM2125RT) at 5µm thickness and set onto positively charged slides before being left to dry overnight. For use as controls, a total of 10 rat liver and 10 rat heart sections were also cut at 5µm and fixed onto positively charged slides. These organs were previously embedded in paraffin and were from female Sprague Dawley rats, obtained from the University of Manchester Animal Facility where they were preserved in 10% formalin for 24 hours. Ten *T. gondii* positive tissue already fixed on a slide were ordered in from Sigma-Aldrich. Most of the slides were prepared by Dr Muyassar Tarabulsi, who was working on a parallel project utilising the same samples.

2.4 Staining for the Presence of *T. gondii*

All 51 samples were stained in a total of 5 batches. Each batch consisted of about 10 samples to be stained, with a negative control for each sample, as well as two of the *T. gondii* positive slides- one that would be stained as normal and the other was treated as a negative control. The negative control slides underwent the same protocol as the other slides with the only exception being the omission of the incubation with primary antibody. This protocol was also used in Bajnok *et al* (2019).

Initially the slides were de-waxed in Histoclear twice for 5 minutes. Rehydration then took place by submerging the slides in 100% ethanol for 5 minutes, then 90% ethanol for 3 minutes, followed by 75% ethanol for 2 minutes, and lastly 50% ethanol for 1 minute. The slides were

then rinsed under running water for 5 minutes, after which a PAP pen was used to draw a circle around the tissue to keep the reagents contained on the tissue. For antigen retrieval, the samples were incubated at 37^{o}C with 1% trypsin/calcium chloride, pH adjusted to 7.8, for 30 minutes in a humidified chamber. After this, the slides were left at room temperature for 10 minutes to cool down and prevent heat shock to the tissue. PBS-tween 20 was used to wash the slides twice for 2 minutes. Any surplus liquid residue was then removed before incubation with 0.3% hydrogen peroxide at room temperature for 30 minutes to block endogenous peroxidase activity. The slides were then washed with PBS-tween 20 for 3 minutes three times. To prevent non-specific antibody binding, the slides were incubated for 30 minutes at room temperature with normal goat serum (Vectastain ABC Systems, Vector Laboratories, UK). All slides except the negative controls were then incubated at room temperature for 1 hour with the primary polyclonal rabbit anti-*T. gondii* antibody, diluted to 1% in PBS, that would bind to any *T. gondii* in the tissue. Afterwards, another PBS-tween 20 wash was performed for 3 minutes, 3 times. All slides were then incubated at room temperature with the 0.5% diluted (in normal goat serum) secondary biotinylated anti-rabbit antibody (Vectastain ABC Systems, Vector Laboratories, UK), that would bind to any primary antibody present on the tissue. A wash was then done three times for 3 minutes with PBS-tween 20. The slides were incubated with ABC-Px mix (Vectastain ABC Systems, Vector Laboratories, UK) for 30 minutes at room temperature to aid attachment of the dye to the secondary antibody. Another PBS-tween 20 three-minute wash was repeated three times before incubation with the secondary antibody binding dye, 3-3'-diaminobenzidine (DAB) for no more than 10 minutes in the dark at room temperature. Rapidly, the slides were washed under running water for 5 minutes. Ehrlich's haematoxylin was used to counterstain the slides for 45 seconds before washing the slides under running water for 5 minutes. The tissue on

the slides was then dehydrated by submerging in 50% ethanol for 1 minute, 75% ethanol for 2 minutes, 90% ethanol for 3 minutes, and 100% ethanol for 5 minutes. The slide tissue was cleared with Histoclear for 5 minutes two times. Lastly, the slides were mounted in DPX using coverslips.

2.5 Staining for the Expression of Arginase-1 and iNOS

As with the *T. gondii* staining protocol, 51 samples were stained in a total of 5 batches, each batch consisting of about 10 samples to be stained. With the protocol for staining for Arginase-1 and iNOS being nearly identical, both were stained together, meaning there were three slides per sample in the batch; one to be stained for the presence of Arginase-1, another for iNOS, and one acting as a negative control. Positive controls were also used: two rat liver and two rat heart slides- one of each of the two being stained as normal and the other was treated as a negative control. Heart tissue typically expressing high levels of iNOS, as opposed to liver tissue of which typically expresses high levels of Arginase-1. All negative control slides underwent the same protocol as the other slides with the only exception the omission of the incubation with primary antibody.

Initially the slides were de-waxed in Histoclear twice for 5 minutes. Rehydration then took place by submerging the slides in 100% ethanol for 5 minutes, then 90% ethanol for 3 minutes, followed by 75% ethanol for 2 minutes, and lastly 50% ethanol for 1 minutes. The slides were then submerged in distilled water for 5 minutes, with the water being refreshed midway though. After this, a PAP pen was used to draw a circle around the tissue to keep the reagents contained on the tissue. For antigen retrieval, the slides were incubated in a Lab Vision™ PT

Module for a 20-minute cycle at 90^{o}C in pH 6 tricitric buffer. The slides were then washed under running water for 10 minutes. To block endogenous peroxidase activity, the slides were incubated with DAKO enzyme block (Dako EnVision Detection Systems, Dual Endogenous Enzyme Block, code number K4065) for 30 minutes at room temperature. The slides were then washed with PBS-tween 20 for 5 minutes, three times. With omission of the negative controls that were instead incubated with PBS buffer, the slides were then incubated with the Arginase-1 (Thermo Fisher Scientific, Catalogue number PA5-29645, Rockford, IL, USA) or iNOS (Thermo Fisher Scientific, Catalogue number PA1-036, Rockford, IL, USA) primary polyclonal rabbit antibody, diluted to 1:200 for 90 minutes at room temperature. After this, another PBS-tween 20 wash was carried out for 5 minutes twice before incubation with the secondary (Labelled Polymer - Dako REAL EnVision-HRP, Rabbit-Mouse, code number K4065) antibody for 1 hour at room temperature. Then, the slides were washed with PBS-tween 20 twice for 5 minutes. 3-3'-diaminobenzidine (DAB) was used as the secondary antibody binding dye and was incubated with the slides at room temperature for a maximum of 10 minutes. Speedily, the slides were washed under running water for 5 minutes. Ehrlich's haematoxylin was used to counterstain the slides for 45 seconds before washing the slides under running water for 5 minutes. The tissue on the slides was then dehydrated by submerging in 50% ethanol for 1 minute, 75% ethanol for 2 minutes, 90% ethanol for 3 minutes, and 100% ethanol for 5 minutes. The slide tissue was cleared with Histoclear for 5 minutes two times. Lastly, the slides were mounted in DPX using coverslips.

2.6 Protocol for Image Collection

Images were taken with the use of a Leica DM500 camera microscope and its accompanying Leica application where the focus and image position could be viewed and adjusted before being taken and saved. A mixture of randomised and selective, serial photos were taken at different magnifications. Figure 2.1 shows five 400x magnified serial photos of one sample as an example. Serial images were also taken at 100x magnification. In addition to this, three randomised photos, as per Bajnok *et al* (2019) protocol, were taken at 400x magnification for each of the five slides in every one of the 51 samples. This randomisation was achieved by moving the positioning dial of the microscope, and then only looking through the eyepiece to correct the focus for the photo taking.

2.7 Data Collection and Statistical Analysis

The images collected of the slide sections formed the basis of this study and were investigated using the software ImageJ, as well as visually through gridded colocalization analysis, and cell/tissue identification and categorisation.

ImageJ was used to calculate tissue coverage and so this was manually factored into the data as well; the reasoning behind this is explored in the Chapters 3 and 4. This was carried out for the randomised photos as well as the photos of the same region of the sample sections, both datasets being analysed separately. Both datasets were adjusted for 'background noise', calculated by taking ImageJ readings from the counterpart negative control slide photos and subtracting them from the sample photo readings. Numerical readings that became negative

figures were omitted from statistical analysis. Microsoft Excel™ and Minitab™ were used for statistical analysis. Where it was found that datasets were not of a normal distribution, non-parametric statistical tests such as Spearman's rank and Kruskal-Wallis tests were performed, otherwise, t-tests or Pearson's correlation tests were used. In some cases, 2 x 2 Fishers exacts tests were used to identify associations. P-values of < 0.05 were considered significant. Percentage of staining coverage data obtained from ImageJ was analysed between Arginase-1 and iNOS, *T. gondii* and Arginase-1, *T. gondii* and iNOS, as well as *T. gondii* and the iNOS/Arginase-1 ratio.

Visual observations were also utilised for analysis, using two different methods. On the serial (matched) photographs, a five by four grid was overlayered to create 20 identical square coordinates. An example of this can be seen in Figure 3.2 of Chapter 3. Coordinates with dark brown or extensive staining were classified as highly expressive; beige or yellow staining was classified as low expression; and only blue haematoxylin staining was classified as nil stained. Any samples with cross-reacting negative controls or had image quality issues were omitted from the analysis.

Lastly, visual observation was also used for cell/tissue identification and categorisation, with all the photos being pooled together to retrieve as much data as possible. Help with identification was provided by lung specialist Dr Lucy Smyth of the University of Salford as well as the use of histology textbooks. Airway epithelia and blood vessel endothelia were chosen for *T. gondii* rate of infection analysis, whereas smooth muscle and macrophages were analysed for *T. gondii* as well as the expression of Arginase-1 and iNOS.

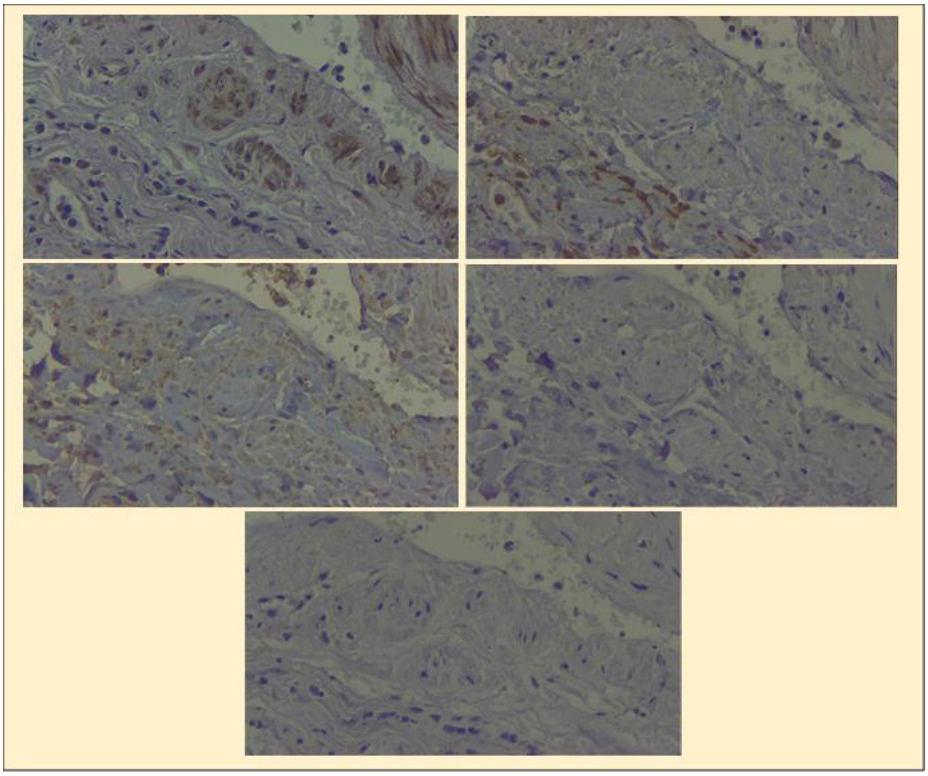

Figure 2.2: photographs taken at 400x magnification of five, 5µm thick, sections of the same lung tissue sample, in the same field of view. Immunohistochemistry was used for staining. Top left was stained for the presence of T. gondii. Top right was stained for Arginase-1 *expression. Middle left was stained for iNOS expression. Middle right and bottom were both negative controls.*

Chapter 3 Results

3.1 Development and optimisation of Immunohistochemical detection and quantitative analysis approaches for the quantification and spatial analysis of *Toxoplasma gondii*, iNOS, and Arginase-1.

3.1.1 Development and optimisation of Immunohistochemistry protocols

Before this study could begin quantitative analysis with the intention of offering insight into the research questions outlined above, functional and effective protocols were developed and optimised with regard to slide preparation, immunohistochemistry staining, as well as precise use of a camera compound light microscope. In this subsection the optimisation process will be described.

Perhaps the most fundamental protocol to develop, and also the most challenging to get right, was the development of the immunohistochemistry protocols to get clear imagery of *Toxoplasma gondii* distribution and iNOS, and Arginase-1 expression. Additionally, a specific challenge was that the paraffin embedded lung tissue biopsy samples had to be thinly cut and mounted onto glass slides. Lung tissue, unlike most other tissues is very porous and delicate, owing to the alveoli that constitute a large proportion of the lungs. This made it difficult to mount the thin tissue slices onto the slides without either damaging the original tissue layout and/or having the tissue fold in on itself. It was crucial for the tissue section to be as level as possible, as was found that irregular sections lead to uneven staining in addition to difficulties focussing in on the area with the microscope. To counteract this issue, the paraffin embedded

tissue samples were kept in an ice box for at least 30 minutes prior to microtoming- this greatly increased the stability of the sections, therefore creating better quality slides.

Immunohistochemical staining was optimised on test slides before the investigation of this study was conducted. Mammalian liver tissue is a natural expresser of high levels of Arginase-1, whereas mammalian heart tissue typically expresses high levels of iNOS. Therefore, rat heart and liver samples were obtained and fixed, before being mounted onto slides. These slides were then used for optimisation of the iNOS/Arginase-1 staining protocol. The *T. gondii* staining on test slides were performed on sections taken from the lung biopsy samples where more tissue was available rather than exhausting more precious samples. Key optimisation outcomes were as follows. Firstly, the time spent incubated with DAB, the brown staining agent that bound with the secondary antibody on the tissue, was reduced from 10 minutes (typical of several protocols) to 8 minutes after the staining was deemed too dark and may interfere with intensity analysis. Another substantial improvement, highlighted in Figure 3.1, was the utilisation of a PT Module in place of the use of a microwave for antigen retrieval in the iNOS/Arginase-1 protocol. It was found that microwaving the slides was damaging to the tissue, and by using the specialist buffer heating equipment instead, meant less tissue destruction and cleaner, crisper images could be taken of the section after staining. Figure 3.1, showing an example slide from these experiments, illustrates the increased clarity of the section and a reduction in the level of tissue damage. Once a level of confidence was established with the protocols, sample processing could be scaled up using larger staining troughs and slide racks with a greater capacity.

This optimisation process on the test slides additionally enabled operator skill development on the techniques needed to take good quality photographs of the stained sections using the

light microscope. Subsection 3.3.2 will discuss how these images taken could then be used for quantitative analysis.

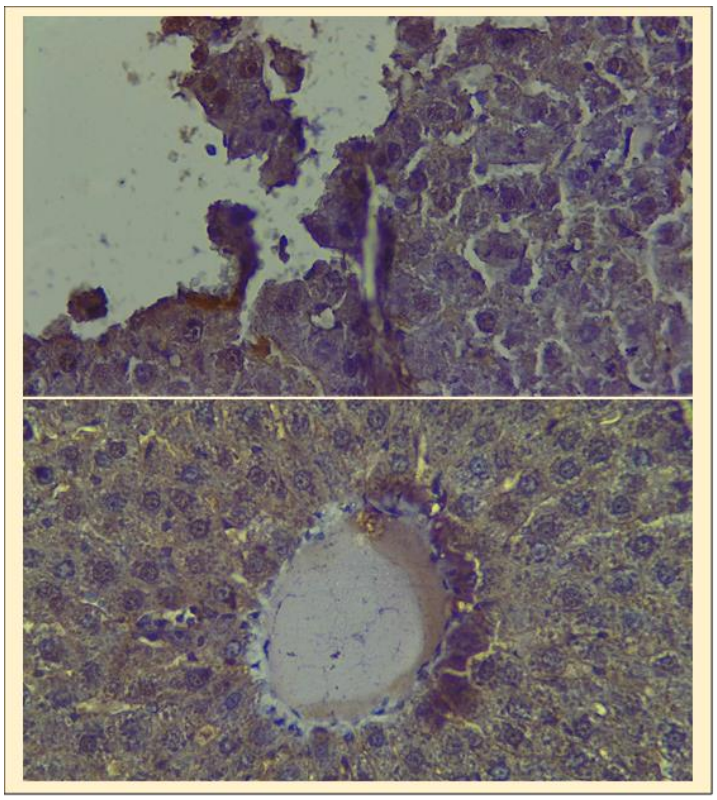

Figure 3.1: Comparison of the use of a PT module with the microwave protocol for preparing slides. Images were taken at 400x magnification of rat liver tissue immunohistochemically stained for the presence of Arginase. Above: The section was incubated for 7 minutes with tricitric buffer in a microwave. Below: The section was incubated with tricitric buffer in PT Module for a 20-minute cycle at 90^{o}C. As shown, the tissue section incubated in the PT Module is clearer to see and has suffered less damage to its overall structure.

3.1.2 Development of approaches for quantitative analysis of *T. gondii* infection using a pilot study

Once the staining had been optimised, a decision was required on the quantity, magnification, and type of images that were required for further analyses with the aim of answering the objectives set out in Section 3.1. Table 3.1 summarises the categories and different types of images and how they were analysed. However, prior to following this arrangement, a pilot study was conducted to assess suitability of the selected analytical models on the first batch of 10 samples.

Influenced by Bajnok *et al* (2019), it was decided that three images would be taken at randomised fields of view at 400x magnification. This allowed for a large pool of images to be collected. For more specific, comparative analysis that was required of this study, it was decided to have one set of "matched" (serial section) photographs also. These would take advantage of the proximity of each of the cut sample sections with the goal of having a visualisation of *T. gondii,* iNOS, and Arginase-1 interactions in a given area of the lung tissue. One set of matched photographs were also taken at 100x magnification to increase the data pool.

Bajnok *et al* (2019) used open-source photo analysis software ImageJ to quantify the proportion of stain coverage on their 400x magnified, *T. gondii* immunohistochemically stained slides. All three randomised photos of each sample were utilized to form a mean percentage of stain coverage figure. It was deemed suitable for this methodology to be applied to both the randomised and the matched 400x magnified images of this study, although an average could not be computed for the results of the matched photos. However, adjustments were made to the Bajnok *et al* (2019) ImageJ protocol. Firstly, the total area of

lung tissue in the photo was calculated through ImageJ before being divided into the percentage stain coverage to ascertain the proportion of staining relative to the tissue present. This alteration will be discussed further in section 3.3.4. Another adjustment was made to account for some non-specific staining in the photos of the negative control samples. This will be discussed further in Chapter 4 as a possible limitation of the study, but it was found that the secondary antibody in the immunohistochemistry protocol could inappropriately bind to alveolar macrophages in the negative control slides, creating false positives. This has been referred to as 'background noise' in this study. To overcome this issue, ImageJ readings were taken of the negative control images, from randomised and matched images, to calculate a baseline staining that was then subtracted from the ImageJ results from those of *Toxoplasma,* Arginase-1, and iNOS stained images to form Dataset C and Dataset I as seen in Table 3.1. Unfortunately, for a few samples, these subtractions led to figures in the negative value. So as to not interfere with further statistical analyses Dataset D and Dataset J were utilised whereby these negative numbers were not included by omission of the affected sample. Table 3.2 lists the lung biopsy samples and each dataset it is included in for each of the three components it was stained for.

Although ImageJ analysis allowed for the generation of a large quantity of data, it was decided a more specific, colocalised analytic method was also required. This would more specifically gauge whether there were interactions between *T. gondii* and Arginase-1, or *T. gondii* and iNOS. Efforts were made to use another ImageJ plugin called Coloc2 that be able to overlay two images of an identical tissue section and calculate as to whether two stain markers were probable of co-occurring, avoidance, or having no relationship. The slight difference in the tissue structure, although there was only 5µm between each section, was too misaligned for the program to work. Instead, colocalised analysis was performed manually with the

superimposition of grid coordinates; this is illustrated in Figure 3.2. This same 5 by 4 grid was overlayed onto each of the matched 400x magnified images. Each grid coordinate was allocated a grading based on the intensity of staining within and could be classified as 'high', 'low' or 'nil'. Coordinates without lung cells or tissue, or those that had cross reaction showing in the negative control were omitted from analysis. A classification of 'high' meant there was dark brown staining; a classification of low meant that there was only beige staining; and in the nil classification, there would be no hint of browning. Therefore, in Figure 3.1 coordinates A2 and C2 would be classified as high, and coordinates B1 and C1 would be classified as low.

Lastly, it was considered important to determine whether there was any preferential staining within the different lung tissue and cell types. If such a preference existed and was not recognised, it may interfere with or artificially inflate other analyses assessing whether there is a relationship between the intensity of infection along with the expression of Arginase-1 and iNOS. This will be discussed further in Chapter 4. The decision as to which tissues and cells to analyse were mainly based on their relative abundance and ease of identification. As such, smooth muscle bundles and alveolar macrophages were identified and a value was calculated for the proportion that stained positive for the presence of *T. gondii,* Arginase-1, and iNOS. Airway epithelial and blood vessel endothelial were only analysed in this way for the presence of *Toxoplasma gondii*.

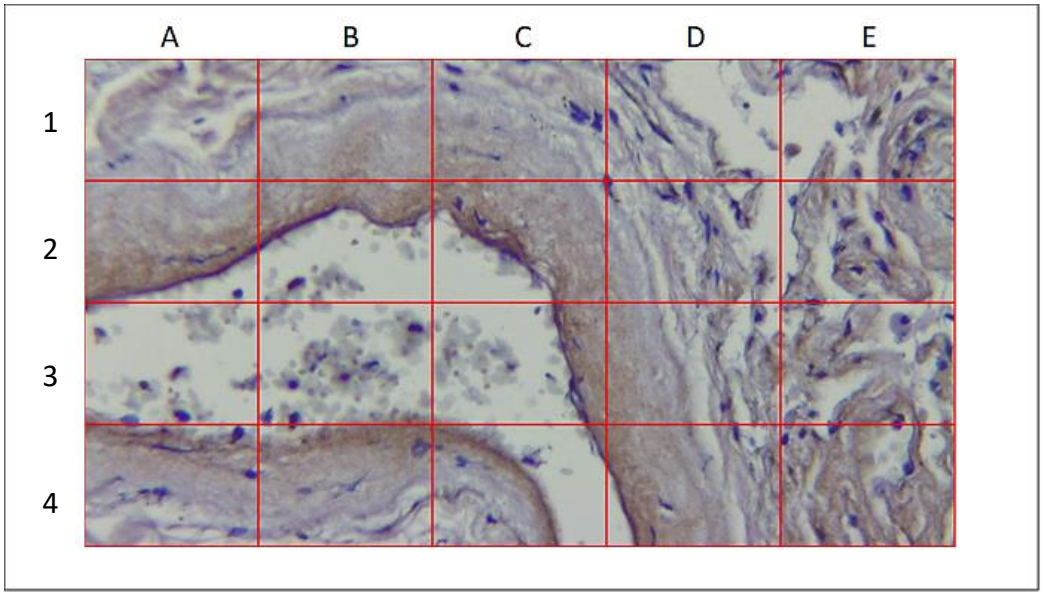

Figure 3.2: Overlayered 4 x 5 grid on a 400x magnified lung tissue biopsy sample immunohistochemically stained for the presence of Toxoplasma gondii. Only the 400x *magnified images taken at the same field of view for each of the 5 sample slides were analysed in this way. Grid coordinates with non-specific staining in the counterpart negative control slides were omitted. Grid coordinates absent of lung tissue were also omitted from study. Grid coordinates were either classified as 'high', 'low', or 'nil'. A high classification would mean staining in dark brown colour, such as that of B2 and C2. A classification of low would mean staining in only a light brown or beige colour, such as that of C1. Nil staining meant no brown staining at all.*

Table 3.1: Summary of the different categories of images and how they were analysed. Photographs taken of each of the stained and negative control lung tissue slide samples were taken at 100x and 400x magnification in randomised and in the same field of view. The randomised images, 3 per slide, were put through specialist staining analysis software ImageJ to calculate percentage of stain coverage, of which an average was calculated. As shown, these averages are represented Dataset G. Similarly, ImageJ analysis was conducted on the matched photos too alongside colocalization analysis with the use of grid coordinates, represented as Dataset A and Dataset E respectively. All images were pooled together for the tissue specific staining analysis, with the omission of some samples due to non-specific staining, termed cross-reacting, of the negative controls. Similarly, 'background noise' also refers to cross-reacting in the negative control samples. Any amendments to the datasets were recategorized as another dataset and as shown here, can be found further along the row to the right.

<table>
<tr><td rowspan="6">400x Magnified images</td><td rowspan="4">Matched images</td><td rowspan="2">ImageJ data</td><td>Percentage stain coverage Dataset A</td><td colspan="2"></td></tr>
<tr><td>Percentage stain coverage data/tissue coverage Dataset B</td><td>With adjustments made for background noise Dataset C</td><td>With omitted samples with negative values Dataset D</td></tr>
<tr><td>Gridded analysis data Dataset E</td><td colspan="3"></td></tr>
<tr><td>Tissue specificity data</td><td>With omitted cross-reacting samples Dataset F</td><td colspan="2"></td></tr>
<tr><td rowspan="3">Randomised images</td><td rowspan="2">ImageJ data</td><td>Average Percentage stain coverage Dataset G</td><td colspan="2"></td></tr>
<tr><td>Average Percentage stain coverage data/tissue coverage Dataset H</td><td>With adjustments made for background noise Dataset I</td><td>With omitted samples with negative values Dataset J</td></tr>
<tr><td>Tissue specificity data</td><td>With omitted cross-reacting samples Dataset F</td><td colspan="2"></td></tr>
<tr><td>100x Magnified images</td><td>Matched images</td><td>Tissue specificity data</td><td>With omitted cross-reacting samples Dataset F</td><td colspan="2"></td></tr>
</table>

Table 3.2: Each lung tissue biopsy sample and its inclusion in the 12 different datasets for the data generated from the sections stained for the presence of Toxoplasma gondii, Arginase-1, and iNOS. As shown, the majority of all samples were utilised for the entirety of this study, whilst others such as sample number 818 had full inclusion with T. gondii and Arginase-1 datasets but omission from tissue specificity analysis from its iNOS datasets.

Biopsy sample	*T. gondii* datasets utilised	Arginase-1 datasets utilised	iNOS datasets utilised
812	A,B,C,D,E,F,G,H,I,J	A,B,C,D,E,F,G,H,I,J	A,B,C,D,E,F,G,H,I,J
818	A,B,C,D,E,F,G,H,I,J	A,B,C,D,E,F,G,H,I,J	A,B,C,D,E,G,H,I,J
819	A,B,C,D,E,F,G,H,I,J	A,B,C,D,E,F,G,H,I,J	A,B,C,D,E,F,G,H,I,J
821	A,B,C,D,E,F,G,H,I,J	A,B,C,D,E,F,G,H,I,J	A,B,C,D,E,F,G,H,I,J
822	A,B,C,D,E,F,G,H,I,J	A,B,C,D,E,F,G,H,I,J	A,B,C,D,E,G,H,I,J
823	A,B,C,D,E,F,G,H,I,J	A,B,C,D,E,F,G,H,I,J	A,B,C,D,E,F,G,H,I,J
827	A,B,C,D,E,F,G,H,I,J	A,B,C,D,E,F,G,H,I,J	A,B,C,D,E,F,G,H,I,J
828	A,B,C,D,E,F,G,H,I,J	A,B,C,D,E,F,G,H,I,J	A,B,C,D,E,F,G,H,I,J
965	A,B,C,D,E,F,G,H,I,	A,B,C,D,E,F,G,H,I	A,B,C,D,E,F,G,H,I
968	A,B,C,D,E,F,G,H,I,J	A,B,C,D,E,G,H,I,J	A,B,C,D,E,F,G,H,I,J
972	A,B,C,D,E,F,G,H,I,J	A,B,C,D,E,F,G,H,I,J	A,B,C,D,E,F,G,H,I,J
973	A,B,C,D,E,F,G,H,I,J	A,B,C,D,E,G,H,I,J	A,B,C,D,E,G,H,I,J
975	A,B,C,D,E,F,G,H,I,J	A,B,C,D,E,G,H,I,J	A,B,C,D,E,G,H,I,J
979	A,B,C,D,E,F,G,H,I,J	A,B,C,D,E,G,H,I,J	A,B,C,D,E,G,H,I,J
985	A,B,C,D,E,F,G,H,I	A,B,C,D,E,F,G,H,I	A,B,C,D,E,F,G,H,I
988	A,B,C,D,E,F,G,H,I,J	A,B,C,D,E,F,G,H,I,J	A,B,C,D,E,F,G,H,I,J
989	A,B,C,D,E,F,G,H,I,J	A,B,C,D,E,F,G,H,I,J	A,B,C,D,E,F,G,H,I,J
997	A,B,C,D,E,F,G,H,I,J	A,B,C,D,E,G,H,I,J	A,B,C,D,E,G,H,I,J
999	A,B,C,D,E,F,G,H,I,J	A,B,C,D,E,F,G,H,I,J	A,B,C,D,E,F,G,H,I,J
1005	A,B,C,D,E,F,G,H,I,J	A,B,C,D,E,F,G,H,I,J	A,B,C,D,E,F,G,H,I,J
1006	A,B,C,D,E,F,G,H,I,J	A,B,C,D,E,F,G,H,I,J	A,B,C,D,E,F,G,H,I,J
1008	A,B,C,D,E,F,G,H,I,J	A,B,C,D,E,G,H,I,J	A,B,C,D,E,G,H,I,J
1013	A,B,C,D,E,F,G,H,I,J	A,B,C,D,E,G,H,I,J	A,B,C,D,E,G,H,I,J
1014	A,B,C,D,E,F,G,H,I,J	A,B,C,D,E,G,H,I,J	A,B,C,D,E,G,H,I,J
1017	A,B,C,D,E,F,G,H,I,J	A,B,C,D,E,G,H,I,J	A,B,C,D,E,G,H,I,J
1018	A,B,C,D,E,F,G,H,I,J	A,B,C,D,E,G,H,I,J	A,B,C,D,E,G,H,I,J
1025	A,B,C,D,E,F,G,H,I,J	A,B,C,D,E,F,G,H,I,J	A,B,C,D,E,F,G,H,I,J
1026	A,B,C,D,E,F,G,H,I,J	A,B,C,D,E,F,G,H,I,J	A,B,C,D,E,F,G,H,I,J
1028	A,B,C,D,E,F,G,H,I,J	A,B,C,D,E,F,G,H,I,J	A,B,C,D,E,F,G,H,I,J
1029	A,B,C,D,E,F,G,H,I,J	A,B,C,D,E,G,H,I,J	A,B,C,D,E,G,H,I,J
1030	A,B,C,D,E,F,G,H,I,J	A,B,C,D,E,G,H,I,J	A,B,C,D,E,G,H,I,J
1032	A,B,C,D,E,F,G,H,I,J	A,B,C,D,E,F,G,H,I,J	A,B,C,D,E,F,G,H,I,J
1033	A,B,C,D,E,F,G,H,I,J	A,B,C,D,E,G,H,I,J	A,B,C,D,E,G,H,I,J
1037	A,B,C,D,E,F,G,H,I,J	A,B,C,D,E,G,H,I,J	A,B,C,D,E,G,H,I,J
1040	A,B,C,D,E,F,G,H,I,J	A,B,C,D,E,F,G,H,I,J	A,B,C,D,E,F,G,H,I,J
1043	A,B,C,D,E,F,G,H,I,J	A,B,C,D,E,F,G,H,I,J	A,B,C,D,E,F,G,H,I,J
1047	A,B,C,D,E,F,G,H,I,J	A,B,C,D,E,F,G,H,I,J	A,B,C,D,E,F,G,H,I,J
1052	A,B,C,D,E,F,G,H,I,J	A,B,C,D,E,G,H,I,J	A,B,C,D,E,G,H,I,J
1054	A,B,C,D,E,F,G,H,I,J	A,B,C,D,E,F,G,H,I,J	A,B,C,D,E,F,G,H,I,J
1064	A,B,C,D,E,F,G,H,I,J	A,B,C,D,E,G,H,I,J	A,B,C,D,E,G,H,I,J
664	A,B,C,D,E,F,G,H,I,J	A,B,C,D,E,G,H,I,J	A,B,C,D,E,F,G,H,I,J
757	A,B,C,D,E,F,G,H,I,J	A,B,C,D,E,F,G,H,I,J	A,B,C,D,E,F,G,H,I,J
813	A,B,C,D,E,F,G,H,I,J	A,B,C,D,E,F,G,H,I,J	A,B,C,D,E,F,G,H,I,J
976	A,B,C,D,E,F,G,H,I,J	A,B,C,D,E,G,H,I,J	A,B,C,D,E,G,H,I,J
1004	A,B,C,D,E,F,G,H,I,J	A,B,C,D,E,F,G,H,I,J	A,B,C,D,E,F,G,H,I,J
1045	A,B,C,D,E,F,G,H,I,J	A,B,C,D,E,G,H,I,J	A,B,C,D,E,G,H,I,J
1067	A,B,C,D,E,F,G,H,I,J	A,B,C,D,E,F,G,H,I,J	A,B,C,D,E,F,G,H,I,J
1068	A,B,C,D,E,F,G,H,I,J	A,B,C,D,E,F,G,H,I,J	A,B,C,D,E,F,G,H,I,J
1069	A,B,C,D,E,F,G,H,I,J	A,B,C,D,E,G,H,I,J	A,B,C,D,E,G,H,I,J
1071	A,B,C,D,E,F,G,H,I,J	A,B,C,D,E,F,G,H,I,J	A,B,C,D,E,F,G,H,I,J
1072	A,B,C,D,E,F,G,H,I,J	A,B,C,D,E,F,G,H,I,J	A,B,C,D,E,F,G,H,I,J

3.1.3 Quantification of the intensity of *T. gondii,* iNOS, and Arginase-1 staining with an approach used in Bajnok *et al*. (2019)

As stated earlier, Bajnok *et al* (2019) had previously worked on these same 51 biopsy samples of this study. All of which had tested positive for the presence of *T. gondii* both through PCR and immunohistochemistry screening. This published study reported a very striking result – namely that 100% of samples showed infection (72/72). A key result from the study reported in this thesis, is that all 51 samples used here also showed staining for *T. gondii* when conducted by an independent operator and using re-optimised approaches (51/51). This demonstrates that the published results are repeatable and thus further validates the striking conclusions. In this study, as discussed in subsection 3.3.2, the published analysis was extended by improved image analysis and inclusion of the expression of Arginase-1 and iNOS.

The methodology used by Bajnok *et al* (2019) of having 3 photos taken at randomised fields of view, before being inputted into ImageJ and then calculating the mean average was used. This data, comprising Dataset G, is summarised in Figure 3.3. Illustrated here is a large range of extent of staining, particularly with *T. gondii* and iNOS datasets. It also appears iNOS is overwhelmingly the dominant gene expression of the two enzymes, with a median of 45.5% staining coverage. Arginase-1, on the contrary, only has a median of 3.9% and a lower range of expression. These show a significant difference in expression ($P = <0.001$).

Although the data generated from ImageJ was deemed intrinsic to this study and was also applied to the 400x magnified matched images to form Dataset A; it was recognised that improvements could be made to this process to make it a more accurate representation of the distribution of *T. gondii* infection, and Arginase-1 and iNOS expression. This is because

this study had more of a comparative element, expanding on the work of Bajnok *et al* (2019) with a view to visualise how Arginase-1 and iNOS are expressed in relation to the extent of *T. gondii* infection.

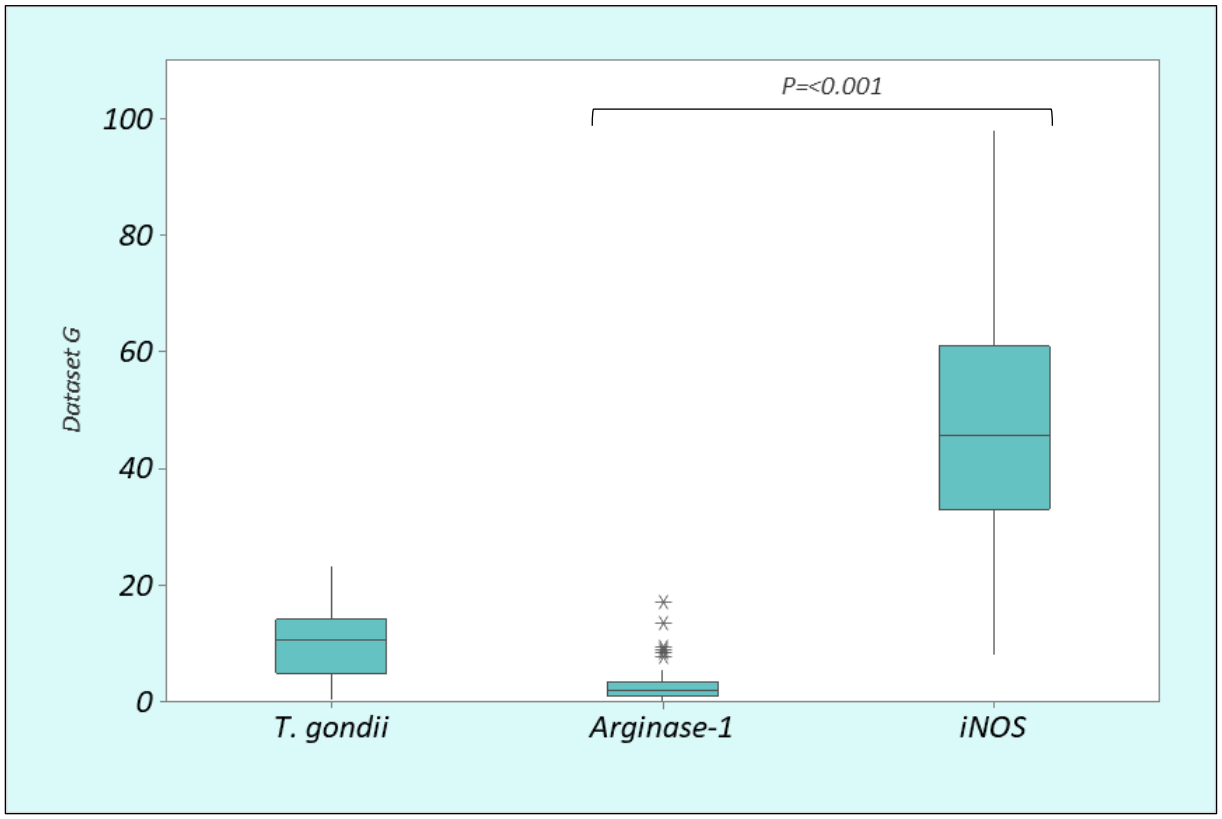

Figure 3.3: A box and whisker plot showing the distribution of Toxoplasma infection, iNOS and Arginase-1 expression in human lung samples. This figure shows the median extent of stain coverage in 51 immunohistochemically stained lung biopsy samples, stained for the presence of T. gondii, iNOS and Arginase-1. These were calculated by percentage coverage analysis with ImageJ on three images of each sample taken at random, before calculating a mean as per the methodology utilised by Bajnok et al (2019). Asterisks denote the presence of outlier results. Dataset G was utilised for this summary figure. As shown, Arginase-1 expression is very minimal, unlike iNOS of which is expressed significantly (p=<0.001) more highly and at a larger range of variability. Similarly, the extent of T. gondii infection is very variable.

3.1.4 Development of an improved quantification of *T. gondii,* iNOS, and Arginase-1 specific staining

As previously discussed, the use of ImageJ for calculation of the percentage coverage of staining was integral to this study. ImageJ analysis was performed on both the 400x magnified, matched images and of the three randomised images for all sample slides to form Datasets A and G respectively. The use of three randomised images to calculate an average reading was used previously by Bajnok *et al* (2019), and so had influenced this study. However, limitations were identified with the Bajnok *et al* (2019) methodology that could have ultimately interfered with the interpretation of the results collected. It quickly became apparent that when ImageJ was calculating the percentage of stain coverage in an image, it did not automatically factor in the amount of tissue on that inputted photo. This was concerning considering the 'patchy' anatomy of lung tissue; particularly when comparing lung connective and interstitial tissue with that of the alveoli. A photo taken at 400x magnification of the latter could easily be filed with lung tissue to analyse, whereas a photo of the former would have large areas of blankness. Therefore, there was the potential for great under- or overrepresentation of the true extent of stain coverage. To correct this and explore the nature of this over representation, the amount of lung tissue present on a photo was factored in, as described below, which culminated in Datasets B and H. The percentage of tissue covering the image was determined separately, in the same manner as the antibody-DAB stain coverage was calculated. The proportion of tissue coverage was calculated by using ImageJ to measure the intensity and spread of the counterstain colour that had stained the lung cells and tissues blue. Once this figure had been calculated for a photo, a percentage coverage of the antibody-DAB stain could be calculated relative to the tissue coverage, to give a

percentage of staining within the tissue only. In order to assess the efficacy of this amendment, a correlation coefficient alongside a paired t-test or Mann-Whitney test (depending on whether the datasets were measured to be normally distributed or not) was calculated between Dataset G and Dataset I for all of the *Toxoplasma gondii,* Arginase-1, and iNOS data.

Figure 3.4 compares Dataset G (percentage of staining coverage only) versus Dataset I (percentage of staining coverage divided by the proportion of lung tissue on the inputted image), for the *Toxoplasma gondii* stained slides.

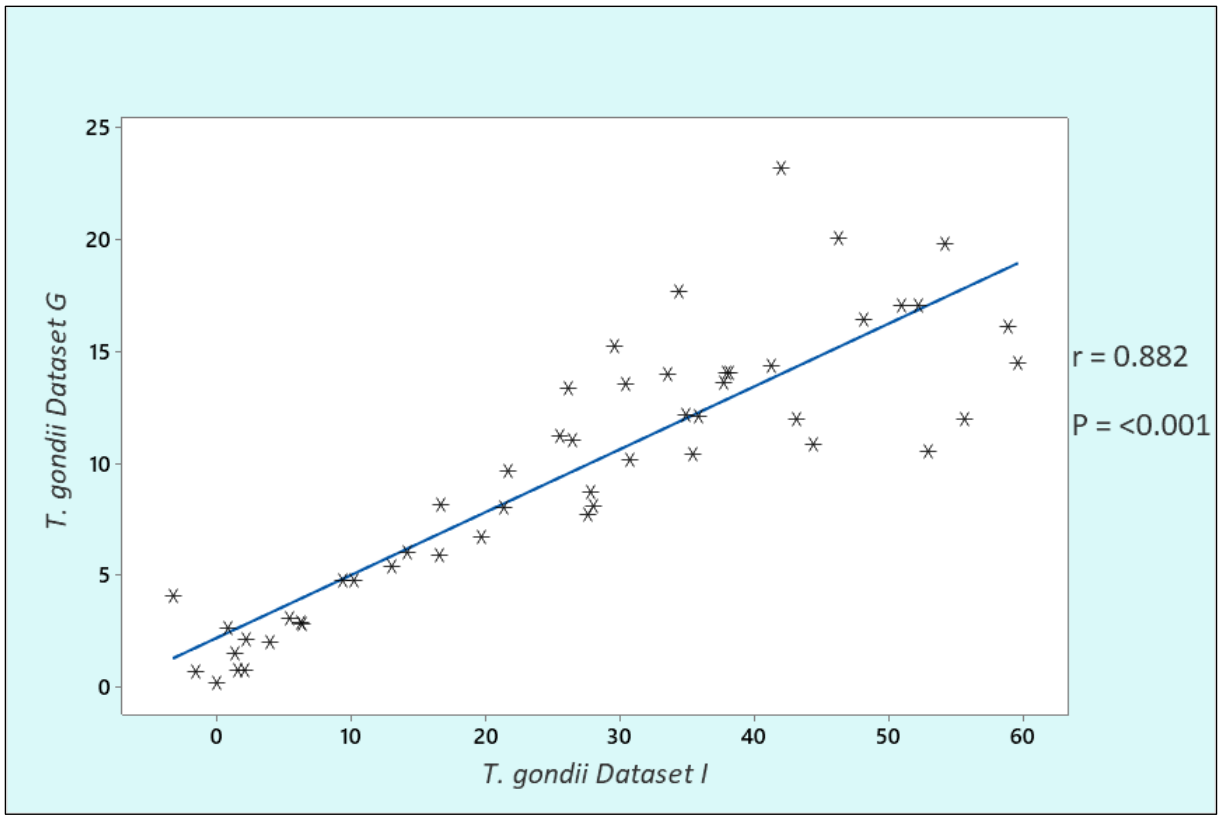

Figure 3.4: A correlation between Dataset G and Dataset I of lung tissue specifically stained for the presence of Toxoplasma gondii. Dataset G comprised data of percentage stain coverage as per the methodology Bajnok et al (2019) used, whereas Dataset I comprised percentage stain coverage divided by the proportion of lung tissue within the analysed image. This Figure determines whether there is a correlation between the two techniques. A strong positive correlation can be seen (r = 0.882; n = 51; P = <0.001) supporting the idea that both datasets strongly align with each other, establishing reliability to this amended methodology.

These datasets were found to be normally distributed and so a Pearson's correlation coefficient was calculated to determine whether there was a correlation. As shown in the

scatterplot in Figure 3.4 a strong correlation was observed (r = 0.882, *P* = <0.001). A paired T-test was also conducted, showing a significant difference between the two datasets (t = -8.96; n = 51; *P* = <0.001). The conclusion is that the data shows a strong correlation between the approach of Bajnok et al (2019) and the improved coverage measures used here this validating the consistency of both methods however the approach taken in this thesis represented a significant improvement the actual distribution quantification of *T. gondii* infection. The next stages were to apply the same analysis to check the effect on iNOS and Arginase-1 expression.

Figure 3.5 compares Dataset G with Dataset I for the Arginase-1 specifically stained slides.

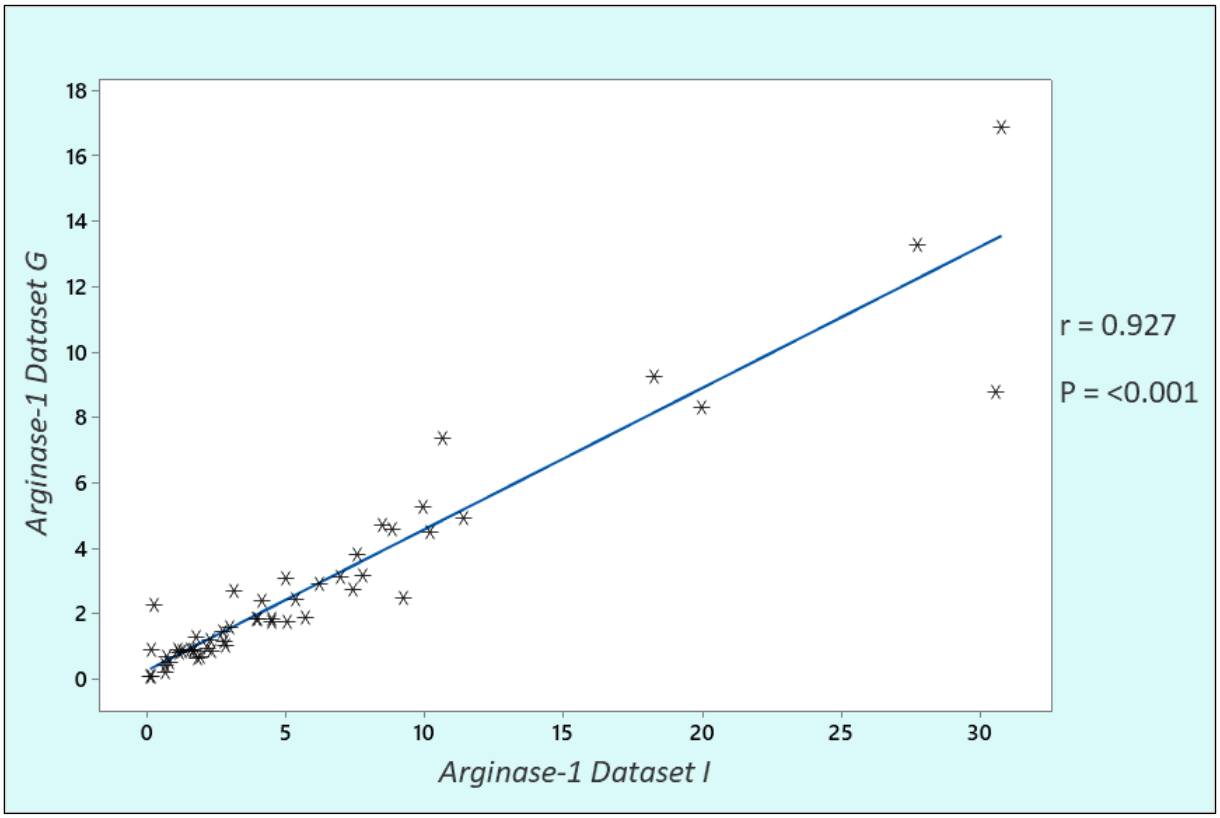

Figure 3.5: A correlation between Dataset G and Dataset I of lung tissue specifically stained for the presence of Arginase-1. Dataset G comprised data of percentage stain coverage as per the methodology Bajnok et al (2019) used, whereas Dataset I comprised percentage stain coverage divided by the proportion of lung tissue within the analysed image. This Figure determines whether there is a correlation between the two techniques. A strong positive correlation can be seen (r = 0.927; n = 51; P = <0.001) supporting the idea that both datasets align with each other, establishing reliability to this amended methodology.

These datasets were found to not to be of a normal distribution, and so the non-parametric Spearman's test was conducted as means of determining the correlation coefficient. A strong positive correlation was observed (r = 0.927; *P* = <0.001), meaning the datasets do align with each other. A Mann-Whitney test was also conducted and showed a significant difference (W = 2217.00; n = 51; *P* = 0.006). This, again, shows that the approach of Bajnok *et al* (2019) and the methods used here produce a consistent outcome (they are correlated) but the method used in this study is a significant improvement.

Lastly, Figure 3.6 summarises Dataset G versus Dataset I, for the slides stained for iNOS.

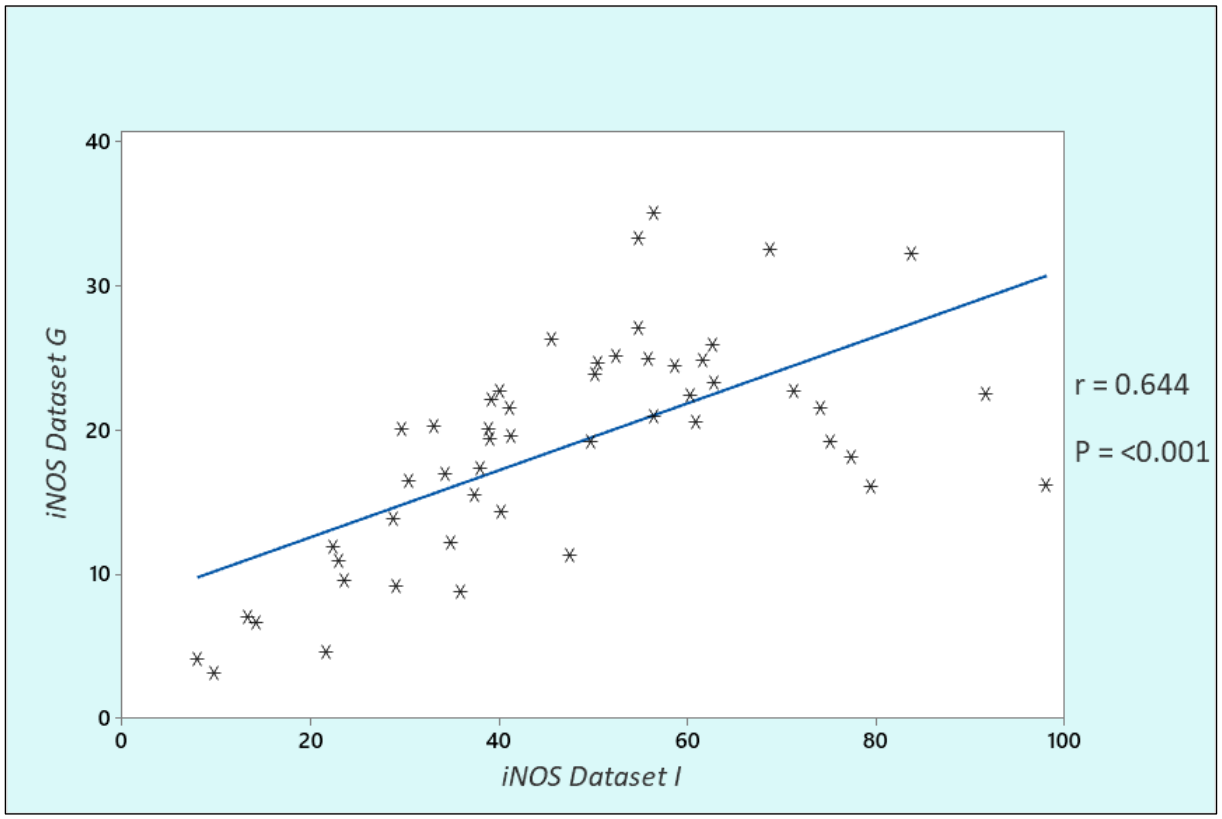

Figure 3.6: A correlation between Dataset G and Dataset I of lung tissue specifically stained for the presence of iNOS. Dataset G comprised data of percentage stain coverage as per the methodology Bajnok et al (2019) used, whereas Dataset I comprised percentage stain coverage divided by the proportion of lung tissue within the analysed image. This Figure determines whether there is a correlation between the two techniques. A moderate positive correlation can be seen (r = 0.644; n = 51; P = <0.001) supporting the idea that both datasets are aligned, in addition to establishing reliability to this amended methodology.

A Pearson's test determined a moderate correlation between Dataset G and Dataset I (r = 0.644; *P* = <0.001). A paired t-test also found a significant difference between the two datasets (t = -11.79; n = 51; *P* = <0.001). This would, again, infer that this amendment does impact the readings and still establishes consistency within the results set, thus can be considered an improvement to the methodology.

As shown in Figures 3.4, 3.5, and 3.6, these combined results all found a statistically significant difference in the two datasets yet also show that there is still the same alignment (a correlation) between them; and so unilaterally support the hypothesis that factoring in tissue coverage appears to make a difference to the results but also reflect the analytical methods employed by Bajnok *et al* (2019), be it *Toxoplasma gondii*, Arginase-1 or iNOS presence in these lung biopsy samples. Thus, the data with the correction for tissue coverage, namely Datasets C, D, I, and J will be used for all further ImageJ data analyses.

3.1.5 Development and use of scales for categorising spatial distribution and intensity of *T. gondii* infection and iNOS and Arginase-1 expression

The aim of this section was to investigate whether dividing *T. gondii* distribution into categories representing low medium and high intensities of infection enabled a better understanding of the relationship between infection and expression of iNOS and Arginase-1. To do this, a suitable categorisation system needed to be developed.

Bajnok *et al* (2019) had developed a methodology for categorising their ImageJ analysis results for the extent of *Toxoplasma gondii* presence and had allocated an infection grade dependent on the mean percentage of stain coverage. This grading system is outlined below:

- Grade 1: <10% coverage
- Grade 2: 10-20% coverage
- Grade 3: >20% coverage

The grading system generated by Bajnok *et al* (2019) was based on the measurement of the percentage of coverage of *T. gondii* staining and therefore did not take into account the instances where fields of view contained large areas of space (*e.g*. alveolar spaces *etc*.). Incorporating this aspect led to a much wider range of percentage coverage than that observed by Bajnok *et al* (2019). Therefore, a more suitable grading system is required that would more accommodate the revised analysis and could be applicable to datasets like dataset J. These amended grades are outlined below:

- Grade 1 (Low): <20% coverage
- Grade 2 (Moderate): 20-36% coverage
- Grade 3 (High): >36% coverage

The development of this improved *T. gondii* grading system meant that smaller groups of Dataset J could be analysed when calculating correlation coefficients, and these smaller groups may enable better opportunities to detect relationships by statistical analysis that larger data pools may not. Figure 3.7 shows the grading system of Bajnok et al (2019) using their original data and compares it with dataset J as analysed in this study. The larger number of higher percentage samples found in dataset J are not adequately expanded under the

system of Bajnok *et al* (2019). Too many fell into grade 3 and are therefore not well discriminated. The new system expands the higher percentage categories into more grades.

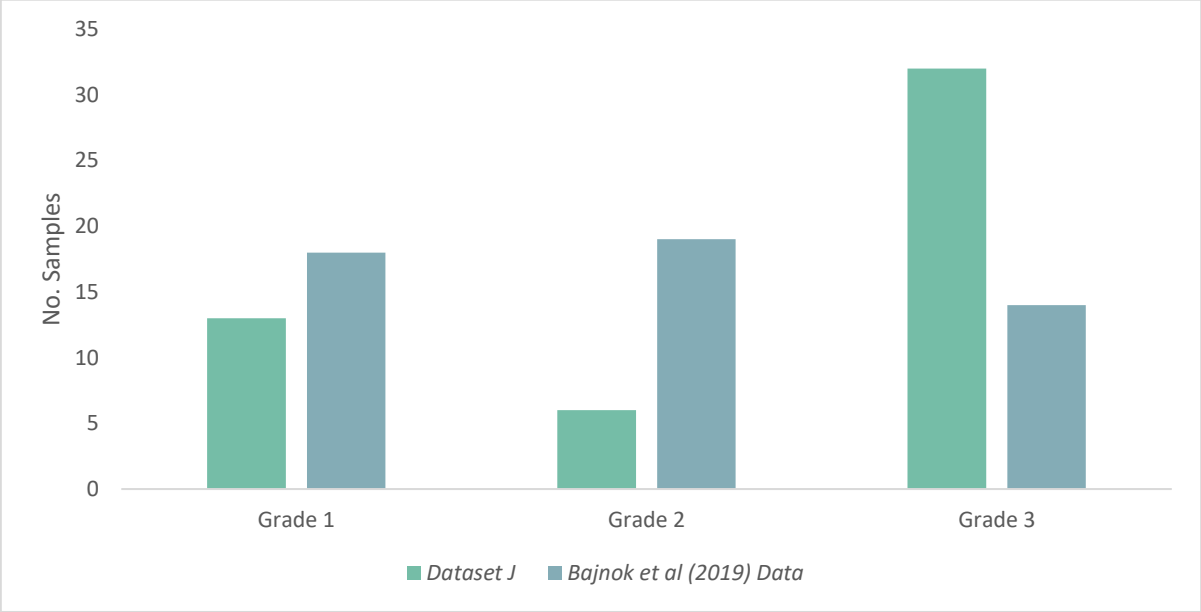

Figure 3.7: A comparison of the number of samples from Dataset J and those of Bajnok et al (2019) when categorised into their infection grades as defined by Bajnok et al (2019). Samples with <10% stain coverage were classified as grade 1, 10-20% stain coverage classified as grade 2, and >20% stain coverage classified as grade 3 infection. As shown, Dataset J are not evenly distributed and are overrepresented in Grade 3.

Having established a new grading system that better categorised Dataset J into categories, it was possible to investigate the relationship between iNOS and Arginase-1 expression within the categories.

To explore the relationship between *T. gondii* distribution and Arginase-1 expression, samples were categorised as the revised grades 1, 2 and 3 as described above. Each grade was compared separately to investigate any correlations between infection and Arginase-1 expression for each grade.

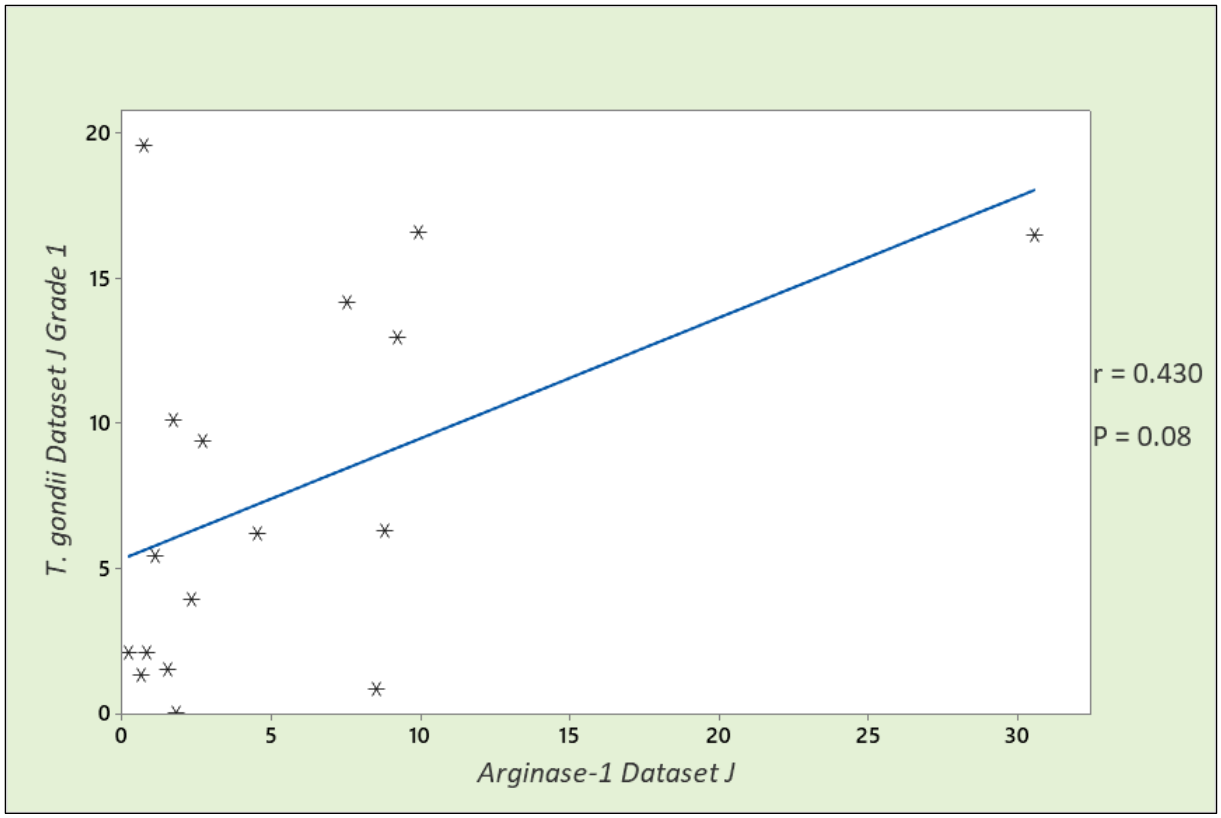

Figure 3.8: A scattergram of Toxoplasma gondii and Arginase-1 percentage coverage of staining for samples in Dataset J that were categorised as having a Grade 1 (low) infection. As shown (r = 0.430; n = 17; P = 0.08), approaching significance is a weak positive correlation between the extent of Arginase-1 staining and Toxoplasma gondii staining for the samples categorised as being Grade 1 infected.

Figure 3.8 shows the relationship between Arginase-1 staining compared to the staining coverage of *T. gondii* from Dataset J in samples that were categorised as a Grade 1 (low) infection. This data was found not normally distributed and so the non-parametric Spearman's correlation test was used. There is no significant correlation between *T. gondii* and Arginase-1 in these Grade 1 samples of Dataset J (r = 0.430; n = 17; *P* = 0.08). However, a weak positive correlation was seen (r = 0.430) which had this achieved a coefficient of 0.488, would have been significant (*P* = < 0.05) for this sample number (n = 17).

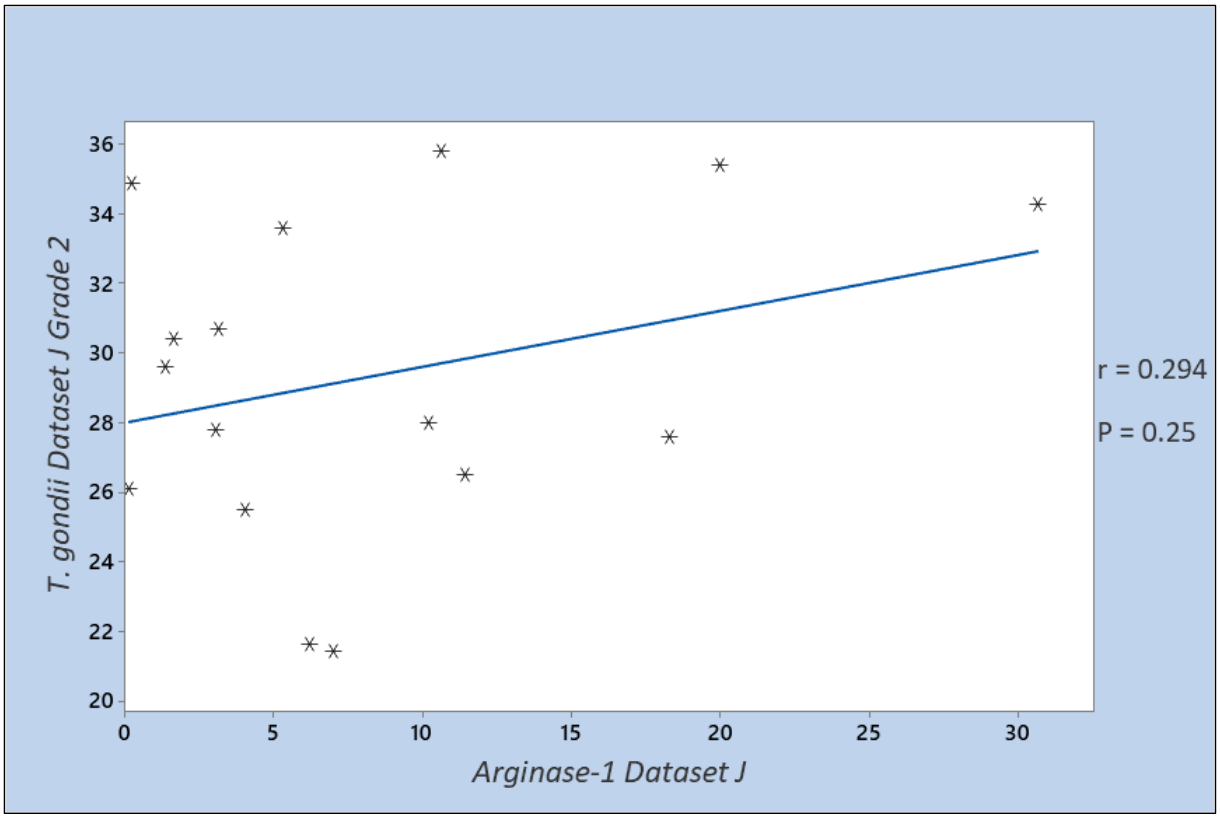

Figure 3.9: A scattergram of Toxoplasma gondii and Arginase-1 percentage coverage of staining for samples in Dataset J that were categorised as having a Grade 2 (moderate) infection. As illustrated above (r = 0.294; n = 16; P = 0.25), no correlation could be determined between the extent of Arginase-1 staining and extent of Toxoplasma gondii staining for the samples categorised as being Grade 2 infected.

Figure 3.9 shows the relationship of Arginase-1 staining with *T. gondii* distribution from Dataset J that were deemed to have a Grade 2 (moderate) infection. This data was found to be normally distributed and therefore the parametric Pearson's correlation test was conducted. There was no correlation between *T. gondii* and Arginase-1 in these Grade 2 samples of Dataset J (r = 0.294; n = 16; *P* = 0.25).

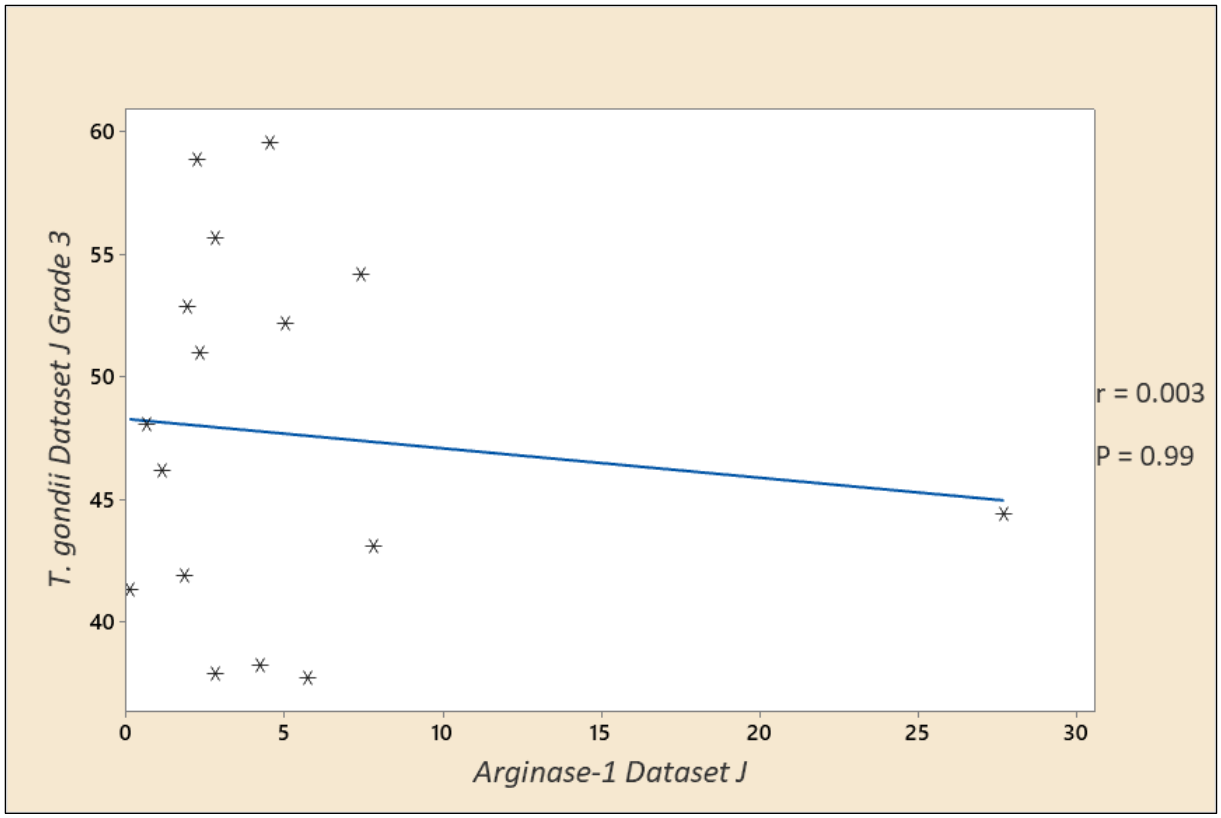

Figure 3.10: A scattergram of Toxoplasma gondii and Arginase-1 percentage coverage of staining for samples in Dataset J that were categorised as having a Grade 3 (High) infection. As shown (r = 0.003; n = 16; P = 0.99), there appears to be no correlation between the extent of Arginase-1 staining and extent of Toxoplasma gondii staining for the samples categorised as being Grade 3 infected. It is also evident that the linear regression fit does not align with the r value obtained from the Spearman's rho (i.e the slope should not be downward sloping). This may have been caused by skewing from the outlier Arginase-1 result.

Figure 3.10 shows the relationship between Arginase-1 staining and *T. gondii* distribution from Dataset J that were deemed to have a Grade 3 (high) infection. This data was found not to be normally distributed and so the non-parametric Spearman's correlation test was used. There was no correlation between *T. gondii* and Arginase-1 staining in these Grade 3 samples of Dataset J (r= 0.003; n = 16; *P* = 0.99). Within this figure it is apparent that the gradient of the linear regression line does not align with the Spearman's coefficient of r = 0.003 (*i.e.,* the gradient should be almost horizontally straight). It may be that the outlying Arginase-1 reading is skewing this finding, it may also be skewing the correlation coefficient. Therefore, it was decided to repeat this statistical analysis on this dataset, with the 1 outlier reading removed. Figure 3.11 demonstrates the impact on the correlation coefficient and linear

regression with this omission. As shown, the correlation coefficient is in alignment with the linear regression, and additionally, removal of the outlier reading has more strongly supported there being no correlation between *T. gondii* and Arginase-1 presence (r = 0.018; n = 15; *P* = 0.95) in these grade 3 categorised infected samples.

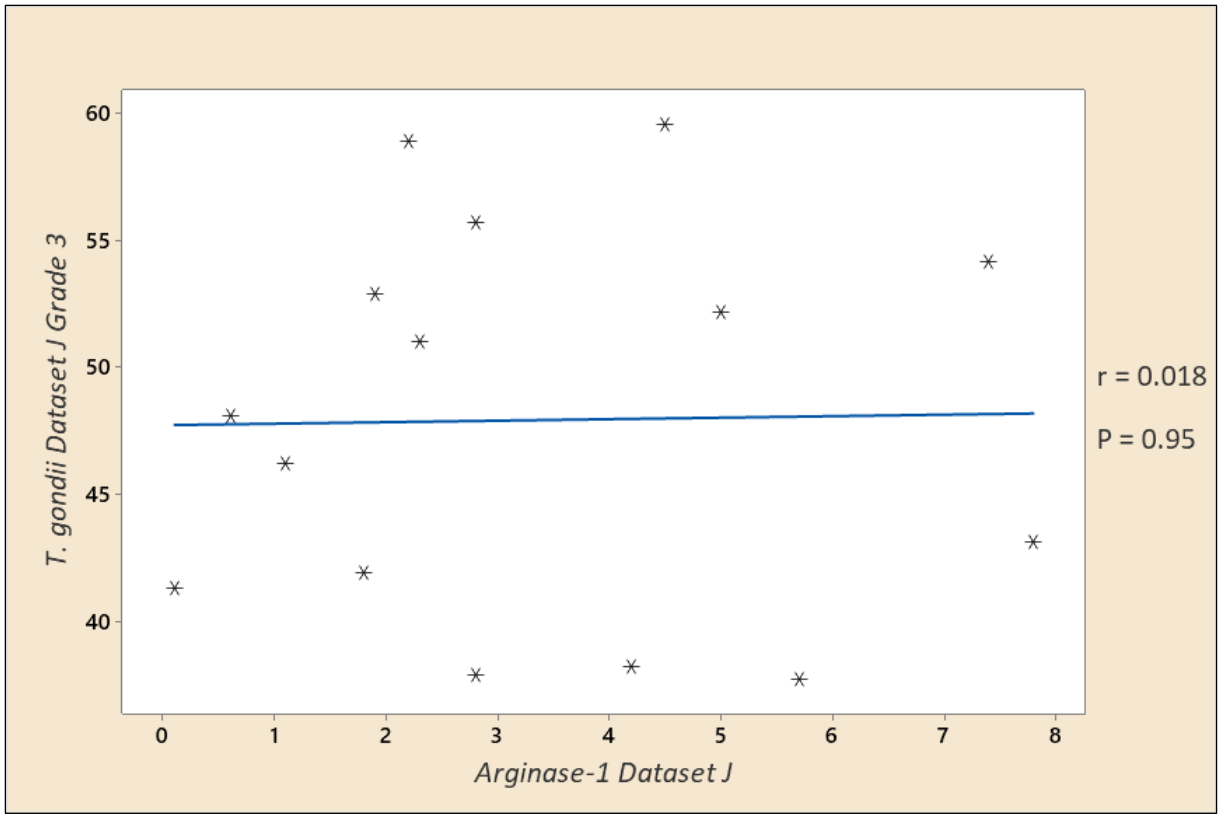

Figure 3.11: A scatterplot of the stain coverage of lung biopsy tissue specifically stained for the presence of Toxoplasma gondii and Arginase-1, with omission of 1 outlier reading. Dataset J was utilised for this analysis, identical to Figure 3.10, but without outlying Arginase-1 reading. As shown (r = 0.018; n = 15; P = 0.95), removal of this outlying result further supports there being no correlation between the staining distribution of T. gondii and that of Arginase-1 in the grade 3 categorised samples.

Figures 3.8, 3.9, 3.10, and 3.11 illustrate the expression of Arginase-1 alongside *Toxoplasma gondii* infection in the three infection intensity grades. As shown, the findings are varied. Grade 2 and 3 identified samples have no correlating relationship between *T. gondii* and Arginase-1 presence. However, the Grade 1 samples, although showing no significant correlation between *T. gondii* and Arginase-1 staining had a co-efficient of correlation that was approaching significance.

To examine the relationship between *T. gondii* distribution and iNOS expression, samples were categorised using the revised grades 1, 2 and 3. Each grade was compared separately to investigate any correlations between infection and iNOS expression using the correlation coefficients within the three defined infection gradients.

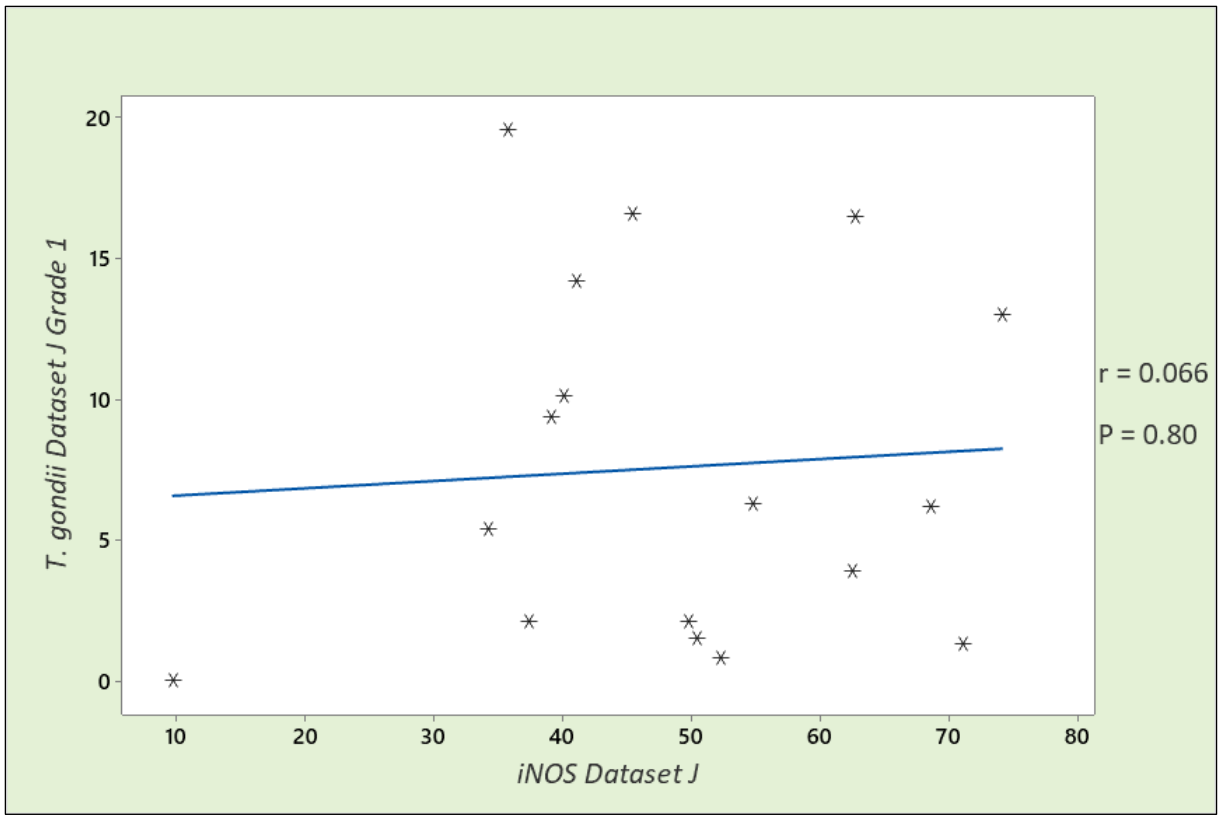

Figure 3.12: A scattergram of Toxoplasma gondii and iNOS percentage coverage of staining for samples in Dataset J that were categorised as having a Grade 1 (low) infection. As shown by the regression line and the Pearson's coefficient of 0.066 (n = 17; P = 0.80), there appears to be no correlation between the extent of iNOS staining and extent of Toxoplasma gondii staining for the samples categorised as being Grade 1 infected.

Figure 3.12 shows the comparison of iNOS staining with of *T. gondii* distribution using samples from Dataset J that were classified as having a Grade 1 (low) infection. This data was found to be normally distributed and the parametric Pearson's correlation test was used. No significant correlation was found between *T. gondii* and iNOS in these Grade 1 samples of Dataset J (r= 0.066; n = 17; *P* = 0.80).

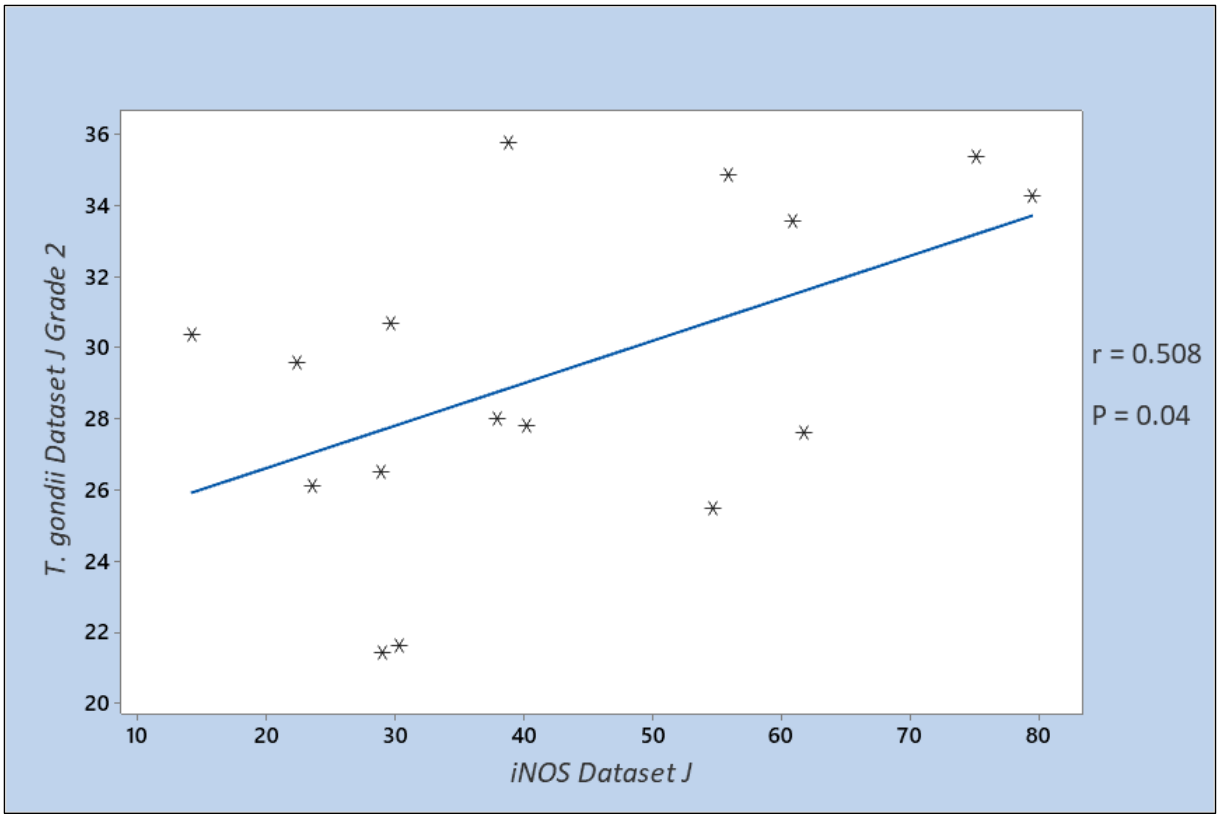

Figure 3.13: A scatterplot of Toxoplasma gondii and iNOS percentage coverage of staining for samples in Dataset J that were categorised as having a Grade 2 (moderate) infection. As shown by the regression line and the Pearson's coefficient of 0.508 (n = 16; P = 0.04), there appears to be a significant moderate positive correlation between the extent of iNOS staining and extent of Toxoplasma gondii staining for the samples categorised as being Grade 2 infected.

Figure 3.13 shows the comparison of iNOS staining alongside the readings with *T. gondii* distribution using samples from Dataset J that were deemed to have a Grade 2 (moderate) infection. This data was found to be normally distributed and therefore the parametric Pearson's correlation test was used. There was a significant positive correlation between *T. gondii* distribution and iNOS in these Grade 2 samples of Dataset J (r = 0.508; n = 16; *P* = 0.04).

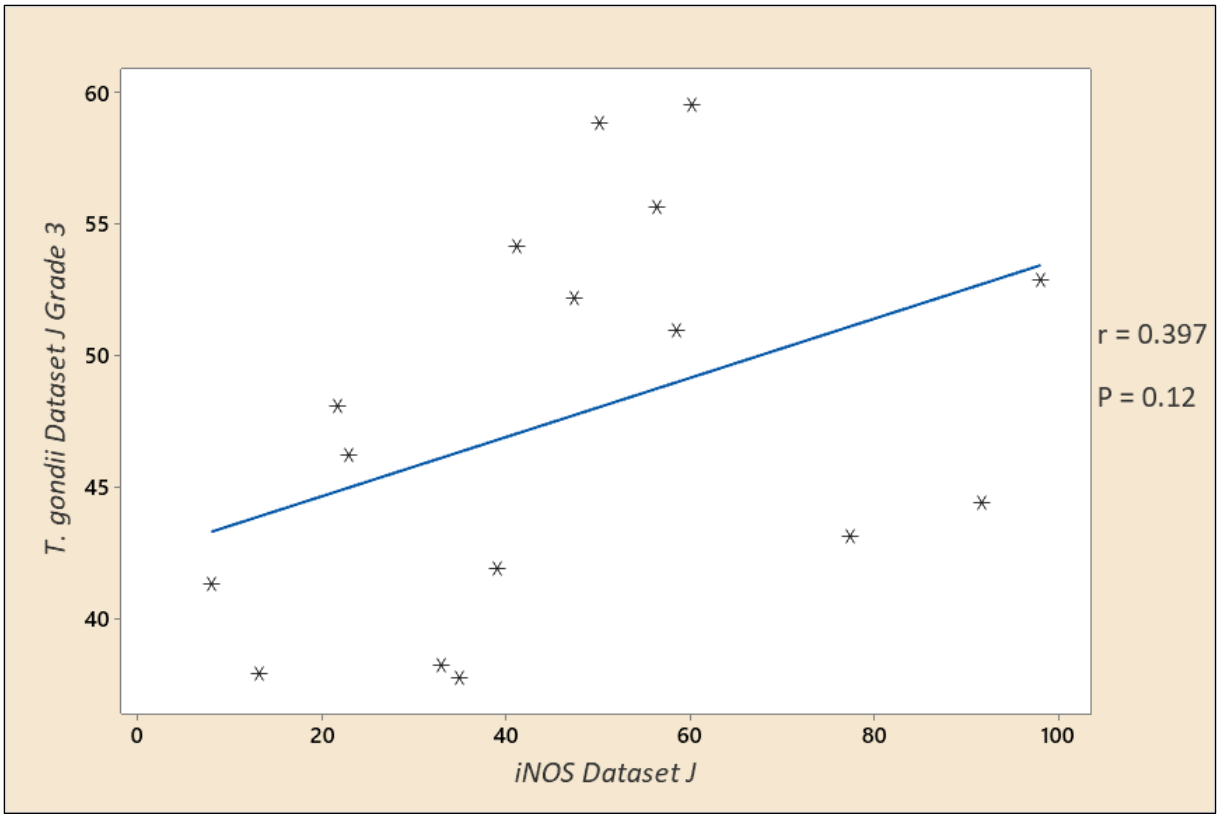

Figure 3.14: A scatterplot of Toxoplasma gondii and iNOS percentage coverage of staining for samples in Dataset J that were categorised as having a Grade 3 (high) infection. As shown by the regression line and the Pearson's coefficient of 0.397 (n = 16; P = 0.12), there appears to be no correlation between the extent of iNOS staining and extent of Toxoplasma gondii staining for the samples categorised as being Grade 3 infected.

Figure 3.14 shows the comparison of iNOS staining with *T. gondii* distribution from Dataset J samples that were deemed to have a Grade 3 (high) infection. This data was found to be normally distributed and so the parametric Pearson's correlation test was used. There was no significant correlation between *T. gondii* and iNOS in these Grade 2 samples of Dataset J (r= 0.397; n = 16; *P* = 0.12).

Figures 3.12, 3.13, and 3.14 illustrate the expression of iNOS alongside *Toxoplasma gondii* infection in the three infection intensity grades. There were no significant correlations between *T. gondii* distribution and iNOS expression in the low- or high-grade *T. gondii* infected samples. However, there was a positive correlation between *Toxoplasma gondii* and iNOS expression in the samples deemed to have a moderate infection grade.

3.2 Analysis of colocalization and coexpression of *T. gondii* with iNOS and Arginase-1

3.2.1 Measurement of spatial overlap of *T. gondii* infection with iNOS and Arginase-1 expression

Following the pilot study, quantification was used to measure spatial overlap of *T. gondii* infection with the expression of Arginase-1 and iNOS at varying degrees of specificity. This subsection uses Datasets D, E, and J to ascertain whether a correlation can be found between *Toxoplasma gondii* infection and how Arginase-1 and iNOS are expressed in these lung tissue samples.

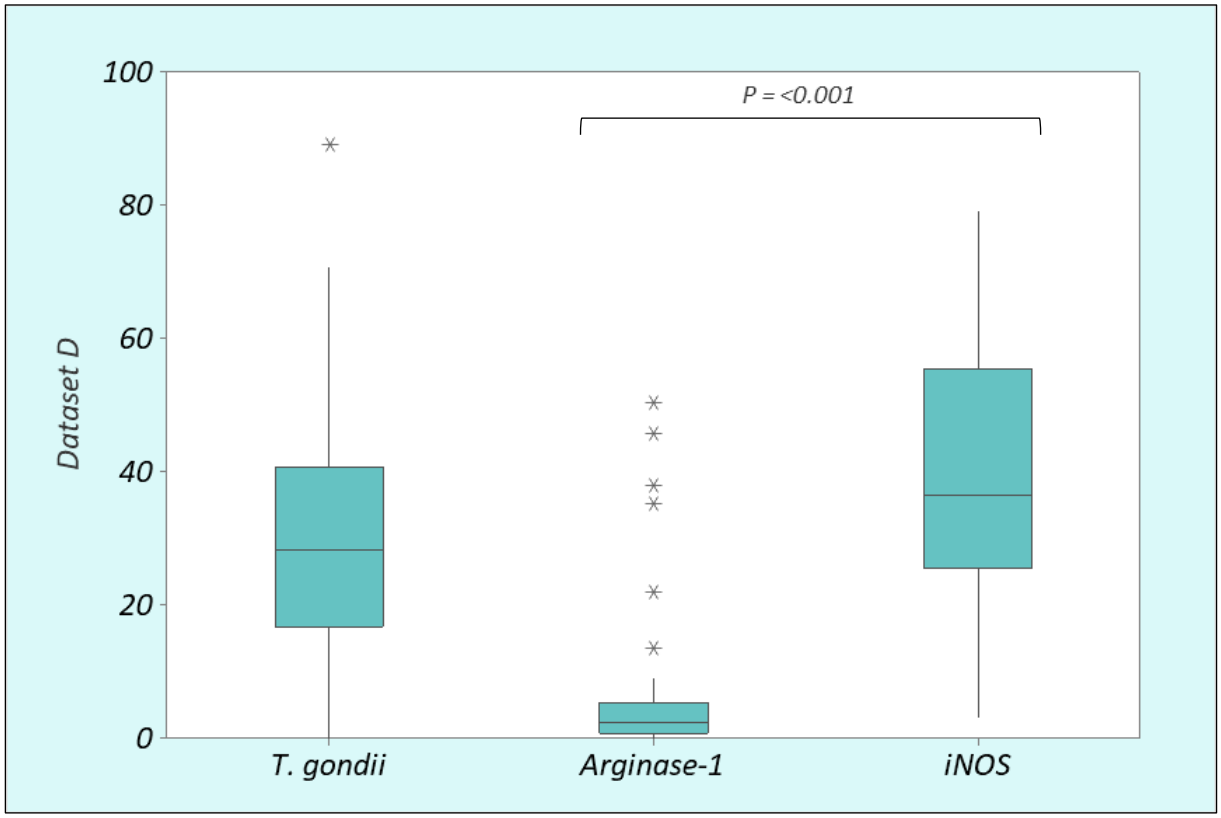

Figure 3.15: Summary of the range and median of Dataset D. This dataset entailed the percentage of stain coverage for lung biopsy samples, specifically stained for the presence of Toxoplasma gondii, iNOS and Arginase-1. These were calculated through ImageJ analysis of photos taken on three separate sections of each sample at the same field of view. Outlying readings are marked with asterisks. As shown, Arginase-1 expression is very minimal, unlike iNOS of which is expressed significantly (P = <0.001) more highly and at a larger range of variability. Similarly, the extent of Toxoplasma gondii infection is very variable.

Figure 3.15 shows an analysis of Dataset D, which entailed ImageJ analysis from matching sets of fields of view from slide sections (n=48). As shown, Arginase-1 expression is minimal, whereas iNOS is expressed far more extensively and with a much larger range of proportions across the different samples. There is a significant difference between the spatial expression levels of iNOS and Arginase-1 (P= <0.001) *Toxoplasma gondii* spatial distribution, in fields of view, was high and showed considerable variation between different lung samples.

Figure 3.16 and Figure 3.17 show scattergrams of the percentage of stain coverage, for each slide, for both the *Toxoplasma gondii* and Arginase-1., using Dataset J (randomised fields of view) and Dataset D (matched fields of view), respectively. Dataset J provides an overall pooled average of the staining proportions for all the samples, as opposed to Dataset D of which is more specific to a single region of each lung tissue sample. Both datasets were plotted on a scatterplot and a correlation coefficient was calculated to ascertain whether any correlating relationship could be found between *Toxoplasma gondii* distribution and Arginase-1 expression for the two separate analyses of Datasets J and D. Both scatterplots show the expression of Arginase-1 as tending to be low with a few outlier heavier readings. The extent of *Toxoplasma gondii* infection is very variable for both also.

As shown in Figure 3.16, there is no correlation between the two in this scatterplot ($r = 0.077$; $n = 49$; $P = 0.60$). A Spearman's correlation coefficient was calculated as the Arginase-1 data of Dataset J is not normally distributed. This shows that there is no correlation between the percentage coverage of *Toxoplasma gondii* staining with the coverage of Arginase-1 staining for Dataset J.

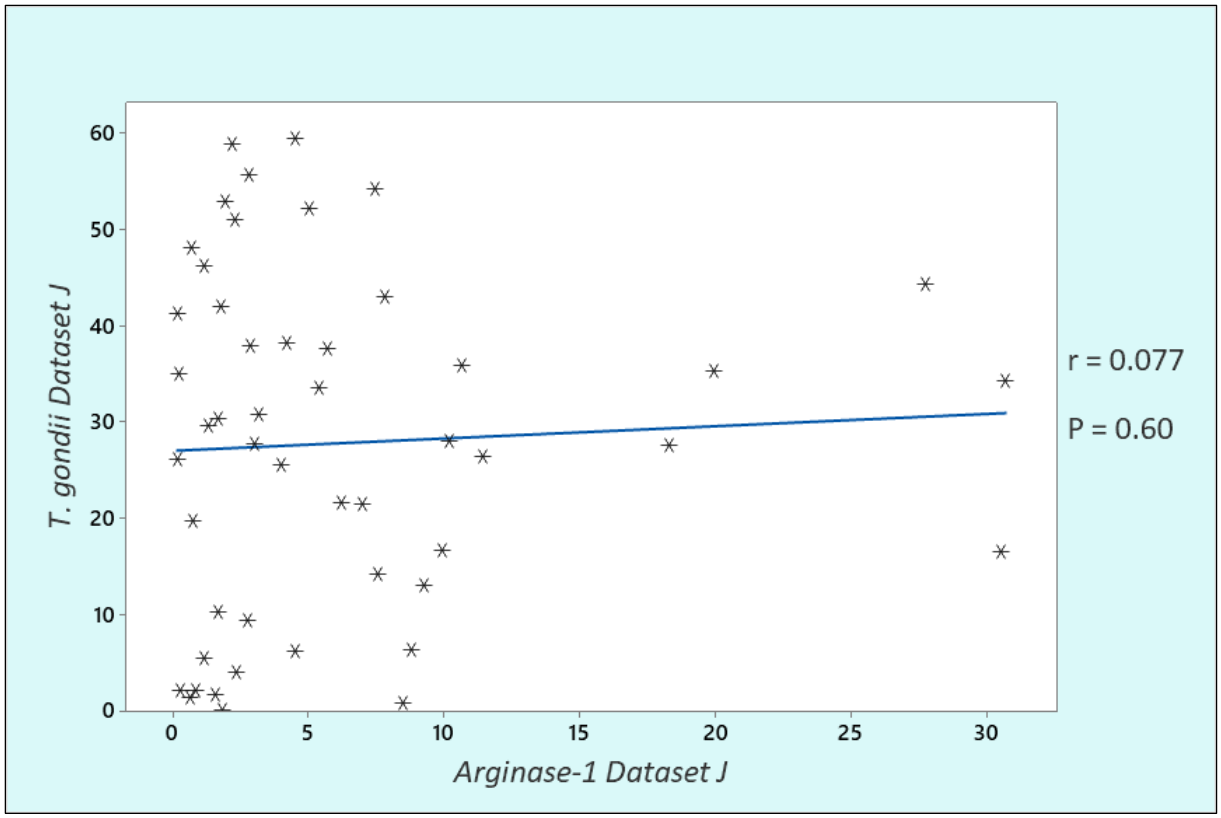

Figure 3.16: A scatterplot of the stain coverage of lung biopsy tissue specifically stained for the presence of Toxoplasma gondii and Arginase-1. This data was extracted from Dataset J, from images taken at randomised fields of view. As shown (r = 0.077; n = 49; P = 0.60) there was no correlation between the T. gondii staining and the expression of Arginase-1.

Figure 3.17 shows the relationship of *Toxoplasma gondii* staining with Arginase-1 coverage in Dataset D. Although similar to Figure 3.16 and dataset J; Dataset D was taken from the matched images, and so offered a more specific analysis of regions of the lung tissue to look for any noticeable patterns between Arginase-1 and *T. gondii* occurrence. As was found with Dataset J in Figure 3.16, there is no relationship between the two in this scatterplot (r = 0.133; n = 48; *P* = 0.36). (Dataset J like dataset D, was non-parametric and hence the use of Spearman's correlation co-efficient). This again showed no correlation between the distribution of *Toxoplasma gondii* staining and the distribution of Arginase-1.

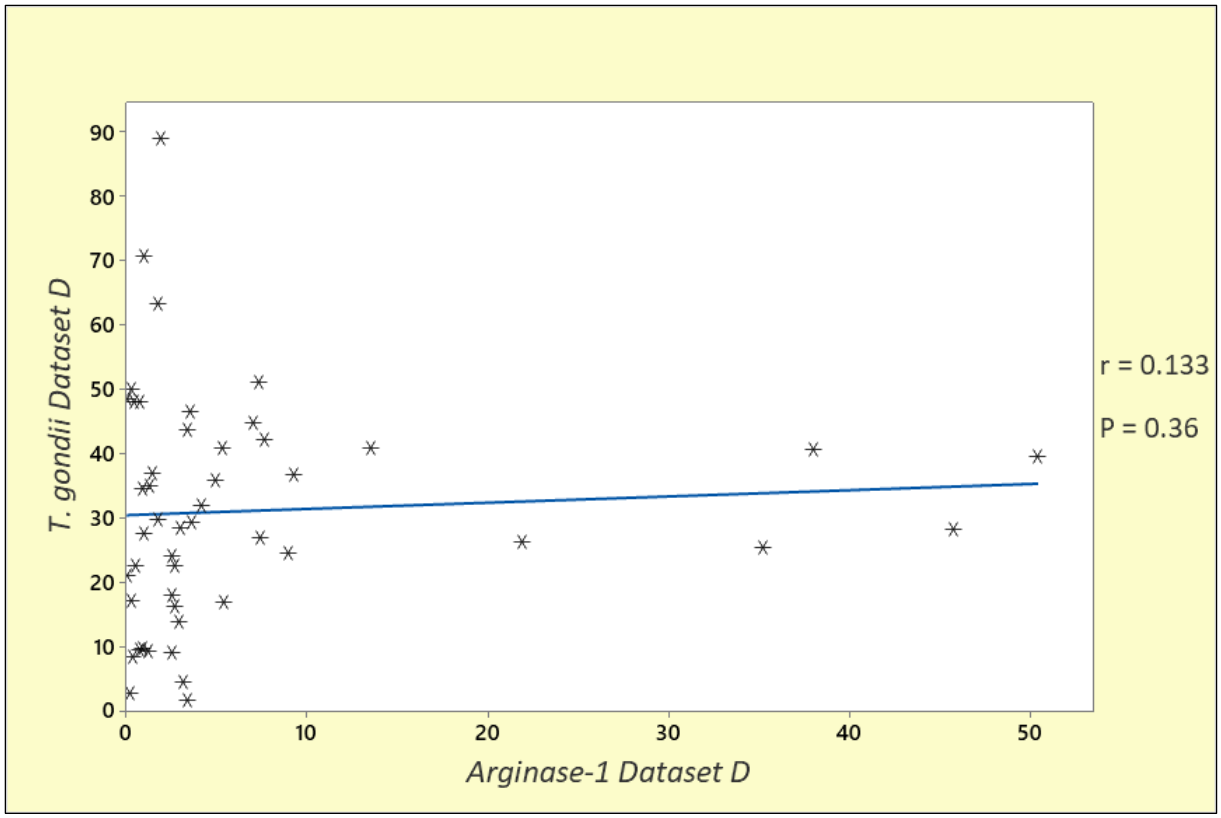

Figure 3.17: A scatterplot of the stain coverage of lung biopsy tissue specifically stained for the presence of Toxoplasma gondii and Arginase-1. This data was extracted from Dataset D, of which was taken from the paired images. As shown (r = 0.133; n = 48; P = 0.36) there is no relationship between the coverage of Arginase-1 expression and coverage of T. gondii infection staining.

Evident in the Figure 3.17 scatterplot were the six outlier Arginase-1 readings (>10% stain coverage). Concern was raised that this may be skewing the results and thus it was deemed necessary to repeat this statistical analysis on the dataset, with these 6 outlier readings removed. Figure 3.18 demonstrates the impact on the correlation coefficient with omission of those readings. As shown (r = 0.099; n = 42; *P* = 0.53), there remains no correlation between the extent of *T. gondii* and Arginase-1 specific staining.

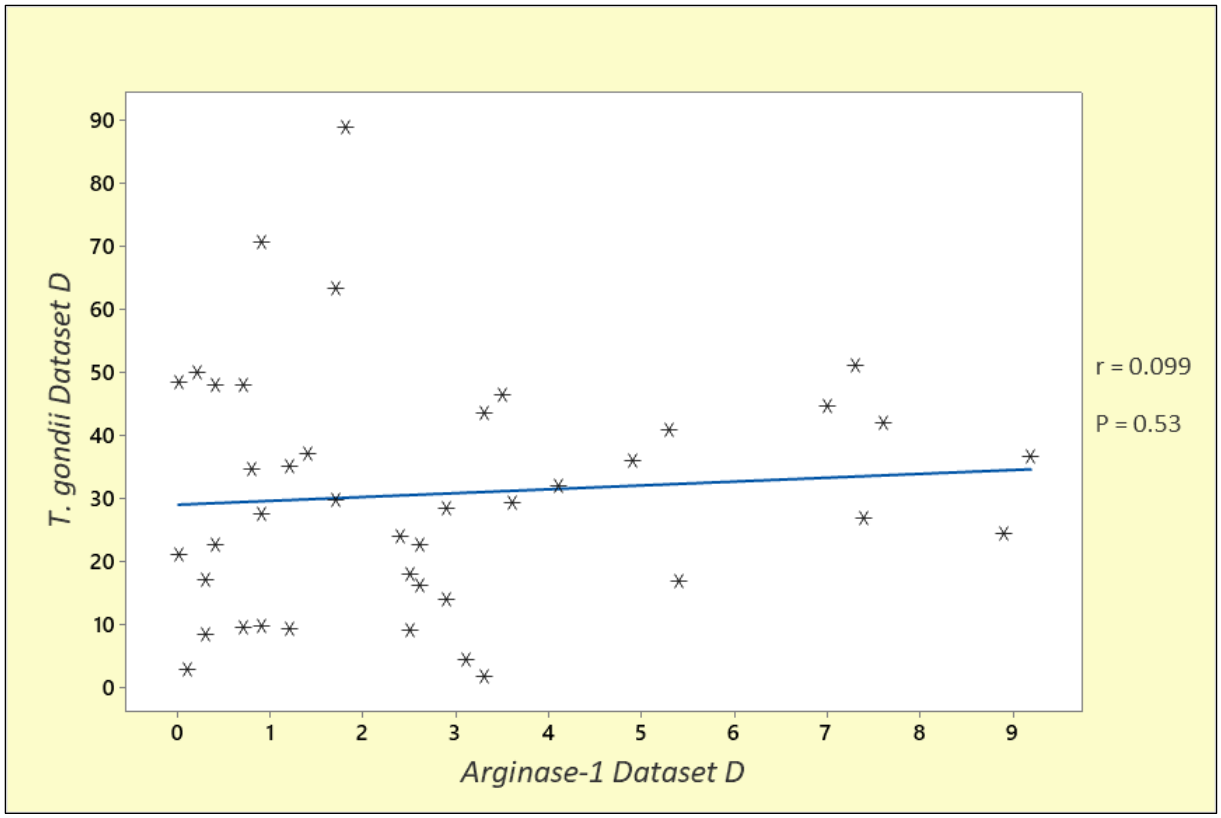

Figure 3.18: A scatterplot of the stain coverage of lung biopsy tissue specifically stained for the presence of Toxoplasma gondii and Arginase-1, with omission of 6 outlier readings. Dataset D was utilised for this analysis, identical to Figure 3.17, but with 6 outlying Arginase-1 readings removed. As shown (r = 0.099; n= 42; P = 0.53), removal of these anomalous results further supports there being no correlation between the staining distribution of T. gondii and Arginase-1.

In order to explore the degree of co-occurrence of Arginase-1 expression and *T. gondii* distribution in more detail, an analysis of the intensity of staining of both was carried out using grids within the fields of view. Dataset E (Table 3.1) was utilised to address this as it comprised the analysis of overlayered specific grid coordinates on each of overlapping matched images. The results are shown in Figures 3.19 and 3.20.

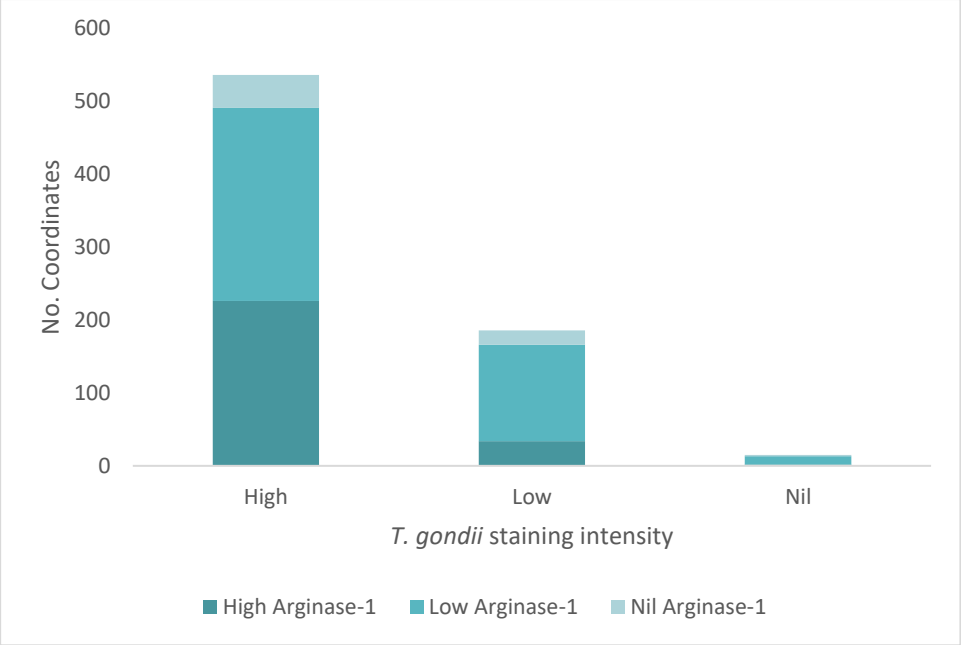

Figure 3.19: A comparison of T. gondii and Arginase-1 intensity of staining in paired images taken at the same field of view. The intensity of staining was designated in grid coordinates of lung tissue specifically stained for the presence of T. gondii and Arginase-1 separately. Coordinates were deemed to have high, low, and no level of specific staining. This data is taken from the Dataset E. As shown above, in coordinates that were found to have high intensity of T. gondii presence, Arginase-1 was expressed more highly, proportionally, than in coordinates with lower or no T. gondii specific staining. Illustrated here is also how Arginase-1 has a tendency towards low expression throughout these lung tissue samples.

Figure 3.19 illustrates the intensity of Arginase-1 staining in grid coordinates that were deemed to have a high, low, and nil intensity of T. gondii specific staining. As shown, Arginase-1 specific staining appears to be more intense, proportionally, in grid coordinates that also have high intensity of *T. gondii* specific staining. To further investigate these findings, categories low and nil were combined. This would allow for more accurate statistical analysis to take place by means of a Fisher's Exact test. This would determine whether a significant difference exists between the intensity of Arginase-1 staining in grid coordinates categorised as having high or low to no *T. gondii* specific staining. This data is presented in Figure 3.20.

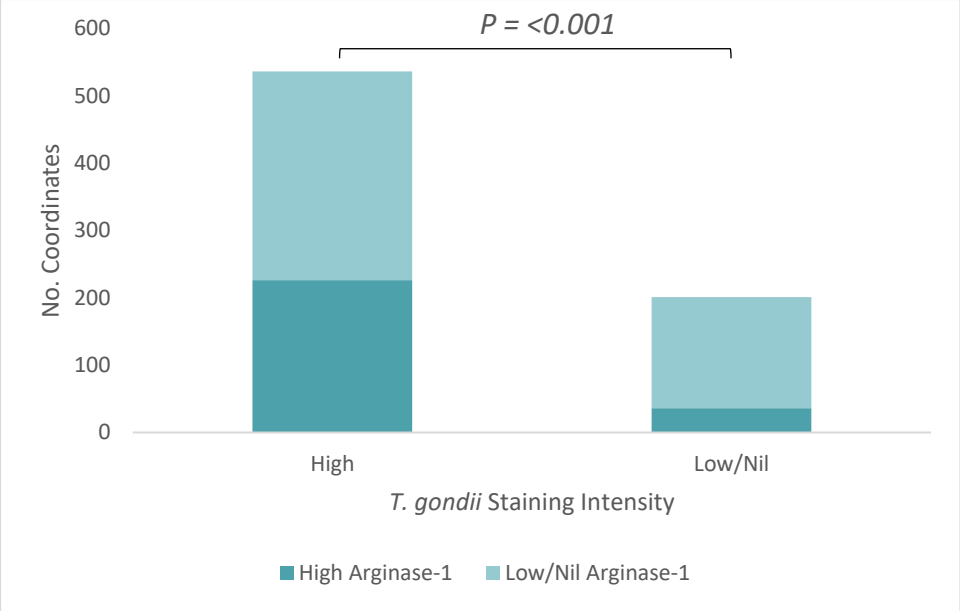

Figure 3.20: A comparison of T. gondii and Arginase-1 intensity of staining in paired images taken at the same field of view. The intensity of staining was designated in grid coordinates of lung tissue specifically stained for the presence of T. gondii and Arginase-1 separately. Coordinates were deemed to have high, low, and no level of specific staining. This data is taken from the Dataset E and is identical to that presented in Figure 3.11, but the low and nil categories are combined. The data was combined to allow for a Fisher's Exact test to be calculated. As shown above (P = <0.001), there is a significant positive association between the intensity of Arginase-1 staining and that of T. gondii specific staining. Arginase-1 was expressed proportionally more highly than in the coordinates with high T. gondii specific staining.

The findings from Dataset E, as expressed in Figure 3.20, indicate a significant difference (*P* = <0.001) in the intensity of Arginase-1 specific staining in coordinates of high compared with low/nil intensity of *T. gondii* specific staining. To conclude, it appears that Arginase-1 has an increased tendency towards higher intensity staining in areas of higher intensity of *T. gondii* staining. However, this does not contradict other findings as it is evident throughout that Arginase-1 is most frequently expressed at a low intensity.

This marks the end of the *Toxoplasma gondii* and Arginase-1 correlative analysis. Next the analysis will focus on *T. gondii* and whether it correlates with the spatial distribution of the other immunomodulating protein, iNOS.

In order to investigate whether there is an association (positive or negative) between iNOS expression and *T. gondii* distribution, similar analyses to those used for Arginase-1 datasets,

were conducted with *T. gondii* and iNOS. Scattergrams were constructed that showed the percentage of stain coverage, for each slide, for both *Toxoplasma gondii* and iNOS, using Dataset J (randomised fields of view) and Dataset D (matched fields of view), respectively. Dataset J provides an overall pooled average of the staining proportions for all the samples, as opposed to Dataset D of which is more specific to a single region of each lung tissue sample. Both datasets were plotted on a scatterplot and a correlation coefficient was calculated to ascertain whether any correlating relationship could be found between *Toxoplasma gondii* distribution and iNOS expression for the two separate analyses of Datasets J and D. The scattergrams undertaken on the ImageJ data of Dataset J and Dataset D of the randomised and matched photos are shown in figure 3.21 and 3.22 respectively.

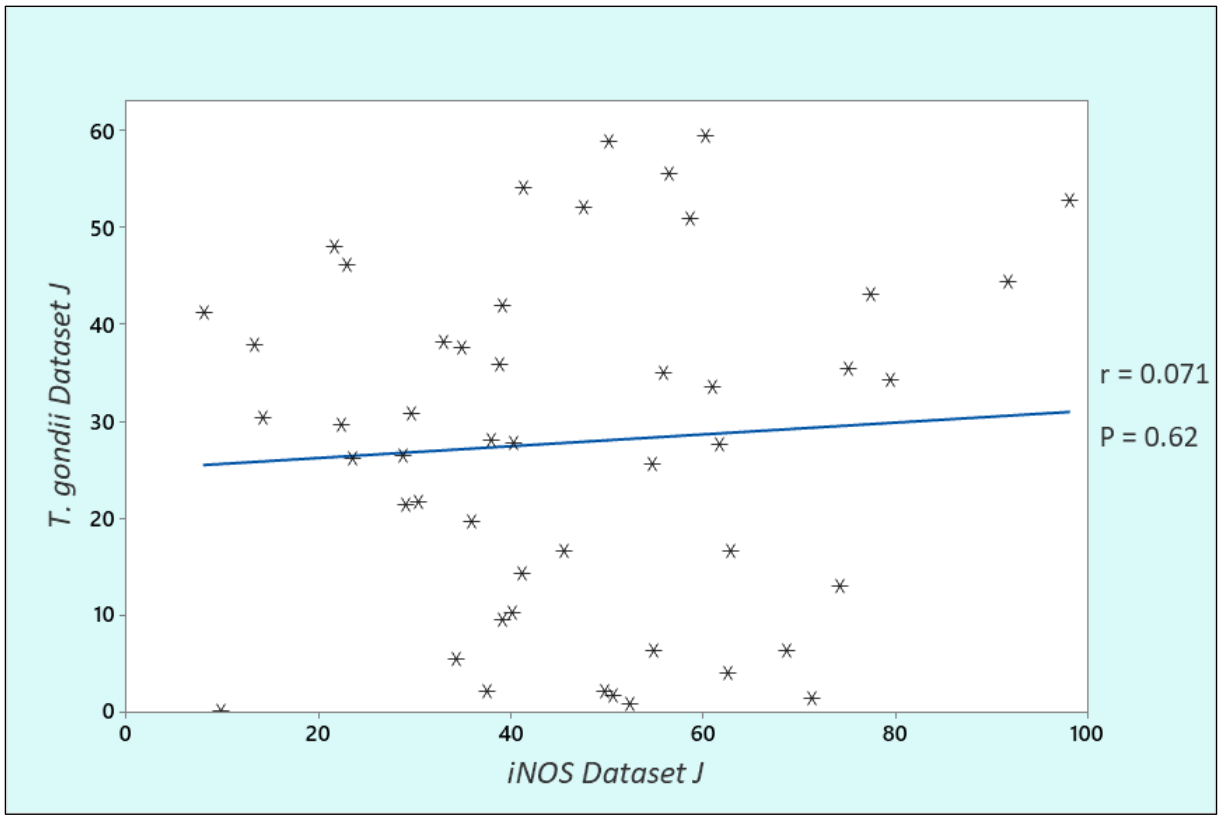

Figure 3.21: A scatterplot of the staining coverage of lung biopsy tissue specifically stained for the presence of Toxoplasma gondii and iNOS. This data was extracted from Dataset J. As shown, (r = 0.071; n = 49; P = 0.62) no correlation can be found between the extent of iNOS specific staining and that of T. gondii.

Figure 3.21 shows the extent of *Toxoplasma gondii* specific staining compared to that of iNOS within Dataset J. Both pieces of data were found to be normally distributed, and so the parametric correlation Pearson's test was performed. As illustrated, there appears to be no correlation between the expression of iNOS and the degree of infection by *Toxoplasma gondii* in this scatterplot (r = 0.236; n = 49; *P* = 0.62).

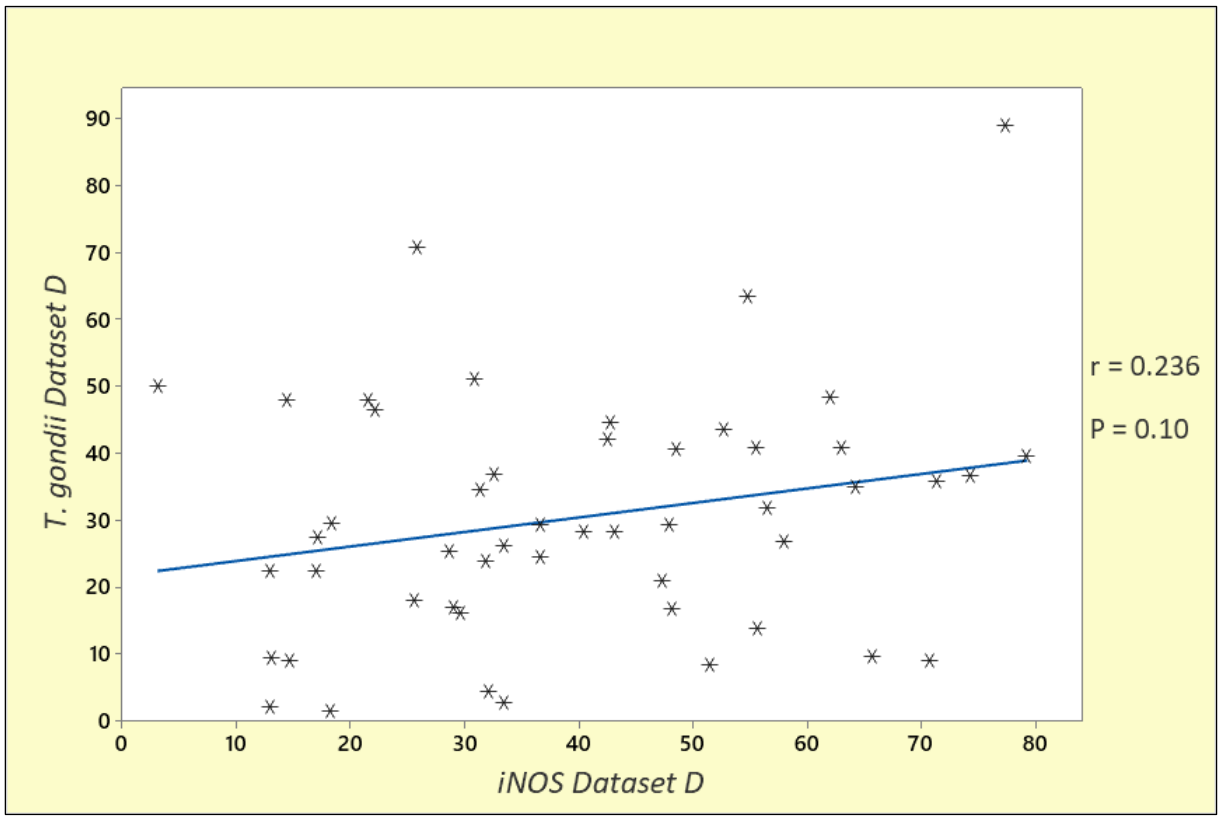

Figure 3.22: A scatterplot of the staining coverage of lung biopsy tissue specifically stained for the presence of Toxoplasma gondii and iNOS. This data was extracted from Dataset D, which was taken from paired images. As shown (r = 0.236; n = 50; P = 0.10) there appears to be no relationship between the extent of iNOS expression and the extent of T. gondii staining.

Figure 3.22 shows the extent of *Toxoplasma gondii* staining compared to that of iNOS in Dataset D. Although similar to Figure 3.21 and dataset J; Dataset D was taken from the matched images, and so offered a more specific analysis of regions of lung tissue to look for any noticeable patterns between iNOS and *T. gondii* occurrence. There is no association between *T. Gondii* distribution and iNOS expression with a Pearson's correlation coefficient

of 0.236 (n= 50; *P* = 0.10). (Both *T. gondii* and iNOS values in Dataset D were normally distributed and so the parametric correlation Pearson's test was used).

In order to explore the degree of co-occurrence of iNOS expression and *T. gondii* distribution in more detail, an analysis of the intensity of staining of both was carried out using grids within the fields of view. Dataset E (Table 3.1) was utilised to address this as it comprised the analysis of overlayered specific grid coordinates on each of overlapping matched images. The results are shown in Figures 3.23 and 3.24.

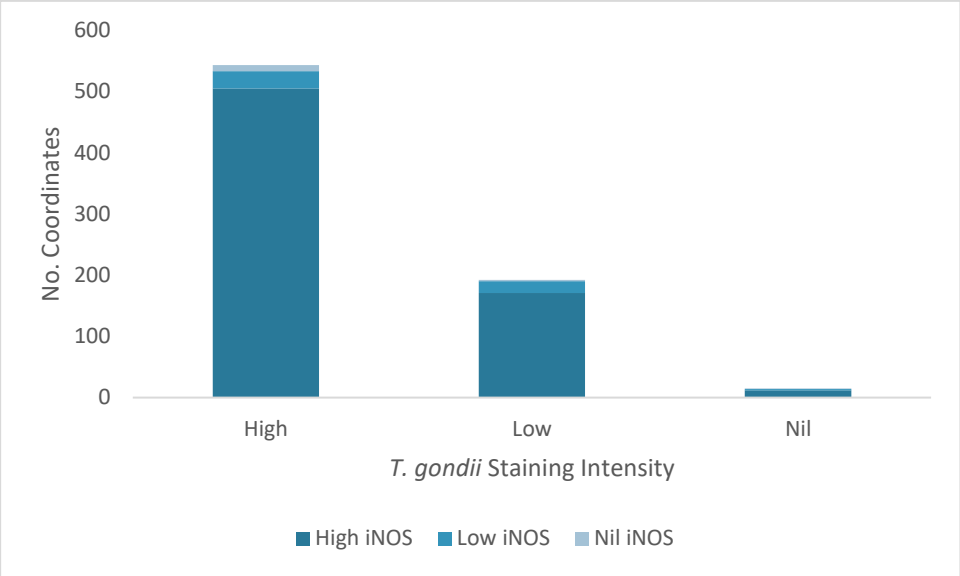

Figure 3.23: A comparison of T. gondii and the intensity of staining of iNOS in paired images taken at the same field of view. The intensity of staining was designated in grid coordinates of lung tissue specifically stained for the presence of T. gondii and iNOS. Coordinates were deemed to have high, low, and no level of specific staining. This data is taken from the Dataset E. As shown above, staining intensity is high throughout these lung tissue samples, seemingly independent of the intensity of T. gondii specific staining.

Figure 3.23 illustrates the intensity of iNOS staining in grid coordinates that were deemed to have a high, low, and nil intensity of T. gondii specific staining. As shown, iNOS specific staining appears to be high, independent of the intensity of *T. gondii* specific staining in the grid coordinates. To further investigate these findings, categories low and nil were combined. This allowed for the more accurate Fisher's Exact test to be conducted. This would determine

whether a significant association exists between the intensity of iNOS staining in grid coordinates categorised as having high or low to no *T. gondii* specific staining. This data is presented in Figure 3.24.

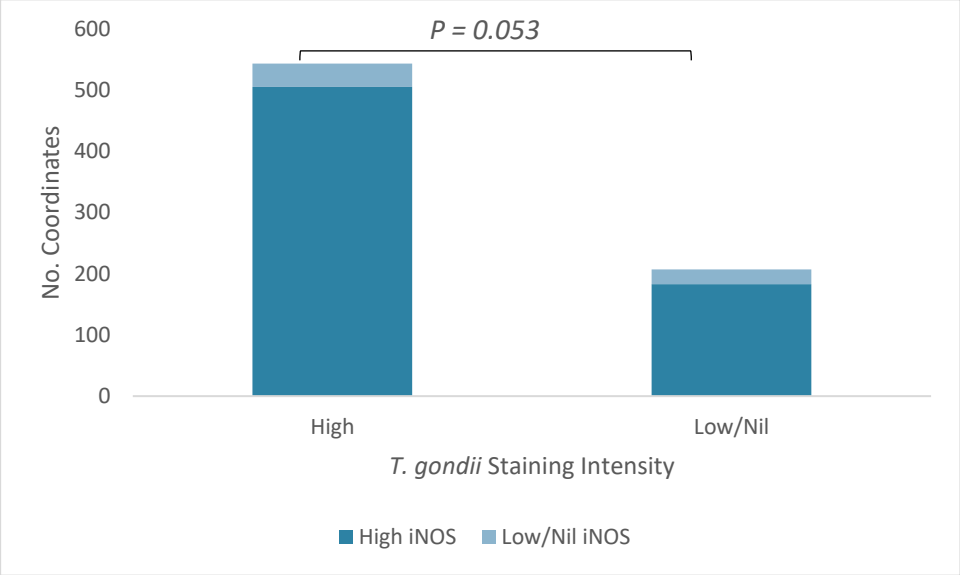

Figure 3.24: A comparison of T. gondii and iNOS intensity of staining in paired images taken at the same field of view. The intensity of staining was designated in grid coordinates of lung tissue specifically stained for the presence of T. gondii and iNOS. Coordinates were deemed to have high, low, and no level of specific staining. This data is taken from Dataset E and is identical to that presented in Figure 3.15, but with combined low and nil categories. This was to allow for a Fisher's Exact test to be calculated. As shown above (P = 0.053), although approaching significance, no association was found for the intensity of iNOS staining between coordinates that were found to have high or low/nil intensity of T. gondii staining.

Figure 3.24 appears to support the observation noted in Figure 3.23. No significant association (*P* = 0.053) was found in the intensity of iNOS specific staining in coordinates of high compared with low/nil intensity of *T. gondii* specific staining. To conclude, it appears that iNOS has high intensity of staining independent of the intensity of *T. gondii* staining.

The findings from Dataset E, as expressed in Figures 3.23, and 3.24 show no clear correlation (*P* = 0.053). iNOS appears to cooccur at high levels independent of the intensity of *Toxoplasma*

gondii presence. In conclusion, the study on co-localisation of iNOS expression and *T. gondii* demonstrated that there was no detectable association or lack of it.

Although a significant difference (P = <0.001) was found in the colocalised analysis of *T. gondii* and Arginase-1 in Dataset E, no other analysis between the two indicated any correlation. Therefore, when considering the relationship between *T. gondii* distribution and both iNOS and Arginase-1 expression, no clear relationship between expression and distribution was seen for either enzyme.

3.2.2 Investigating the relationship between iNOS/Arginase-1 expression ratios and *T. gondii*

As previously mentioned, many lung cells express both Arginase-1 and iNOS; but due to the competition for L-arginine, one of these proteins tends to be expressed more than the other, as opposed both proteins being expressed at the similar levels (Brüne, Weigert, & Dehne, 2015; Munder, Eichmann, & Modolell, 1998; Yoon & Ryoo, 2013). Therefore, it was deemed important to explore the Arginase-1-iNOS dynamic in these lung biopsy tissue samples, before then comparing this dynamic with the extent of *T. gondii* staining. Utilizing Dataset E, the extent of Arginase-1 staining was assessed in grid coordinates with high, low and no iNOS staining.

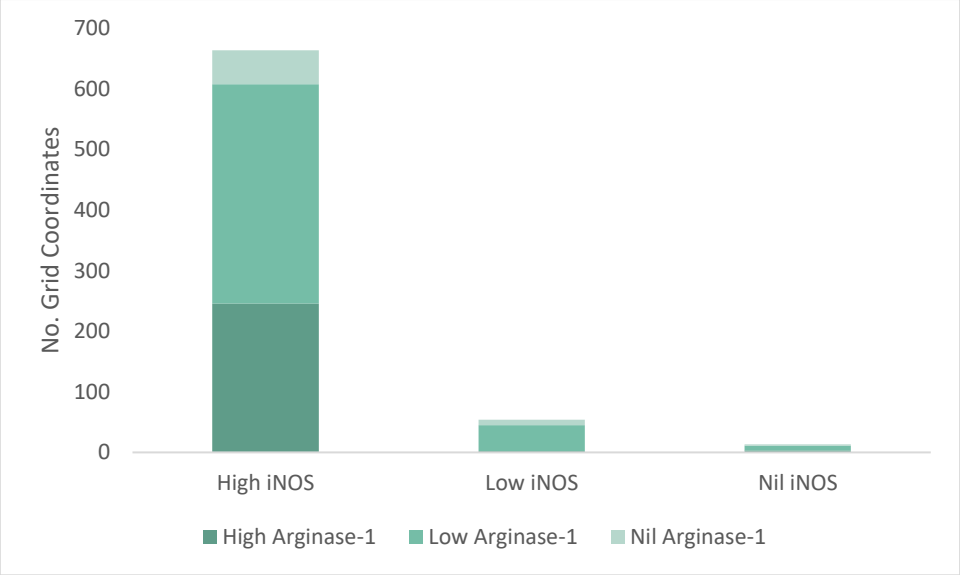

Figure 3.25: The intensity of Arginase-1 specific staining in coordinates with high, low, and nil iNOS specific staining. This data was collated from a 5 x 4 grid overlaid onto paired images taken at the same field of view (Dataset E). The intensity of Arginase-1 and iNOS specific staining was designated high, low, and no level of staining within these grid coordinates. As shown above, iNOS staining intensity is high whereas Arginase-1 staining tends to be low throughout these lung tissue samples. Curiously, the largest proportion (by far) of high intensity Arginase-1 coordinates also cooccur where iNOS is deemed to have high intensity.

Figure 3.25 illustrates the intensity of Arginase-1 staining in grid coordinates that were deemed to have a high, low, and nil intensity of iNOS specific staining. As shown, iNOS specific staining appears to be high throughout. Conversely, Arginase-1 has a tendency towards low intensity of expression of staining. To further investigate these findings, categories low and nil were combined. This allowed for the more accurate Fisher's Exact test to be conducted. This would determine whether a significant difference exists between the intensity of Arginase-1 staining in grid coordinates categorised as having high or low to no iNOS specific staining. This data is presented in Figure 3.26.

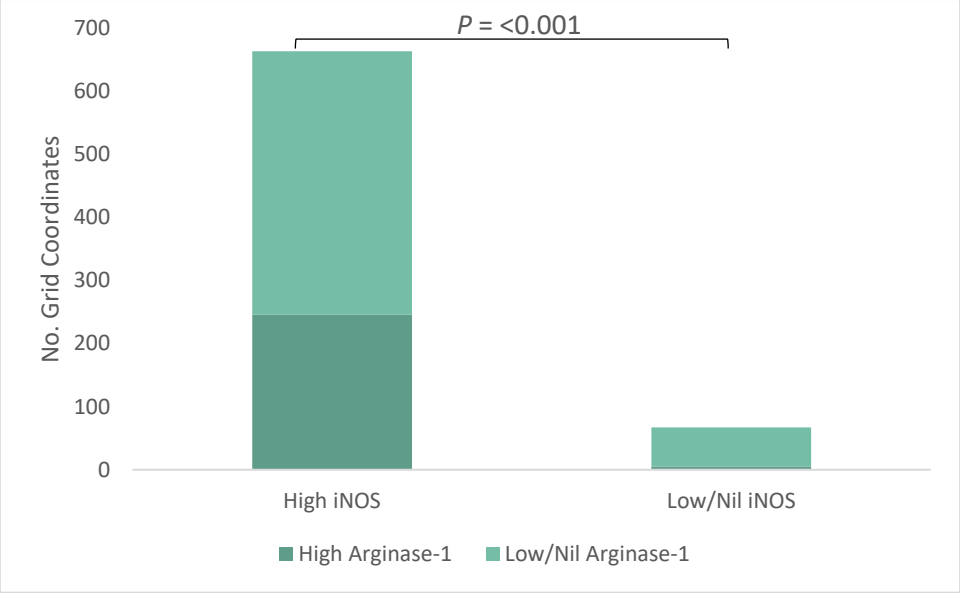

Figure 3.26: A comparison of Arginase-1 and iNOS intensity of staining in paired images taken at the same field of view. The intensity of staining was designated in grid coordinates of lung tissue specifically stained for the presence of immunomodulating proteins Arginase-1 and iNOS. Coordinates were deemed to have high, low, and no level of specific staining. This data is taken from Dataset E and is identical to that presented in Figure 3.25, but with combined low and nil categories. This was to allow for a Fisher's Exact test to be calculated. As shown above (P = <.001), a significant positive association was found for the intensity of Arginase-1 and iNOS staining.

Figure 3.26 found a significant positive association (*P* = <0.001) in the intensity of Arginase-1 and iNOS specifically stained coordinates.

To conclude, the findings from Dataset E, as expressed in Figures 3.25, and 3.26 show there to be a clear difference (*P* = <0.001) in the intensity of Arginase-1 staining in the different intensities of iNOS specific staining. iNOS staining was found to be mostly at high levels of intensity, contrary to Arginase-1 of which tended towards lower intensities of staining. Strikingly, the largest proportion of high intensity Arginase-1 staining also cooccurred in coordinates with high intensity iNOS staining. In conclusion, the study on co-localisation of the expression of iNOS and Arginase-1 demonstrated that there was no obvious association or lack of it.

Having established the relationship between iNOS and Arginase-1 expression using dataset E, the next question to address was whether there was a relationship between the ratio of iNOS

expression and Arginase-1 expression and the distribution of *T. gondii* infection. Introduced by Gao *et al* (2015), in their research into resistance and sensitivity to *Toxoplasma gondii* in mice and rats, the ratio of Arginase-1 to iNOS was found to have a strong relationship with resistance/susceptibility to *T. gondii*. When using this ratio, they had found a negative correlation between the iNOS/Arginase-1 ratio and the intensity of *T. gondii* infection in rat peritoneal macrophages. This same finding was not observed in their analysis of *T. gondii* presence with just iNOS or Arginase-1. Therefore, this raised the question as to whether this could be examined in human lung tissue and was applied to the larger dataset from the randomised images (Dataset J) in addition to the smaller, but more precise data from the matched images (Dataset D). The iNOS/Arginase-1 ratio was calculated for the ImageJ data of Dataset J and Dataset D, separately and can be found in Table 3.3.

Table 3.3: The iNOS/Arginase-1 ratio of Dataset J and Dataset D. Additionally, mean averages and standard deviations were calculated for both datasets. Omitted from calculation and analysis are ratios from samples with an Arginase-1 or iNOS negative reading. Here it can be inferred that the iNOS/Arginase-1 ratio for the paired images of Dataset D has slightly less variation in the range of values than the ratios calculated for Dataset J of the randomised images.

Sample	Dataset j iNOS/Arginase-1 ratio	Dataset d iNOS/Arginase-1 ratio
812	30.0	8.1
818	3.6	0.9
819	5.5	13.9
821	27.1	
822	6.2	42.3
823	14.3	9.0
827	4.6	0.8
828	4.9	52.2
965	11.3	76.8
968	32.7	13.5
972	61.4	179.5
973	6.2	5.4
975	150.7	
979	112.7	7.8
985	21.2	10.3
988	24.3	238.9
989	15.4	59.4
997	13.8	6.1
999	3.3	5.6
1005	8.0	11.3
1006	2.1	14.6
1008	8.6	5.9
1013	11.4	1.5
1014	3.4	1.3
1017	3.8	4.2
1018	2.6	1.6
1025	25.7	10.5
1026	10.0	4.7
1028	13.5	16.0
1029	20.3	19.2
1030	202.2	30.6
1032	5.6	36.4
1033	51.2	115.2
1037	334.4	
1040	9.4	32.7
1043	51.9	23.1
1047	23.1	
1052	7.9	10.9
1054	34.0	27.5
1064	13.6	12.9
664	2.5	4.1
757	3.7	14.7
813	20.4	29.3
976	5.4	21.3
1004	9.5	38.4
1045	57.4	6.4
1067	22.1	6.3
1068	6.1	13.0
1069	17.7	18.5
1071	4.7	19.7
1072	4.2	10.3
Average	30.3	27.5
Standard Deviation	56.6	44.2

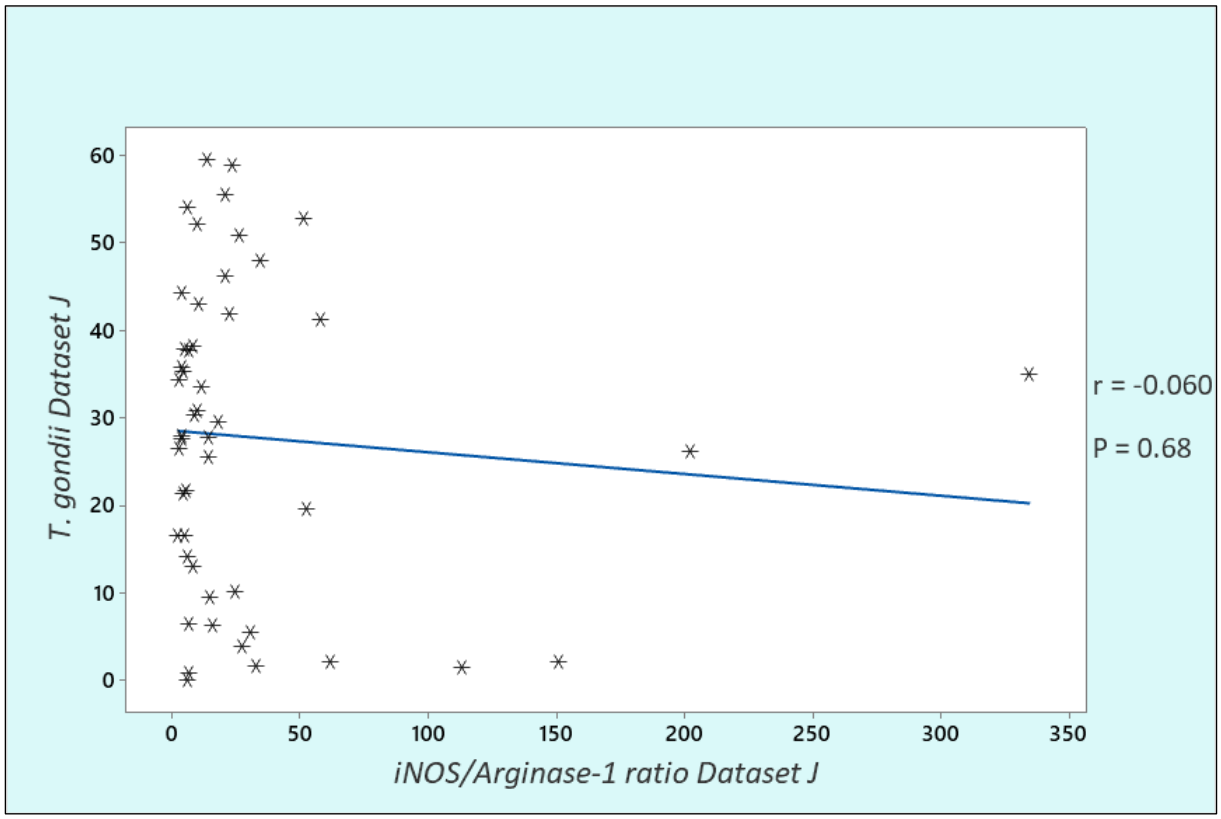

Figure 3.27: A scattergram of the stain coverage of lung biopsy tissue specifically stained for the presence of Toxoplasma gondii and the iNOS/Arginase-1 staining ratio. This data was extracted from Dataset J, which was taken from randomised images. As shown (r = -0.060; n = 49; P = 0.68) there appears to be no correlation between the extent of T. gondii staining and the ratio of iNOS/Arginase-1 staining.

Figure 3.27 shows the extent of *Toxoplasma gondii* specific staining against the ratio of iNOS/Arginase-1 for Dataset J. The iNOS/Arginase-1 ratio data were found not to be normally distributed and so a non-parametric correlation test (Spearman's) was performed. There was no correlation between the intensity of *Toxoplasma gondii* specific staining and the ratio of iNOS to Arginase-1 expression (r = -0.06; n = 49; *P*= 0.68). However, it may be that the two outlier readings above the 150% mark within the ratio dataset may be interfering with the correlation coefficient. Therefore, it was decided to repeat this statistical analysis, omitting the 2 outlying readings. Figure 3.28 demonstrates the impact on the correlation coefficient and linear regression with this omission.

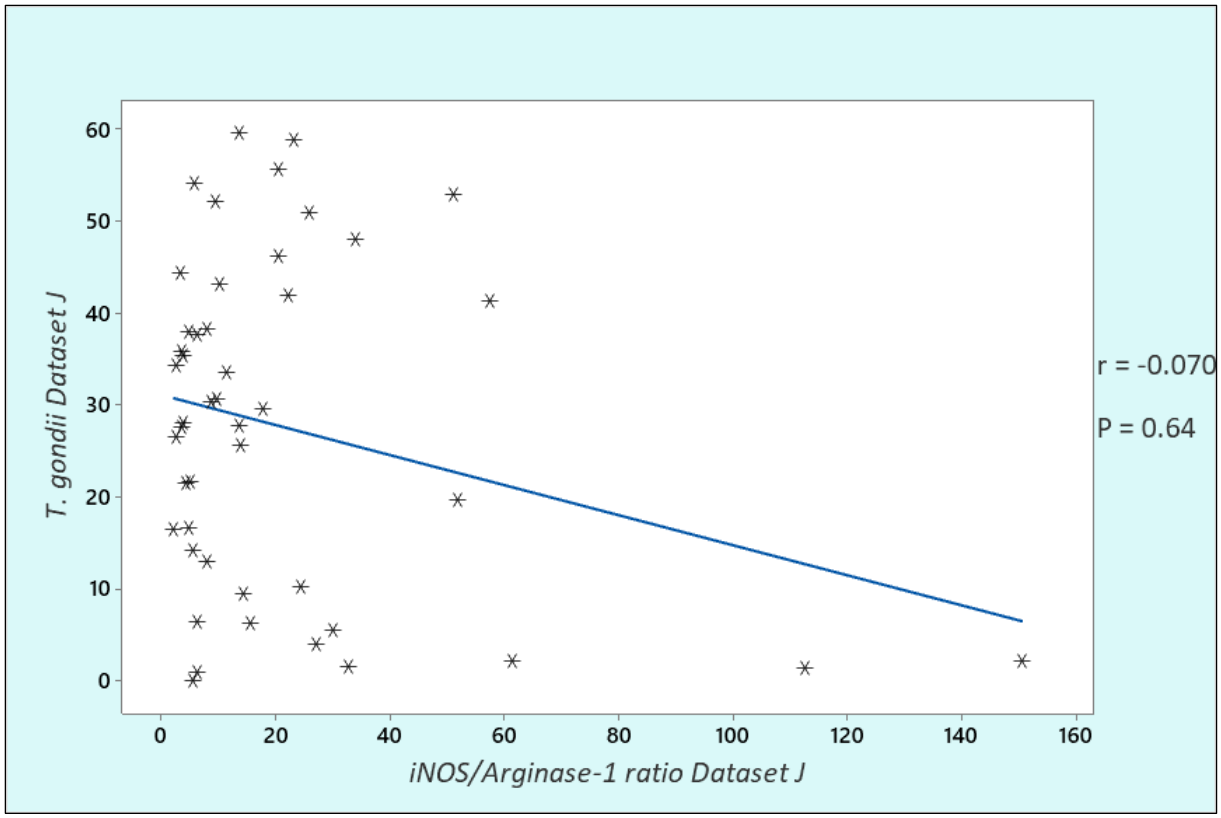

Figure 3.28: A scatterplot of the stain coverage of lung biopsy tissue specifically stained for the presence of Toxoplasma gondii and the ratio of iNOS/Arginase-1 specific staining. These readings are identical to those of Figure 3.27, utilising Dataset J, but with the omission of 2 outlier readings. As shown (r = -0.070; n = 47; P = 0.64), removal of these outlier results further supports the hypothesis of there being no correlation between the staining distribution of T. gondii and that of the ratio of iNOS/Arginase-1 within Dataset J.

As shown, removal of the outlier readings has barely altered the correlation coefficient. This further supporting the conclusion of there being no correlation between *T. gondii* and the iNOS/Arginase-1 ratio (r = -0.070; n = 47; *P* = 0.64). However, it is notable that this amendment has increased the decline on the linear regression line- again it appears that it may be skewed due to the two readings above 100 of the iNOS/Arginase-1 ratio data. As it appears as though removal of those readings and repetition of the correlation analysis is unlikely to alter the findings that much, it was decided not to repeat the analysis.

Figure 3.29 shows the extent of *Toxoplasma gondii* specific staining against the ratio of iNOS/Arginase-1 for Dataset D. The iNOS/Arginase-1 ratio data were found not to be normally distributed and so a non-parametric correlation test was performed. There is no correlation

between the intensity of *Toxoplasma gondii* specific staining and the ratio of iNOS to Arginase-1 expression (r= -0.081; n= 46; *P* = 0.59).

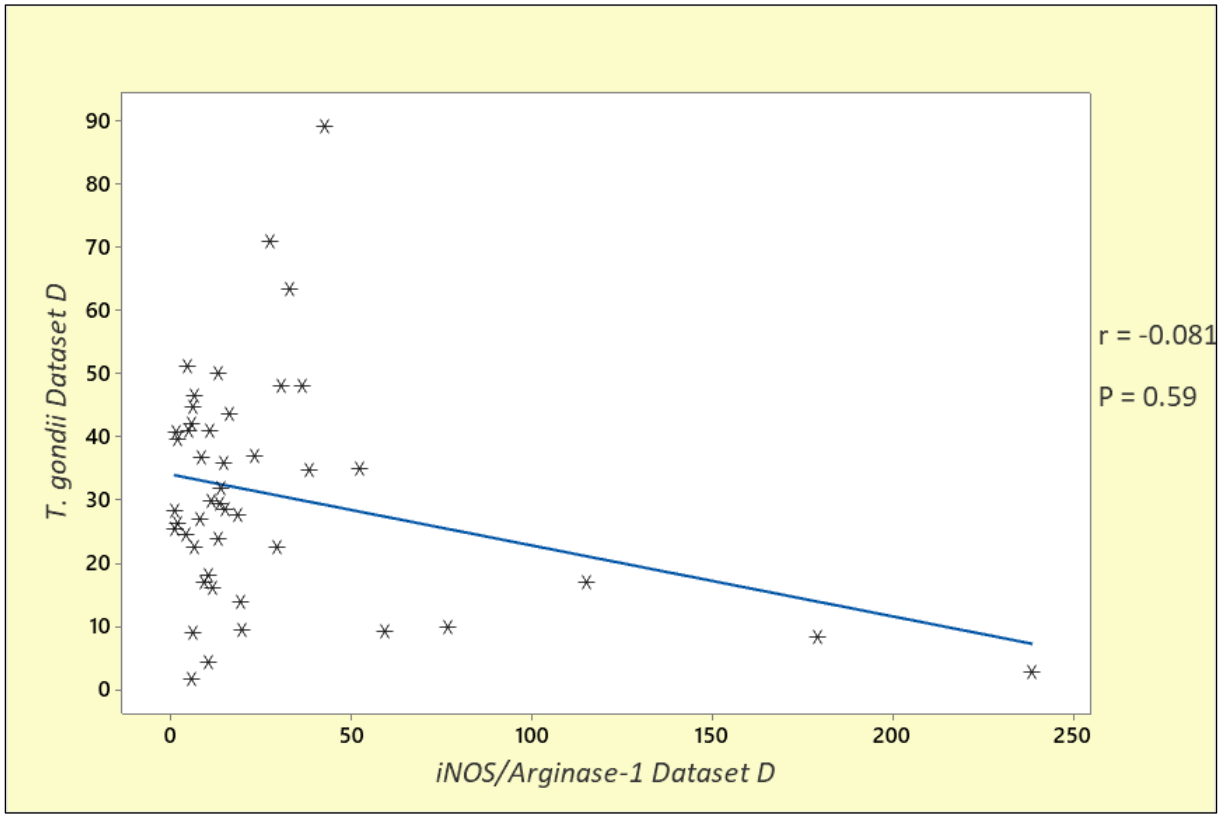

Figure 3.29: A scattergram of the stain coverage of lung biopsy tissue specifically stained for the presence of Toxoplasma gondii and the iNOS/Arginase-1 stain ratio. This data was extracted from Dataset D, of which was taken from matched images. As shown (r = -0.081; n = 46; P = 0.59) there appears to be no correlating relationship between the extent of T. gondii staining and the ratio of iNOS/Arginase-1 staining within Dataset D.

As was seen in Figure 3.27, there appears to be outlier readings in Figure 3.29 that may be skewing the results. Therefore, this analysis was repeated with omission of the 3 iNOS/Arginase-1 ratio readings above 100 and is shown in Figure 3.30.

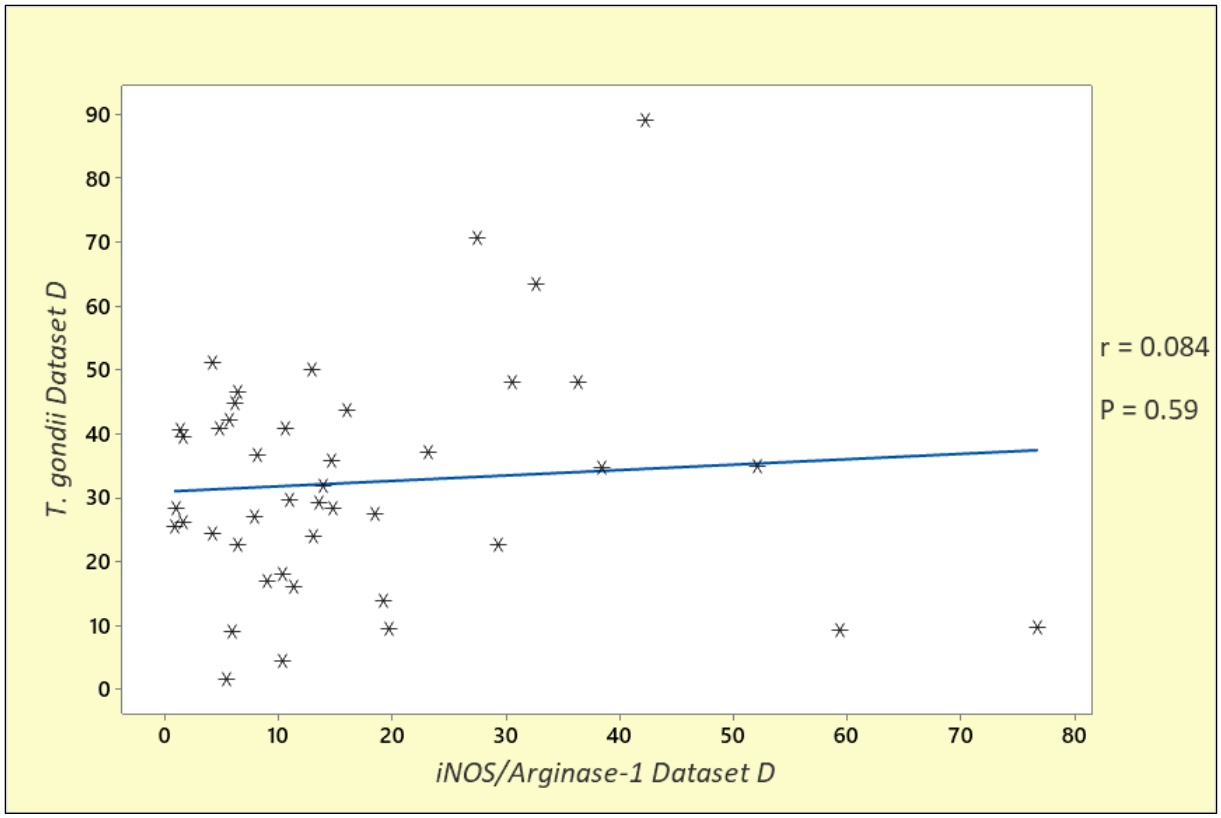

Figure 3.30: A scatterplot of the stain coverage of lung biopsy tissue specifically stained for the presence of Toxoplasma gondii and the ratio of iNOS/Arginase-1 specific staining. These readings are duplicated to those of Figure 3.29, but with the omission of 3 outlier readings. As shown (r = 0.084; n = 43; P = 0.59), removal of these outlier readings does alter the correlation coefficient and regression line, but there remains no correlation between the staining distribution of T. gondii and that the ratio of iNOS/Arginase-1 staining within Dataset D.

Figure 3.30 further supports there being no correlation (r = 0.084; n = 43; *P* = 0.59) between the extent of *T. gondii* specific staining and the ratio of iNOS/Arginase-1 staining within Dataset D.

A comparison of the iNOS/Arginase-1 ratio with *T. gondii* distribution, as utilized by Gao *et al* (2015), for both Dataset J and Dataset D, show no correlation between *Toxoplasma gondii* and the ratio of iNOS/Arginase-1 expression.

3.3 Investigation of tissue specific distribution of *T. gondii* infection and expression of iNOS and Arginase-1

The aim of this analysis was twofold. Firstly, to understand if there are any tissue/cell type specific differences in expression of iNOS and Arginase-1 and *T. gondii* distribution. Secondly, to use comparison of specific tissues as a criterion for investigating co-localisation of expression of iNOS or Arginase-1 and *T. gondii* infection distribution. This was done by selecting specific lung tissues or cells that could be identified and then calculate the proportion of those tissues/cell that were positive for expression or infection. An example of this methodology can be seen in Figure 3.31.

Smooth muscle was chosen as *Toxoplasma gondii* preferentially invades this tissue in an active infection. *Toxoplasma gondii* also tends to invade macrophages and so this cell type was chosen to be studied too. The Gao *et al* (2015) study had a heavy analysis on peritoneal macrophages as means of evaluating sensitivity to infection associated with Arginase-1 and iNOS expression in rats and mice. Therefore, it is of interest to see if human alveolar macrophages replicate this in these lung biopsy samples. As such a preference has been noted, it was also decided to research the proportion of alveolar macrophages and smooth muscle with Arginase-1 and iNOS specific staining.

As discussed earlier, *T. gondii* influences circulating monocytes to stick to the blood vessel endothelium to aid movement out of the cell into the peripheral tissues. Therefore, there may be a higher infection rate of blood vessel endothelium than other lung tissues, particularly if the infection is new. As it was unclear how favourable airway epithelia is to *Toxoplasma gondii* infection, this was studied too. The latter two tissues may also offer evidence of directionality

of infection. Though the consensus is that most *Toxoplasma gondii* infections arise from ingestion, even without direct contact with a cat, the localised nature of infection has raised questions among medical practitioners (Montoya & Liesenfeld, 2004; Shen *et al*, 2015). To investigate the tissue distribution of *T. gondii* Dataset F was interrogated and four tissue/cell types were scored for the presence or absence of infection in that tissue type. The tissue/cell types used were airway epithelia, vessel endothelia, smooth muscle, and macrophages. All images were pooled for analysis (with exception for samples with cross-reaction staining in their negative controls for the macrophage analysis only) and were extensively checked for the tissue/cell type listed above. Once identified (separately), both the stained positive and the total number were counted. An epithelial or endothelial lumen would count as one result only. Similarly, a bundle of smooth muscle fibres would count as one result only. Macrophages, being freely movable cells, where able to be counted on a singular (one cell) basis. The results are shown in Figure 3.32.

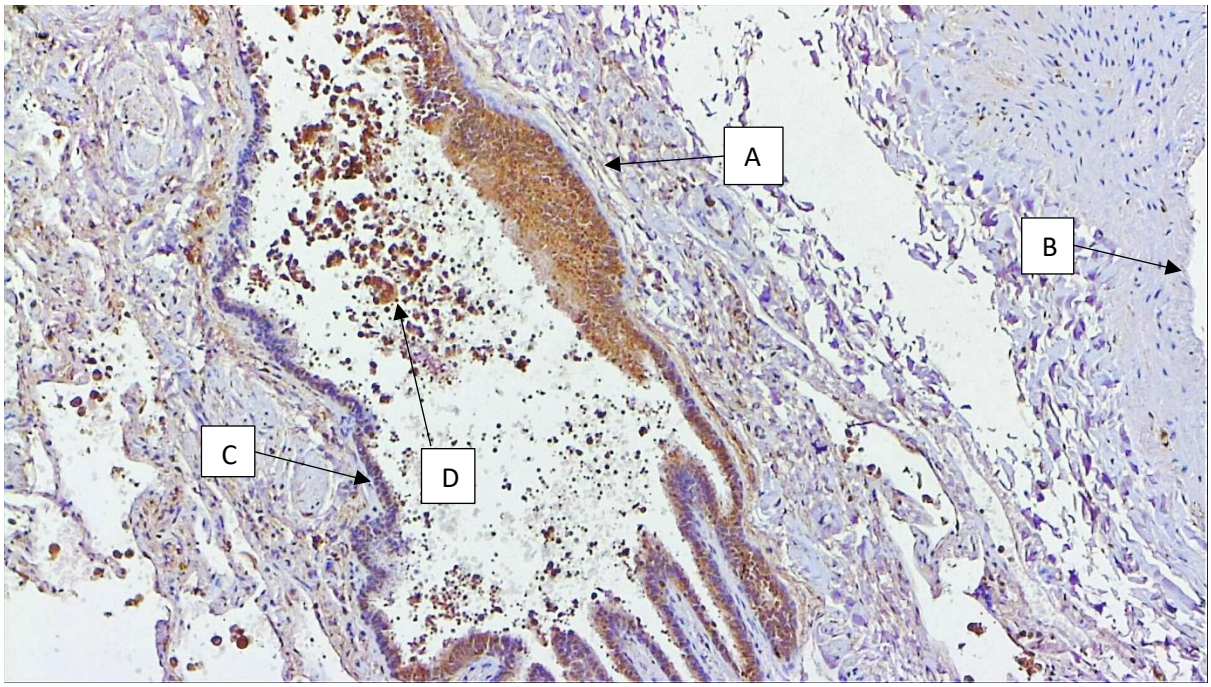

Figure 3.31: Microphotograph (100x magnification) of a section of lung tissue immunohistochemically stained for the presence of iNOS with identified cell/tissue types and their positive/negative status. Brown staining is indicative of a positive result. A) iNOS positive smooth muscle. B) iNOS negative airway epithelial tissue. C) iNOS positive airway epithelial tissue. D) iNOS positive macrophages.

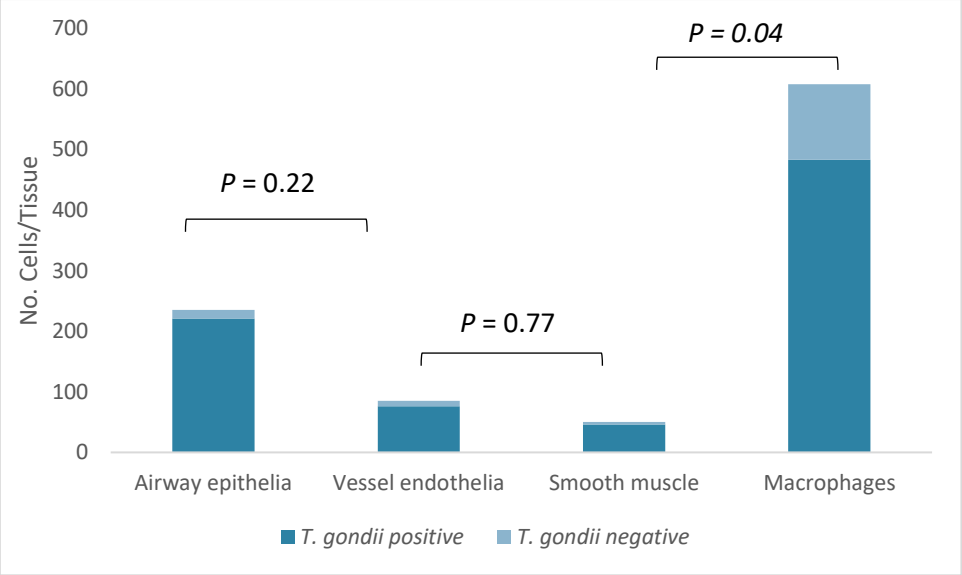

Figure 3.32: The tissue or cell type and the quantity that were found to be positive or negative for Toxoplasma gondii specific staining within 51 lung biopsy samples (n = 23 samples for macrophage identification and analysis) (n = 51 samples for epithelia, endothelia, and smooth muscle identification and analysis). This graph comprises data extracted from Dataset F that was subjected to a Fisher's Exact Test. As shown, no significant difference was found in the quantities of T. gondii positive and negative counts between airway epithelia and vessel endothelia (P = 0.22), as well as smooth muscle and vessel endothelia (P = 0.77). Conversely, a significant difference (P = 0.04) between the number of macrophages and smooth muscle that were found to be positive or negative for the presence of Toxoplasma gondii.

Figure 3.32 summarises the amount of epithelia, endothelia, smooth muscle, and macrophages found to be positive or negative for the presence of *Toxoplasma gondii*. As shown, the infection rate is high, with little variation for the three lung tissue types identified. No significant association (negative or positive) was established between epithelia and endothelia ($P = 0.22$) *T. gondii* staining. The lack of substantial difference between the airway epithelial tissue and the blood vessel endothelia likely indicates there being no discernible directionality to infection. No significant negative or positive association was also found between smooth muscle and endothelia ($P = 0.77$) *T. gondii* specific staining. This would likely indicate there being no clear tissue preference for *T. gondii* that can be ascertained from this data.

However, Alveolar macrophages were less likely to be positive, the proportion that were found to be positive was still high at 79.4% of all identified macrophages and this differed

significantly (P = 0.04) between the findings in smooth muscle. This was a driving force behind the second question raised, and that is whether specific tissue or cell types differentially express Arginase-1 and iNOS. To investigate this question, Dataset F was interrogated, and smooth muscle and macrophages were scored for the presence or absence of infection (data as collected for Figure 3.31) and also for iNOS and Arginase-1 Expression. The results are shown in Figure 3.32.

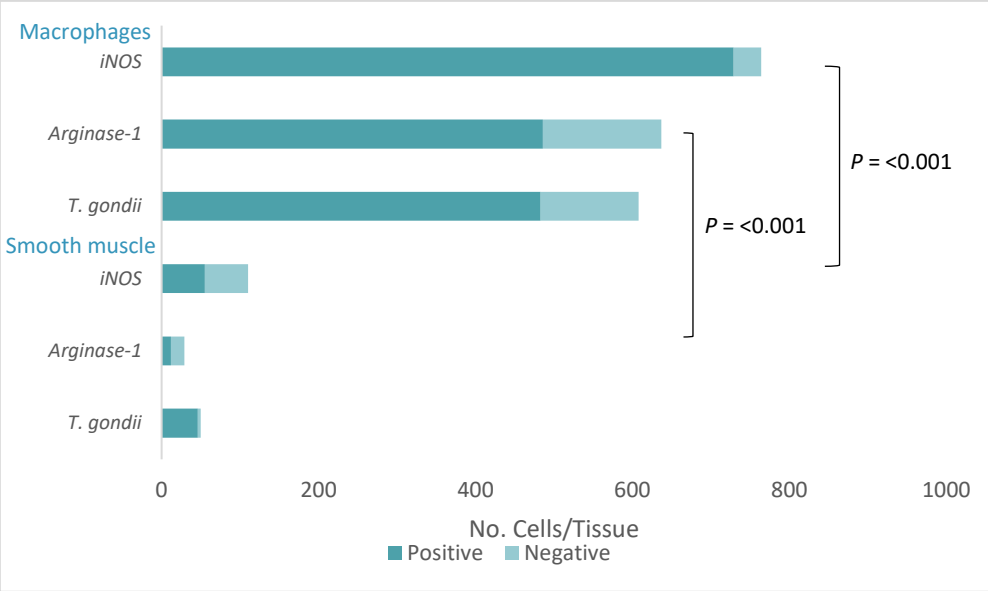

Figure 3.33: The amount of smooth muscle and alveolar macrophages positive and negative for the presence of Toxoplasma gondii, Arginase-1, and iNOS. Previous analysis (Fig. 3.31) had found a significant difference (P = 0.04) in the amount of T. gondii positive and negatively identified macrophages and smooth muscle. This graph comprises data from Dataset F and sought to compare the expression of Arginase-1 and iNOS between the two cell/tissue types. As shown, there is a significant difference (P = <0.001) between the proportion of Arginase-1 positive and negative macrophages versus that of smooth muscle. Similarly, there is a significant difference (P = <0.001) between macrophages and smooth muscle that are positive or negative for the presence of iNOS.

Figure 3.33 summarises the proportion of smooth muscle and alveolar macrophages positive for the presence of *T. gondii*, Arginase-1, and iNOS. A significant difference (P = <0.001) could be found between the proportion of smooth muscle and macrophages positive for the presence of Arginase. Likewise, the proportion of smooth muscle and macrophages positive

for the presence of iNOS were found to be significantly different (P = <0.001). It appears that an increase in the proportion of iNOS positive tissue is cooccurring with a decrease in the proportion of *T. gondii* positive tissue type. However, there is a major difference in the quantities of the two tissue types, increasing the probability of data errors, and so it is difficult to come to a definitive conclusion.

Overall, there is little evidence to conclude that *Toxoplasma gondii* preferentially infects some tissues over others. Arginase-1 and iNOS expression seem to mimic that of what has been found in other analyses- that the level of iNOS specific staining is much higher than Arginase-1.

3.4 Summary of Conclusions

In conclusion, the intensity of *Toxoplasma gondii* infection has been variable, but all samples could still be categorized as having significant infections. iNOS is consistently highly expressed, whereas Arginase-1 expression has tended to be low and in pockets of areas. Statistical analysis of ImageJ percentage coverage data as well as the more specific gridded colocalization analysis collectively support the hypothesis of there being very little or no relationship between *Toxoplasma gondii* presence and the expression of Arginase-1 or iNOS. These same findings were seen when analysing *Toxoplasma gondii* with the ratio of Arginase-1 to iNOS.

Similarly, selective tissue/cell analysis also suggest there being little or no tissue specificity to infection with *Toxoplasma gondii*; with expression of Arginase-1 or iNOS again seeming to

have no influence. Airway epithelia and blood vessel endothelia shared similar infection rates and so a directionality of infection could not be determined from this. For example, a higher proportion of *T. gondii* positive airway epithelial tissue could have been indicative of infection being acquired through inhalation, whereas high positivity in blood vessel endothelia would be more indicative of infection via ingestion or through endogenous reinfection from a chronic *T. gondii* infection.

Chapter 4 Discussion

As part of a previous study, seventy-two lung biopsy tissue samples were previously acquired from the University Hospital of South Manchester and all tested positive for the presence of *Toxoplasma gondii* (Bajnok *et al,* 2019). This was in contrast to lung lavage samples, taken from 10 healthy volunteers as a control group, where the 10% *Toxoplasma* prevalence was found to be in line with the UK national average. In this study, using immunohistochemical analysis, they found evidence of both the active infectious stages of the parasite, tachyzoites and infected macrophages, as well as the dormant bradyzoites in cysts (Bajnok *et al,* 2019). Few studies have shed light on the immunological interactions occurring in the human lung with respect to infection with *T. gondii*. In rodents, the two enzymes, iNOS and Arginase-1, have been shown to act antagonistically to influence sensitivity and resistance to *T. gondii* infection (Gao *et al,* 2015; and Li *et al,* 2012). In these studies, they found a higher ratio of iNOS expression to Arginase-1 expression was linked to a more marked resistance to infection by *Toxoplasma gondii*. The reverse was also true, with a lower iNOS to Arginase-1 ratio being more likely to be associated with sensitivity to *T. gondii* infection. These studies showed that rats had a higher resistance to *T. gondii* infection than mice and that this was associated with the higher expression ratio of iNOS to Arginase in the rats. Interestingly though, when peritoneal and alveolar macrophages were compared within inbred rat strains, epigenetic differences were seen in the iNOS to Arginase expression ratio (Zhao *et al,* 2013). Alveolar macrophages were much more sensitive to *T. gondii* infection and had a low iNOS to Arginase

expression ratio while the much more resistant peritoneal macrophages had a higher iNOS/Arginase expression ratio. This raises the question as to whether the lung may be a more permissive tissue with respect to *T. gondii* infection. Furthermore, glucocorticoids are commonly used as both anti-inflammatory drugs and, in some cases, anticancer drugs were also found to depress iNOS expression and thereby promote infection with *T. gondii* in rats (Wang *et al* 2014). These findings, in laboratory rodents, raise important questions as to whether there is a role for iNOS and Arginase-1 expression in relation to *T. gondii* infection in human lung tissue. As far as could be determined, there are no previously published studies on the involvement of iNOS and Arginase-1 in human lung tissue infection with *T. gondii*. The previous studies by Bajnok *et al* (2019) generated a source of many human lung tissue samples, which could be guaranteed to be infected with *T. gondii*, thereby providing a good sample set to investigate the relationship between the parasite and iNOS/Arginase expression in human lungs.

In this study, immunohistochemistry was used to stain, separately, for the presence of *T. gondii*, iNOS, and Arginase-1 on cut sections of fixed human lung biopsy samples. Following the development of suitable approaches, examination of the tissue distribution of parasite infection and iNOS and Arginase gene expression, using specific antibodies, enabled an investigation of spatial interrelationships.

To be capable of measuring intensity of both extent of infection and protein expression, immunohistochemistry was developed and optimised. This technique was used successfully by Bajnok *et al* (2019) for the detection of *T. gondii* and this was further developed to include localisation of iNOS and Arginase gene expression. However, a process of development and optimisation was needed before analysable slide sections could be made. Owing to the

amount of lung tissue left available in the sample sets, only 51 of the original 72 samples, used previously (Bajnok *et al* 2019), could be utilised for this study. Once completed, the optimisation process provided a successful methodology that could be applied to the 51 lung biopsy samples and enabled spatial visualisation of *T. gondii* infection and iNOS or Arginase-1 expression. One of the problems encountered was that faint background staining was seen in some negative control slides probably caused by residual non-specific binding of secondary antibodies to macrophages. The effect was clearly distinguishable from genuine binding but required modifications to the image analysis to subtract the non-specific effects from some samples.

Three main analytical methods were developed that involved taking images at 400x and 100x magnification with matched and unmatched fields of view.

Challenges were encountered in developing a method for consistent co-localisation. Initially, specialist software capable of performing colocalization analysis was tried on the matched images. This type of software was based on analysing the distance between pixels from two or more images to look for overlapping patterns on the slides. This form of analysis potentially could be used in assessing colocalization of *T. gondii* staining with Arginase-1 and iNOS staining. One such method tried was with the ImageJ plugin, EZColocalization, and the other was via the use of GIS mapping software. The paired images, although precise, were not identical enough to overlay and analyse through the EZColocalization plugin. Some of this misalignment was likely due to normal variations in tissue shape and structure, when considering its 3-dimensional shape. Similarly, there was no success in applying a GIS system software to these images. Again, this was partially due to the misalignment issue, but also in part to the inability to find an adequate quantity of points of reference to base the analysis

on. To overcome these limitations, an approach was developed in which a five by four grid pattern was superimposed of on overlayed images. This is the dataset designated Dataset E. Although lacking in the mathematical precision of the ImageJ and GIS software, by adhering to the given guidance, by the software, on what constituted a 'high' or 'low' stain intensity, an accurate snapshot of staining activity was captured on a much smaller, localised, area of tissue when compared with the ImageJ stain coverage data provided in Dataset A.

Another, more precise, methodology utilised in this study was to analyse the images for tissue specific staining. Here a few specific tissues were identified and noted on whether they were positive or negative for the presence of *T. gondii,* Arginase, or iNOS expression. As discussed in Chapter 1, there is little knowledge as to the expression of Arginase-1 and iNOS dynamics in different human lung tissues. Additionally, little is known whether there is any tissue infection preference by *T. gondii* in infected human lung tissue. This enabled detailed co-localisation to be measured but also enabled a critical evaluation as to whether tissue type may be influencing the findings. For example, correlating relationship between *T. gondii* and Arginase-1 or iNOS may be coincidental due to the expression profiles of different tissues. Limitations were discovered, though, with using this methodology. These centred mainly around trying to accurately identify specific lung tissues, hence only a small repertoire of lung cells and tissues were chosen for analysis where certainty over identity could be established. It was discovered that positive stained tissues were more easily identifiable than those only stained with the background Erhlich's haematoxylin, and so there was the potential for an overinflation of the positively identified tissue types. This potential inaccuracy was and is still difficult to overcome but efforts were made to be especially detailed-orientated when observing the slides for specific tissues. If these studies were extended in future, cell type

specific antibody markers would be recommended to assist with cell/tissue type identification.

Analysis of stain coverage, using ImageJ to calculate proportional coverage of immunochemical staining, represents the bulk of data obtained in this study. This software proved useful when trying to get a larger, generalised overview of the expression of Arginase-1 and iNOS and the distribution of *T. gondii* infection. ImageJ provided numerical data that could be statistically analysed with a range of tests. In particular, this type of analysis was suitable for investigating whether correlations existed between *T. gondii* distribution coverage and iNOS/Arginase-1 expression coverage. The outcomes of these analyses differed from the grid coordinate analysis or the tissue specificity analysis, described earlier, where the associations and differences could be analysed. The grid coordinate analysis and tissue specificity analysis were more localised and specific, and this was a strength over the proportional cover analysis as measured by the ImageJ approach. Bajnok *et al* (2019) used ImageJ software in their measurement of coverage of *Toxoplasma gondii* infection within the same collection of lung biopsy samples as this study has utilised. Their methodology included taking 3 photos of randomised fields of view, before putting them through ImageJ analysis that would generate a percentage of staining coverage for each of the inputted images. An average reading was then calculated from these three readings, and this was then used as the finding for the sample, as a calculation of the percentage coverage of *T. gondii* specific staining. One of the limitations of the previous study (Bajnok *et al* 2019) was that they just measured the coverage of *T. gondii* infection without considering that fact that some slides possessed more tissue that others. In some cases, especially where sections covered alveolar tissue, large airspaces could potentially cause an over estimation of the proportion of parasite distribution. This same ImageJ methodology was utilized in this study but was improved upon

by accounting for the extent of lung tissue present in the image (see later). Initially, the slides were analysed following the Bajnok *et al* (2019) ImageJ methodology and this resulted in the data presented in Dataset G and was summarised in Figure 3.3. iNOS was expressed highly in all fields of view and had a larger range of distributions than Arginase-1. Arginase-1 expression was minimal in most of the fields of view with a handful of outlying readings which suggested an overall low level of expression with localised pockets of high expression. The difference between the expression of iNOS and Arginase was very highly significantly different (P = 0.001). The distribution of *Toxoplasma gondii* staining in different fields of view had some variability, but lesser so than iNOS.

In addition to utilising ImageJ as Bajnok *et al* (2019) had done, this analysis was expanded to include matched photographs, taken of the same field of view of the closely sectioned lung samples. This gave a more localised representation of what was happening regarding *Toxoplasma gondii* colocalization with Arginase-1 and iNOS in these lung biopsy samples. However, due to the need to compare parasite distribution with gene expression, the previously used method of ImageJ analysis (Bajnok *et al* 2019) needed to be adapted to consider differing proportions of tissue coverage in each field of view.

This study, although expanding on the Bajnok *et al* (2019) data, had differences that required adjustments to improve the reliability of the results. This was because there was a comparative element to this study whereby the presence of the parasite would be compared with how Arginase-1 and iNOS were expressed in these samples, as opposed to another sole *T. gondii* stain intensity study. To improve the accuracy, it was decided to calculate the amount of lung tissue in each image so that antibody staining could be expressed as a proportion of tissue coverage. This was calculated in a similar way to how the stain coverage

was calculated in ImageJ. The counterstain used was Ehrlich's haematoxylin, and this had stained the lung tissue blue - with darker shades signifying a higher tissue density. Therefore, the ratio of lung tissue to blank background could be calculated through ImageJ by isolating and counting the number of blue pixels in the inputted image. This reading was divided into the reading taken of the percentage of DAB staining and converted to a percentage of lung tissue specifically stained for the presence of *T. gondii,* Arginase-1, and iNOS. This data was collated into Dataset H for the randomised photos and Dataset B for the matched images.

To evaluate that these amendments compared to the published data of Bajnok *et al* (2019), two questions were addressed. Firstly, were the revised approach and the previously published approach correlated when the samples were compared as a collection? On the assumption that the improved approach would lead to a more precise representation of the coverage of staining, the second question is whether the improved method produced results that were significantly different to the previously published method. Dataset G (Bajnok *et al* 2019 approach) and Dataset I (revised methodology) were utilised for these analyses for *T. gondii,* Arginase-1, and iNOS with each of these being examined separately from both datasets. For each of the analyses, there was a significant correlation between the outcomes of using both approaches (*i.e.,* samples with low to high staining coverage were correlated when using both methods). This suggested that the two methodologies both broadly supported each other and were therefore providing consistent patterns of distribution. However, there was a significant difference between the actual values of coverage between pairs of samples when the two datasets were compared. This suggests that the use of the revised method is making a significant improvement over the Bajnok *et al* (2019) ImageJ methodology. Therefore, all further ImageJ results analysis were with the datasets with this amendment.

With this adapted ImageJ methodology, the *T. gondii* intensity-based grading system developed by Bajnok *et al* (2019) for the lung samples ill fitted Dataset J (ImageJ readings from the randomised photos). Therefore, these three categories were adjusted to better fit, and more equitably distribute the readings of this study. Following on from Bajnok *et al* (2019), it was considered important to establish whether any subtle correlations could be detected based upon the assigned grade of infection intensity. Here, Grade 1 (low) represented samples with the lowest level of *T. gondii* specific staining, at <20% average stain coverage of lung tissue. Grade 2 (moderate) represented the samples with between 20-36% average *T. gondii* specific stain coverage. Samples with >36% average *T. gondii* specific stain coverage were categorised as Grade 3 (high), having the highest level of infection in the sample set.

Correlation coefficients were calculated for Arginase-1 and the *T. gondii* ImageJ readings within each of the three infection grades. All grade categories showed no significant correlation between the *T. gondii* and Arginase-1 expression. Although, had there been a larger sample size, Grade 1 and 2 infection categories may have expressed a weak positive correlation between *T. gondii* and Arginase-1. Grade 3 had one outlier Arginase-1 reading. As this had the potential to skew the results, this analysis was duplicated with omission of this one outlying reading to address this possibility. Removal of this reading provided stronger support for there being no correlation between Arginase-1 and *T. gondii* ($r = 0.018$; $n = 15$; $P = 0.95$).

When the modified version for measuring coverage was used for the matched images the differences seen were not as detrimental as when comparing the data from the randomised images. This is because the tissue coverage would be expected to be very similar, given these photos were taken of the sample sections same field of view. Nevertheless, for consistency,

this amendment was also applied to the ImageJ readings of the matched photos, and these represented the ImageJ data that were utilised in the analysis of *Toxoplasma gondii* presence with that of Arginase-1 and iNOS.

In order to compare the distribution of iNOS and Arginase, the proportional coverage of the two enzymes was determined by ImageJ analysis. Coverage data (Dataset D) showed that Arginase-1 expression tended to be very low with some 10% of samples having higher readings as seen in Figure 3.7. This is indicative of a 'patchy' distribution, with most samples showing a low proportion of Arginase-1 coverage within the sample tissues. iNOS expression was found in a very significantly higher (P = <0.001) proportional coverage than Arginase's, demonstrating that it was much more widely expressed in lung tissue. *T. gondii* distribution was also found to be much more widely distributed than that of Arginase-1 and had a larger range of readings. This latter was presumably due to the fact that some patients could have had higher intensities of infection that others. It also suggested the *T. gondii* infection could be widely distributed in lung tissue and was not restricted to specific areas.

To investigate whether there was any relationship between the coverage of Arginase expression and localisation of *T. gondii* infection, the extent of *Toxoplasma gondii* specific staining was compared with that of Arginase-1 specific staining. A correlation analysis was conducted using Dataset J (ImageJ readings of the randomised images) between the percentage coverage of *T. gondii* distribution and Arginase expression. No correlation was observed between *T. gondii* infection and Arginase-1 expression (r = 0.060; n = 49; P = 0.60). To gauge if a more precise correlation existed, this same correlation coefficient was applied to Dataset D (ImageJ readings of matched photos). *T. gondii* and Arginase-1 readings of Dataset D also showed no correlation (r = 0.133; n = 48; P = 0.36). Though still in the remit of

classification of no correlation, the correlation coefficient was slightly higher than that of the *T. gondii* and Arginase-1 correlation coefficient found with Dataset J. However, it was apparent that there were 6 outlier readings that may be skewing the regression line as well as the correlation coefficient. To assess whether the results had been skewed, this statistical analysis was repeated but without the 6 Arginase-1 readings above 10% staining coverage. Here it was confirmed again that no correlation could be found ($r = 0.099$; $n = 42$; $P = 0.53$) between *T. gondii* and Arginase-1 in these ImageJ results. From these analyses, there was no correlation found between the proportions of coverage of Arginase expression and *T. gondii* distribution. This provides little support for the situation found in laboratory rodents where Arginase-1 expression was associated with *T. gondii* infection (Li *et al* 2012; Gao *et al* 2015). However, the analyses above merely looked at coverage proportion and not co-localisation.

To specifically address the question of colocalization, more detailed coverage data was interrogated. Dataset E provided an even more colocalised viewpoint of *T. gondii* staining and how Arginase-1 was expressed. This dataset comprised the data obtained from analysis of an overlaid 4 x 5 grid, superimposed on to the 400x magnified images. Each grid was assigned a category based on the intensity of staining. Categories included 'high', 'low', and 'nil' as defined previously. The correspondence between high, low, and nil Arginase-1-stained coordinates were determined with grid coordinates with high, low, and nil *T. gondii* staining. It was found that in coordinates with high intensity of *T. gondii*, Arginase-1 was expressed more highly, proportionally, than when in matching coordinates with lower or no *T. gondii* specific staining. Also confirmed was the tendency of Arginase-1 towards low expression throughout these lung tissue samples. To establish whether this difference was significant, the low and nil categories were each combined for Arginase-1 and *T. gondii*, so that a 2 x 2 contingency analysis could be conducted (using Fisher's Exact Test). This test is more robust

than a larger Chi^2 test with more rows and columns. There was a highly significant positive association (P = <0.001) between Arginase-1 expression and *T. gondii* presence. Thus, in contrast to the less specific analyses, these data supported the observations found in laboratory rodents where Arginase expression was associated with *T. gondii* infection (Li *et al* 2012; Gao *et al* 2015).

To summarise, no correlation was found between *Toxoplasma gondii* and Arginase-1 expression in these lung tissue biopsy samples when looking at overall coverage proportions. However, when a more specific analysis of colocalization, using analysis of grids within the sample fields of view, was carried out there was a significant association between expression of Arginase-1 and *T. gondii* presence. Clearly, the results obtained from the correlation analysis contradict those from the association analysis. This raises the question as to why this might be, and which more truthfully reflects the situation. The correlation analysis is a relatively imprecise analysis which was trying to correlate the percentage coverage of *T. gondii* distribution compared to Arginase-1 expression. Such an approach could erroneously produce a correlation if the same proportion of a field of view was stained even if the locations were different. On the other hand, it could equally be the case that correlation might be low even though there is a significant amount of overlap in staining distribution. The association analysis was carried out on a much more precise area of a field of view. The field of view was divided into 20 sectors which were compared across matching fields of view. Thus, the colocalization precision was higher using this method. It is likely therefore that this method could be a better reflection of the colocalization of *T. gondii* and arginase expression. Thus, these analyses support the notion that arginase may be associated with *T. gondii* infection as determined in rodent models (Li *et al* 2012; Gao *et al* 2015). However, to fully establish this further work would need to be conducted. This could be investigated by using confocal

microscopy and fluorescent labelled antibodies for *T. gondii* and arginase. This would enable demonstration of precise colocalization. Alternatively, the analysis could be carried out at the cellular level. Identification of individual cells and determination of colocalization of expression of arginase and distribution of *T. gondii* could be used to establish whether an association exists. The outcomes of this study lend support to a possible association.

Next this study analysed the relationship between *T. gondii* distribution with the other immunomodulator protein, iNOS, using the same approach used with *T. gondii* and Arginase-1.

For detection of any variations in how iNOS interacts with *T. gondii* in samples designated different infection intensities, *T. gondii* and iNOS were analysed within assigned infection gradings. Analysis of *T. gondii* and iNOS distribution within their designated infection grade categories (Grade 1, 2, and 3) of Dataset J, was varied. Within the lowest (Grade 1) and highest (Grade 3) grades of infection, no significant correlation was found between intensity of *T. gondii* infection and the expression of iNOS. However, had there been a larger sample size, a weak positive correlation could have been found. Grade 2 (moderate) infected samples differed in that a significant moderate positive correlation ($r = 0.508$; $n = 16$; $P = 0.04$) was found between *T. gondii* and iNOS. This result is significant and will be discussed further later in this chapter. It is interesting that a correlation is found for one of the intensity grades but not the two others. It is possible that these contrasting results are related to the fact that iNOS is very highly expressed in these cells. It may be that in samples the entire field of view is swamped by iNOS expression and thus the discriminatory power of these approaches may be insufficient. In the case of the moderately infected samples, it is possible that there is sufficient overlap versus non overlap to enable the correlation to be tested.

In order to establish whether there was a correlation between *T. gondii* parasite distribution and iNOS expression, Dataset J (ImageJ readings from randomised fields of view) was analysed for any correlation. No correlation was found between *T. gondii* and the expression of iNOS ($r = 0.071$; $n = 49$; $P = 0.062$). When this approach was repeated for the more localised data contained within Dataset D (ImageJ readings taken from the matched fields of view), no correlation was also found between *T. gondii* and the expression of iNOS ($r = 0.236$; $n = 50$; $P = 0.10$). Curiously, this correlation coefficient was markedly higher than that of the Dataset J analysis, although both supportive of a lack of correlation between *T. gondii* and iNOS. Likewise, this occurred with the Dataset J and D analysis between *T. gondii* and Arginase-1. This could be indicative of the data collection not being specific enough to notice any subtle correlations or also may have no significance at all. Hence why a collection of different analytical methods has been applied to the images of the stained lung section tissue slides.

To improve the precision of the analysis, Dataset E was analysed to compare iNOS expression in grid coordinates deemed to have high, low, or no presence of *T. gondii* specific staining. No clear difference could be seen in their comparative intensities of staining, with iNOS being expressed highly regardless of the extent of *T. gondii* specific staining. To confirm this, the smaller groups of low and nil staining were combined, so that a statistical test of association, 2 x 2 continency analysis (using Fisher's Exact Test), could be performed. There was no significant association ($P = 0.053$) between iNOS expression and *T. gondii* presence. However, it should be noted with $P = 0.053$, this negative association is approaching significance ($P < 0.05$). As found with the co-localisation studies between *T. gondii* and Arginase-1, determination of association with iNOS using the more precise grid approach resulted in a suggestion that an association is occurring. This would need to be verified by future work which could involve the use of a larger sample set.

In summary, most of these analyses are supportive of there being no correlation between how iNOS is expressed and the intensity of *T. gondii* infection. iNOS was found to be highly expressed throughout the lung tissue, seemingly independent of the intensity and distribution of *Toxoplasma gondii.* However, exceptions were found with the Grade 2 category of infected samples as well as with the Dataset E analysis. A significant moderate positive correlation was found in the moderately infected lung samples. This does not align with what was found in the research conducted by Gao *et al* (2015) and Li *et al* (2012). It does support the findings of Bando *et al* (2018a), who did find an association between *T. gondii* and an increase in iNOS in human cells. This will be expanded later in this Chapter. Conversely, Dataset E analysis was approaching significance for a negative association for *T. gondii* and iNOS, supporting the research in rat and mice models (Gao *et al* 2015; and Li *et al* 2012).

In this study, it was also deemed important to gain an understanding on the interaction between Arginase-1 and iNOS, given that the two proteins are in competition for L-Arginine. Significant differences (P = <0.001) were found between the median expression of the two proteins. More colocalised analysis was included with the interrogation of Dataset E. Here, it was shown that most samples had a tendency towards high expression of iNOS, and low expression of Arginase-1 throughout. Strikingly, it appeared the largest proportion of high Arginase-1 regions, colocalised with those with high iNOS expression.

The research of Gao *et al* (2015) showed that the ratio of iNOS to Arginase-1 expression was related to *T. gondii* infection with a high ratio of iNOS/Arginase being associated with low infection rates. Based on this, a ratio of iNOS/Arginase-1 was calculated for both Dataset J (ImageJ readings from the randomised photos) and Dataset D (ImageJ readings from the matched photos). No significant correlations were found for Dataset J (r = -0.060; n = 49; P =

0.68) or Dataset D (r = -0.081; n = 46; *P* = 0.59). As there were some very noticeable outlier values for iNOS/Arginase from both datasets, any possible influence of these were explored by repeating the correlation analyses with the outlying results omitted. With this amendment, Dataset J (r = -0.070; n = 47; *P* = 0.64) and Dataset D (r = 0.084; n = 43; *P* = 0.59) still showed no significant correlation between the intensity of *Toxoplasma gondii* infection and the ratio of iNOS to Arginase-1.

The availability of large sample sets to analyse the distribution of *T. gondii* in naturally infected human lung tissue is sparse. This study offered the opportunity to investigate whether the parasite had any specific tissue or cellular preferences. Furthermore, it was an opportunity to explore the detailed distribution of arginase and iNOS within human lung tissue. Specific lung tissue/cell types were selected for identification in order to understand if there were any tissue/cell type specific differences in expression of iNOS and Arginase-1 and intensity of *T. gondii* infection and distribution. Secondly, some of these specific tissues/cells were investigated for co-localised expression of iNOS or Arginase-1 and the presence of *T. gondii* infection. This was done by identifying these specific lung tissues or cells using the 100x and 400x pooled images, counting them and quantifying whether they were positive or negative for expression or infection.

Smooth muscle and alveolar macrophages were investigated to see if a preference for infection could be determined, as well as their status for iNOS or Arginase-1 expression, in these lung tissue samples. Blood vessel endothelia and airway epithelial tissue were also opted for investigation into their rate of infection by *T. gondii*. Little is known if the latter tissues are favoured infection sites for *T. gondii,* but it has been observed that *T. gondii* is able to influence macrophage adherence to the endothelial wall to assist migration into the

peripheral tissues (Baba *et al,* 2017). It was also examined whether a directionality of infection could be ascertained from comparison of the proportion of infected epithelial tissue with the infection rate of endothelial tissue. A higher proportion of infected endothelial tissue would likely be indicative of *T. gondii* active infection arising from ingestion of the parasite or from endogenous reactivation of chronic toxoplasmosis. While infection by inhalation of oocysts might favour higher parasite detection in airway epithelia.

All analysed tissue types had high levels of infectivity. The proportion of *T. gondii* infected epithelial tissue was found not to be significantly different (P = 0.22) from that of the endothelial tissue. Thus, a directionality of infection could not be determined. Similarly, no significant difference (P = 0.77) was found between infectivity of endothelia and smooth muscle. This also made it difficult to determine whether tissue specific preferential *T. gondii* infection was present, or whether the parasite infection was distributed throughout.

A significant difference (P = 0.04) was found between the infection rate in smooth muscle and macrophages. Smooth muscle was infected at a higher rate than that of the macrophages. This motivated further study into the whether the proportion of Arginase-1 or iNOS positive counts were different between smooth muscle and macrophages. Similarly, there was a significant negative association between how Arginase-1 was expressed in smooth muscle and macrophages (P = <0.001). This was also found for iNOS within the two tissue/cell types (P = <0.001). Smooth muscle expressed proportionally less Arginase-1 as well as less iNOS than the macrophages.

In summation, *Toxoplasma gondii* appeared to have preferentially infected smooth muscle, endothelial and epithelial tissues over macrophages. Both Arginase-1 and iNOS expression was found to be proportionally higher in the macrophages than in smooth muscle tissue.

As previously stated, as far as could be determined through database searches, no literature could be retrieved about areas of lung tissue that the parasite preferentially infects. Therefore, no comparison to literature could take place. Arginase-1 and iNOS expression appears to support that of what has been found in the other analyses- that the level of iNOS specific staining is much higher than Arginase-1. As mentioned earlier, excessive Arginase-1 expression has been linked to the damage done in chronic inflammatory lung conditions (Durante, 2013; Lucas *et al,* 2014; Popovic *et al,* 2007; Yang & Ming, 2014). The subsequent reduction of NOS associated with this may also add to the damage (Hamad, Johnson, & Knox, 1999; Hamad & Knox, 2001; Kizawa *et al,* 2001; Patel *et al,* 1999; Wani *et al,* 2007). Therefore, it can be assumed that healthy lung tissue would not be expected to have high levels of Arginase-1. As far as could be determined, data could not be found on the healthy Arginase-1 to iNOS dynamic in lung tissue. Arginase-1 has been confirmed to be expressed in lungs. More specifically, macrophages and the epithelial, endothelial tissues, as well as fibroblasts are particularly important expressers of Arginase-1 (Carraway *et al*, 1998; Klasen *et al,* 2001). As previously mentioned in Chapter 1, this likely to do with its role in regulating airway dilation, blood vessel permeability, as well as immunosuppression and tissue repair (Grasemann *et al,* 2013; Hernandez *et al,* 2010; Lucas *et al,* 2013).

Like Arginase-1, iNOS is vital for lung health, but if highly expressed, can cause harmful effects to the tissue (Bagasra *et al,* 1995; Eizirik *et al,* 1996; Grabowski *et al,* 1997; Hamid *et al,* 1993; Kröncke *et al*, 1991; McInnes *et al,* 1996). Additionally, no research could be found on what a healthy baseline of iNOS consists of in healthy human lung tissue. However, Emert *et al* (2002) had sought to analyse different healthy lung tissues in Sprague Dawley rats for a quantification of iNOS expression with and without immune stimulation. In their study they had found lack of iNOS expression in lung endothelial tissue and smooth muscle surrounding

the large arteries, in normal conditions. Bronchial smooth muscle, as well as smooth muscle of smaller blood vessels were found to be expressed moderately. Alveolar macrophages as the epithelial cells of the first- and second-generation bronchus where also confirmed highly positive for iNOS expression in these rat lung control samples. Once stimulated with endotoxin (LPS), all the above tissues that were already expressing iNOS had increased their expression of iNOS, dose dependently. These findings are supportive of what was discussed in Chapter 1, about the need for balance, with reduced iNOS expression when it is not immediately required (Darnell, Kerr, & Stark, 1994), as in an active infection. Also previously mentioned was the increase in iNOS expression in regions of chronic inflammation (Bagasra *et al,* 1995; Eizirik *et al,* 1996; Grabowski *et al,* 1997; Hamid *et al,* 1993; Kröncke *et al*, 1991; McInnes *et al,* 1996) and cancer (Aaltoma, Lipponen, & Kosma, 2001; Kojima *et al,* 1999; Marrogi *et al,* 2000; Vakkala *et al,* 2000). This could explain why the expression of iNOS was found to be very high in these lung biopsy samples. As noted in Chapter 2 (Table 2.1), many of the patients had comorbid COPD alongside a lung cancer diagnosis as well as intense *T. gondii* infections.

Therefore, even though it appears that Arginase and iNOS play an important role in determining sensitivity and resistance to *Toxoplasma gondii* in mice and rats, this link is less clear in humans.

There are a number of strengths and limitations that can be attributed to this study. These will be explored next. Having access 51 lung biopsy samples that were previously confirmed to be *Toxoplasma gondii* positive was a substantial strength to this study. As the prevalence of *T. gondii* is estimated to be around 10% in the UK, obtaining a sample set of this magnitude would require over 500 subjects with a considerable amount of testing for the parasite and

additional preliminary diagnostics. This meant research could begin right away on how Arginase-1 and iNOS are expressed, and whether any interaction occurs with the intensity and spatial distribution of *T. gondii.*

Perhaps the most notable limitation was that imposed by the non-specific staining and cross-reaction of the secondary antibody. This is a common setback encountered in immunohistochemistry (Bussolati & Leonardo, 2008; Daneshtalab *et al,* 2010; Fritschy, 2008; Ramos-Vara, 2005), owing to the affinity of antibodies to macrophages- a vital component of the immune response. To counteract this major setback within the dataset, efforts were made to account for this over-staining. For the observational based analysis, such as that of Dataset E and F, the only option was omission. For the randomised images, samples with cross-reacting negative controls were omitted entirely. Whereas matched photos had more flexibility, allowing for small regions of tissue to be omitted from analysis only. For ImageJ based analysis, a measure was taken of the negative control photos to calculate a baseline 'background noise' reading for each of the samples. This reading was then subtracted from that taken of the stained photos; in the case of the randomised images an average reading from three negative control images were subtracted from the average ImageJ reading of the sample.

Another limitation regarding the data generation process was encountered with ImageJ. Occasionally ImageJ would incorrectly calculate the intensity and spread of staining - usually understating rather than overstating. When this occurred, there was the option to manually adjust the detection threshold by comparing the original photo with the ImageJ generated image isolating the stain pattern on a blank background. The intensity gradient could then be adjusted to increase or reduce intensity by lowering or increasing the threshold at which

yellow to brown hues of the image would be considered a positive DAB stain indication. Naturally, this was susceptible to unconscious manipulation of the readings. However, the benefit of having the generation of lots of data in addition to trying to be as impartial as possible, limited the scope of the impact of this.

Software ImageJ was a substantial asset to this study; being able to calculate the percentage of stain coverage of *T. gondii,* Arginase-1, and iNOS in a photo snapshot of the stained lung section slide was highly advantageous. The amendments made to the Bajnok *et al* (2019) ImageJ methodology also improved the precision of the analysis. Processing of the images in this way quickly uncovered a substantial risk of data skewing- particularly with those obtained from the randomised images. This was due to the absence of the factoring in of the amount of lung tissue present on the field of view under analysis. Fluctuations massively under or overstating the stain percentage of coverage would greatly impact on the reliability of the results of this study, particularly impacting on the comparisons (*i.e., T. gondii vs* Arginase-1 or iNOS). Accounting for tissue coverage in lung tissue is especially important, due to the variability in tissue density of the lung structures. For example, the structure of the alveolus is thin, and sponge like in appearance as they are the site of gas exchange, where inhaled oxygen diffuse into the bloodstream and somatic carbon dioxide diffuses out of the bloodstream and into the alveoli sac. Contrastingly, areas of connective tissue surrounding major blood vessels and airways will have a higher density of tissue coverage. As such, comparing the proportion of staining between the two without reference to the amount of tissue on an analysed image presented a risk of bias to the analysis. Therefore, by calculating a percentage of tissue coverage in a photo, then dividing this into the percentage coverage of the *T. gondii,* Arginase-1, or iNOS specific staining; stronger, more reliable results were generated.

Investigating selected lung tissue or cell types for *T. gondii,* Arginase-1, or iNOS specific distribution and expression was an important analytical tool to strengthen the reliability. Although not observed in these results, if significant (positive or negative) correlations were found between *T. gondii* and either Arginase or iNOS in the other analyses, this type of investigation could help determine whether this correlation was incidental (*i.e.,* due to tissue specific infection or expression, independent of one another), or was occurring independent of the type of lung tissue (*i.e.,* a true correlative relationship). Thus, strengthening the outcomes. However, limitations were recognised with this methodology. These mainly centred around precise identification of the cell or tissue. Smooth muscle was difficult to distinguish between areas of lung connective tissue, as well as similarities were found between some smaller airways and smaller blood vessels. Most major though, was the potential bias towards the positively stained tissues. The brown DAB stain made cells, such as macrophages, more easily identifiable. Although human error will always factor into this type of analysis, efforts were made to be as precise as possible.

Additionally, human error will have also factored into the generation of Dataset E. This type of data had been collected from overlaid grid coordinates assigned categories based on the intensity of staining; whereby brown to dark brown staining represented a 'high', and beige staining represented 'low'. Unstained coordinates were categorised as 'nil'. As with any subjectively assigned category, precision limitations are met- with there being the potential for a level of overlap in readings that could be classified into more than one category.

As discussed earlier, different levels of localised analysis were utilised in the study. There was a need for an optimal balance between larger datasets and specificity of data. One critique of this study would concern whether analysis was specific enough. It would have been very

advantageous to be able to compare *T. gondii* infection and within that same cell to look and see if Arginase-1 or iNOS was expressed- particularly if this type of study could be scaled up. Unfortunately, this type of analysis was not possible with these immunohistochemically stained slides. This is because one stain could be applied to a section slide only. Therefore, for each of the three (and two negative controls) stains, one slice of the tissue sample block was required. Each slice thickness was 5µm, and not all slices were cut entirely consecutively, so it was not possible to ensure the same cell was present, even in matched fields of view of the sections. However, tissue structures and groupings could be analysed- and this was utilised in this study. Multi-staining and analysis of a single slide is possible with immunofluorescence staining and confocal microscopy, and this will be discussed further later as a potential methodology for further study. One finding where this may have had a notable impact was that of the analysis of the Grade 1 (low) infected categorised samples (between *T. gondii* and Arginase-1). Here the P-value was approaching significance ($P = 0.08$), and had this P-value been <0.05, the correlation coefficient of 0.430 would have indicated a weak positive correlation between *T. gondii* and Arginase-1 expression these low-grade infected samples. Though the finding concludes there being no correlation, this cannot be fully ruled out. The potential lack of precision in the data is driven by this larger spread of the results (*i.e.,* lack of specificity to individual cells). It is possible that this data precision could be overcome with a larger sample set, or it could be that due to the technical limitations, this remains close to the optimum accuracy of what can be achieved with this type of study conducted in this way.

Similarly, this data imprecision impacts on the quality of the conclusions that can be drawn from this investigation. Throughout most of this study no correlation could be found between *T. gondii* and Arginase-1 or iNOS expression, with iNOS expression being significantly high throughout the sample set independent of *T. gondii.* However, in the higher precision

analyses, where fields of view were divided into grids, there was evidence of an association between *T. gondii* distribution and higher Arginase expression. In terms of iNOS, these studies also showed that *T. gondii* distribution was approaching a significant association with higher levels of *T. gondii* infection and lower iNOS distribution.

With the exception of the analysis of Dataset E (colocalised grid data), as well as part of the analysis within the assigned infection grade categories, all results unilaterally supported the hypothesis of there being no correlation between the spatial distribution of *Toxoplasma gondii* with the expression of Arginase-1 and iNOS in these lung biopsy tissue samples. Although, iNOS was expressed significantly (P = <0.001) higher than Arginase-1, the extent of *T. gondii* presence remained high. This conclusion did not align with what was found by similar studies in model mice and rat lines (Gao *et al,* 2015; Li *et al,* 2012; Zhao *et al,* 2013). These studies had found an association between increased Arginase-1 expression and sensitivity to *T. gondii* infection; as well as the reverse for iNOS whereby an increase in expression was associated with resistance to the parasite. Even after calculation and comparison of the ratio of iNOS/Arginase-1 to *T. gondii* infection, as was used by Gao *et al* (2015), no correlation (positive or negative) could be found. As was discussed in the previous paragraph, it may be that analyses utilised in this study are not precise enough to detect any dynamics between *T. gondii* and Arginase-1 or iNOS and so it would be imprudent to definitively conclude that no such correlation within these lung tissues is present. Additionally, it must be noted that the comparable studies discussed here were carried out on peritoneal macrophages of rats and mice as well as the alveolar macrophages of rats *in vitro* and *in vivo.*

Moreover, to be considered was that most of this investigation was conducted on a section of lung tissue, rather than solely on alveolar macrophages, as were studied in the Zhao *et al*

(2013) article. However, alveolar macrophages were looked at and compared against smooth muscle in these biopsy tissue samples, and a significant negative association (P = 0.04) was found between the proportion of cells/tissue that were *T. gondii* infected. Because of this, the number of alveolar macrophages and areas of smooth muscle that were also positive or negative for Arginase-1 or iNOS expression were calculated. The expression of both Arginase-1 and iNOS were significantly different (P = <0.001) between the tissue/cell types. Curiously, smooth muscle had a lower overall proportion of Arginase-1 and iNOS positives but also a higher proportion of *T. gondii* positive tissues. Again, this is partially supportive of the Zhao *et al* (2013) findings, but also indicative of the likelihood of no such correlation being detectable within the data of this study. As suggested earlier, it may be the broadness of this analysis that has contributed to this outcome.

As previously mentioned earlier, there may indeed be a positive correlation between *T. gondii* and Arginase-1 in this lung tissue, but the datasets are not specific enough for this to be picked up. Two results not aligned with findings where that of Figure 3.18 and Figure 3.23- both from the analysis of Arginase-1 and iNOS with *T. gondii* in samples assigned to a group based on their infection intensity. Figure 3.18, approaching significance (P = 0.08), indicated a weak positive correlation between *T. gondii* and Arginase-1 for the Grade 1 (low) infected samples. Whereas Figure 3.23 indicated a significant moderate positive correlation between *T. gondii* and iNOS for the Grade 2 (moderate) infected samples. This seemingly appears contradictory and could either be a sign that the obtained results are unable to form strong conclusions with or could be indicative that of the more intensely infected samples, those that were on the higher range of infectivity, also saw more iNOS expression. Similarly, those at the higher range of the low infected sample grouping, where more likely to occur at areas of higher Arginase-1 expression. Emert *et al* (2002) would support the former finding. They had found

dose-dependent increased iNOS expression in a range of different lung tissues, not just immune system cells, in response to endotoxin stimulation. This may also support the idea of the high intensity of iNOS expression impeding detection of any correlative relationships between *T. gondii* and Arginase-1 or iNOS. In regards to human lung tissue, some recent research is highlighting the importance of iNOS to promotion of *T. gondii* infection (Bando *et al,* 2018a; Bando *et al,* 2018b), rather than just an immune response effect. As described in Chapter 1, *T. gondii* has a repertoire of effector proteins for host manipulation. Here the Bando *et al* (2018) studies found, in *in vitro* human cell lines, that effector protein GRA15 inhibited the important anti-*T. gondii* IDO1 protein. In doing this, it had the effect of stimulating the expression of iNOS. Indole 2,3-deoxygenase 1 (IDO1) is an important protein in the immune response against *T. gondii*, and is induced by IFN-γ. With inhibition of this pathway, the parasite was able to proliferate in the cell cultures- irrespective of the increased expression of iNOS resulting from this. This would infer that disarming the inducement of IDO1 is more critical for survival and proliferation than the avoidance of iNOS in human cells.

Although *in vivo* studies in various mammals have established a high likelihood of *Toxoplasma gondii* presence in the lungs in an active infection (Dubey, 1997b; Dubey and Carpenter, 1993; Meyer, Allen, & Beaman, 2000), as far as can be determined, little is known about the typical distribution of *T. gondii* specific to the lungs during active infection in animals and humans alike. Similarly, a medical case study of an immunocompromised child as well as another of a lung cancer patient (but with no immunosuppressive ongoing treatment), had found diffuse *T. gondii* presence in their lung tissue with no reference to specific, favoured regions, or were deemed to be exocytic (Arnold *et al,* 1997; Lu *et al,* 2015). It may be that the ubiquity of this parasite to infect a large variety of tissue types mean that there is no distinct pattern to the distribution- the findings of this study would seem to support this. The vascular anatomy of

the lungs would certainly aid distribution and the tendency towards inhibition of a strong immune response offers an idyllic host organ for parasitism (Newton, Cardani & Braciale, 2016). This might be why no significant difference was observed between endo and epithelial tissue ($P = 0.22$) and also between smooth muscle and endothelial tissue ($P = 0.77$).

In piecing together conclusions, it is important to also consider that the lung samples utilised in this study were not from healthy volunteers, but instead taken from a region surrounding a malignant carcinoma. As previously discussed in Chapter 1, It has been noted that there tends to be a localised area of immunosuppression within the tumour microenvironment and that iNOS, bizarrely, could be the causative agent in this (Ekmekcioglu, Grimm, & Roszik, 2017; Jayaraman *et al,* 2014). This could explain both the high expression of iNOS as well as the intense *T. gondii* infections observed in these lung biopsy samples. Or it could be that *T. gondii* itself is driving some of this increase in iNOS expression (Bando *et al,* 2018a; Bando *et al,* 2018b). Although it is beyond the scope of this study to be able to conclude either explanation.

Ultimately, likely due to the difficulty in such experiments, much is unknown about many of the dynamics of *T. gondii* when inside its human host, and it appears it may be much more complicated than what has been found in mice and rat models.

There are a number of avenues of future work that could be explored from this project. Firstly, a major impact on interpreting these results is the lack of precision of the data used in these studies. A method of improving this precision would be to either increase the sample size or to implement more cell specific analysis.

One way to increase the dataset would be to partner up with more NHS Foundation Trusts and try to obtain more lung biopsy tissue samples, taken from lung cancer patients. These

samples would need to be screened for the presence of *Toxoplasma gondii* prior to any similar study.

Alongside this and going forward, it would be useful to extend this study into *in vivo* mice models. Specifically, it would be useful to obtain a baseline of Arginase-1 and iNOS expression in healthy mouse lung tissue as well as within mice with lung cancer- with and without *T. gondii* infection. Perhaps looking at lung tissue as a whole, as well as extending the research into alveolar macrophages and their susceptibility to *T. gondii* in health and disease. This type of study could mirror that executed by Emert *et al* (2002), whereby the lungs of control rats were analysed as well as those that were stimulated with LPS endotoxin.

Similarly, and perhaps more informative, it would be useful to expand this study into *T. gondii* and Arginase-1 and iNOS within human cell lines. This may address the difficulties in obtaining healthy human lung tissue samples in addition to the inability to study *T. gondii* infection *in vivo* in humans. CRISPR/CAS9 editing of the genes could then be applied to investigate the impact of removal of one of the proteins has on the distribution of the parasite.

Specificity has been mentioned as a major limitation to this study. Therefore, it would be beneficial to expand this research using immunofluorescence techniques. Like with the immunohistochemistry utilized in this study, immunofluorescence relies on specialist dyes for very specific staining. However, with this technique, analysis can occur on a cell-by-cell basis, achieving the specificity that was lacking in this study.

Overall, this is an important, novel area of research that requires more study.

Appendix

Percentage stain coverage obtained from the matched images (Dataset A-D) as well as of lung tissue on the ImageJ inputted photo. See Table 3.1

Sample	*T. gondii*				Arginase-1				iNOS			
	Tissue Coverage	Dataset A	Dataset B	Dataset C	Tissue Coverage	Dataset A	Dataset B	Dataset C	Tissue Coverage	Dataset A	Dataset B	Dataset C
812	49.5	18.3	36.9	36.6	57.1	7.0	12.2	9.2	45.4	35.1	77.3	74.3
818	52.6	14.9	28.4	28.2	61.5	28.3	46.0	45.8	68.8	27.9	40.6	40.4
819	54.5	17.4	31.9	31.9	60.6	2.5	4.1	4.1	54.8	31.0	56.5	56.5
821	40.2	19.6	48.9	48.4	34.1	0.1	0.3	0.0	45.1	28.2	62.4	62.1
822	35.6	31.9	89.6	89.2	45.2	1.0	2.2	1.8	25.5	19.8	77.8	77.4
823	47.1	7.9	16.8	16.8	52.1	2.8	5.4	5.4	52.3	25.2	48.2	48.2
827	56.5	14.4	25.4	25.4	46.6	16.4	35.2	35.2	47.1	13.5	28.7	28.7
828	29.8	10.4	35.0	35.0	32.6	0.6	1.7	1.2	23.2	15.0	64.7	64.2
965	56.4	5.9	10.4	9.7	58.7	0.6	1.0	0.9	57.9	38.2	65.9	65.7
968	45.8	13.4	29.3	29.3	52.3	1.9	3.6	3.6	64.9	31.2	48.0	47.9
972	48.7	4.1	8.3	8.3	42.6	0.2	0.5	0.3	39.5	20.4	51.6	51.4
973	53.5	10.6	19.9	1.5	58.8	4.7	8.0	3.3	62.8	14.3	22.8	18.2
975	32.1	7.9	24.6	2.2	39.7	4.5	11.3	-6.8	43.1	13.3	31.0	12.9
979	50.2	13.9	27.7	26.9	44.6	3.4	7.7	7.4	47.1	27.4	58.3	58.0
985	30.1	1.7	5.8	4.3	59.4	2.2	3.7	3.1	63.1	20.6	32.7	32.1
988	57.4	2.2	3.8	2.7	65.8	0.1	0.1	0.1	60.6	20.3	33.4	33.4
989	57.7	5.7	9.9	9.1	56.2	0.7	1.2	1.2	31.5	22.3	70.8	70.8
997	43.4	19.4	44.7	44.7	48.4	3.4	7.0	7.0	59.4	25.4	42.7	42.7
999	44.2	18.7	42.2	42.1	54.5	4.2	7.7	7.6	51.8	22.1	42.7	42.5
1005	45.5	7.3	16.1	16.1	46.7	1.2	2.6	2.6	50.4	15.0	29.7	29.7
1006	51.5	18.5	35.9	35.9	47.6	2.3	4.9	4.9	53.2	38.0	71.4	71.4

1008	49.7	4.5	9.0	9.0	53.4	1.3	2.5	2.5	66.4	9.7	14.6	14.6
1013	52.0	13.6	26.2	26.2	53.3	11.7	21.9	21.9	63.2	21.1	33.4	33.4
1014	59.4	24.2	40.7	40.7	54.5	20.8	38.1	38.1	67.5	32.8	48.5	48.5
1017	40.8	20.8	51.1	51.1	46.1	3.4	7.3	7.3	46.7	14.4	30.8	30.8
1018	45.9	18.3	39.9	39.6	52.5	27.8	53.0	50.4	41.9	34.3	81.9	79.3
1025	50.2	20.6	41.0	40.8	53.9	2.9	5.3	5.3	53.6	29.8	55.5	55.5
1026	55.2	22.5	40.8	40.8	46.9	6.3	13.5	13.5	43.3	27.3	63.1	63.1
1028	38.8	16.9	43.6	43.6	26.2	0.9	3.3	3.3	30.3	16.0	52.7	52.7
1029	49.2	7.3	14.9	13.8	32.3	1.2	3.7	2.9	51.0	28.8	56.4	55.7
1030	41.1	19.8	48.1	48.1	61.4	0.4	0.7	0.7	67.0	14.4	21.5	21.5
1032	51.3	24.8	48.2	48.0	58.5	0.2	0.4	0.4	56.6	8.1	14.3	14.3
1033	58.9	10.3	17.4	16.9	75.1	0.2	0.3	0.3	59.3	17.2	29.0	29.0
1037	38.1	11.3	29.6	29.4	33.1	0.1	0.3	-1.3	51.3	19.6	38.3	36.6
1040	31.4	20.1	64.0	63.4	27.6	0.5	1.7	1.7	24.0	13.1	54.8	54.8
1043	33.5	12.4	37.2	37.0	31.9	0.6	1.7	1.4	38.5	12.7	32.9	32.6
1047	46.7	10.1	21.6	21.1	40.9	0.2	0.4	0.0	42.0	20.0	47.7	47.3
1052	48.7	14.4	29.7	29.7	48.4	0.8	1.7	1.7	60.7	11.2	18.4	18.4
1054	37.9	27.0	71.2	70.8	52.1	0.5	0.9	0.9	48.5	12.5	25.9	25.9
1064	41.5	20.8	50.1	50.1	46.0	0.1	0.2	0.2	51.6	1.6	3.1	3.1
664	33.6	8.2	24.4	24.4	38.0	3.4	8.9	8.9	44.2	16.2	36.6	36.6
757	47.5	13.5	28.4	28.4	46.6	1.5	3.2	2.9	55.6	24.1	43.4	43.2
813	65.9	14.8	22.5	22.5	67.6	0.4	0.6	0.4	65.3	8.6	13.1	13.0
976	44.0	0.2	0.5	-1.8	57.8	1.5	2.6	1.9	34.7	14.0	40.5	39.7
1004	39.5	13.7	34.8	34.6	53.9	0.6	1.1	0.8	45.6	14.5	31.7	31.4
1045	40.0	9.0	22.5	22.5	27.2	0.7	2.6	2.6	39.2	6.6	16.9	16.9
1067	69.1	32.2	46.6	46.5	57.5	2.5	4.4	3.5	61.7	14.2	23.0	22.1
1068	53.3	13.1	24.5	23.9	56.7	1.7	3.0	2.4	51.7	16.7	32.4	31.8
1069	56.8	16.5	29.0	27.5	60.2	1.0	1.6	0.9	61.7	11.0	17.8	17.1
1071	69.2	6.8	9.8	9.4	46.1	0.3	0.7	0.7	75.9	9.9	13.0	13.0
1072	54.0	9.7	18.0	18.0	60.1	1.5	2.5	2.5	52.9	13.5	25.5	25.5

ImageJ readings of the percentage of stain coverage obtained from the randomised images (Dataset G-J). See Table 3.1

Sample	*T. gondii*			Arginase-1			iNOS		
	Dataset G	Dataset H	Dataset I	Dataset G	Dataset H	Dataset I	Dataset G	Dataset H	Dataset I
812	3.1	5.5	5.4	0.8	1.4	1.1	17.0	34.5	34.2
818	12.1	36.0	35.8	7.4	11.6	10.6	20.0	39.7	38.8
819	6.0	14.2	14.2	3.8	7.5	7.5	21.6	41.1	41.1
821	2.0	4.2	3.9	0.8	2.7	2.3	25.9	63.0	62.6
822	2.8	6.5	6.3	4.6	9.1	8.8	33.3	55.1	54.8
823	4.8	9.4	9.4	1.4	2.7	2.7	22.1	39.1	39.1
827	8.1	16.6	16.6	5.2	9.9	9.9	26.3	45.5	45.5
828	9.6	21.6	21.6	2.9	6.7	6.2	16.5	30.8	30.3
965	4.0	7.6	-3.3	3.1	5.2	5.0	35.1	56.7	56.4
968	0.7	1.5	1.5	0.9	1.9	1.5	24.6	50.9	50.5
972	0.7	2.1	2.1	0.5	1.1	0.8	19.1	50.0	49.8
973	2.6	5.5	0.8	4.7	9.8	8.5	25.1	53.7	52.3
975	2.1	5.0	2.1	2.2	4.0	0.2	15.5	41.1	37.4
979	1.5	3.6	1.3	0.4	0.9	0.6	22.7	71.5	71.2
985	0.6	1.5	-1.6	1.8	4.3	3.9	32.3	84.1	83.8
988	4.7	11.9	10.1	0.9	1.7	1.7	22.7	40.1	40.1
989	2.9	7.0	6.2	1.8	4.5	4.5	32.5	68.7	68.7
997	11.2	25.5	25.5	1.8	4.0	4.0	27.0	54.7	54.7
999	10.8	45.0	44.4	13.3	28.2	27.7	22.5	92.2	91.7
1005	5.4	13.0	13.0	2.5	9.2	9.2	21.5	74.2	74.2
1006	5.9	16.5	16.5	8.8	30.6	30.6	23.3	62.8	62.8
1008	13.5	30.4	30.4	0.8	1.6	1.6	6.6	14.1	14.1
1013	14.0	33.6	33.6	2.4	5.3	5.3	20.5	60.9	60.9
1014	7.7	27.6	27.6	9.2	18.3	18.3	24.9	61.7	61.7
1017	10.4	35.4	35.4	8.3	20.0	20.0	19.2	75.1	75.1
1018	17.7	37.3	34.3	16.9	33.1	30.7	16.1	81.9	79.5
1025	17.0	51.2	51.0	1.2	2.3	2.3	24.5	58.6	58.6
1026	12.0	43.1	43.1	3.2	7.8	7.8	18.1	77.4	77.4
1028	14.5	59.6	59.6	1.7	4.5	4.5	22.4	60.3	60.3
1029	12.0	55.9	55.7	1.2	2.9	2.8	21.0	56.5	56.4
1030	13.4	26.1	26.1	0.0	0.1	0.1	9.6	23.5	23.5
1032	19.8	55.4	54.2	2.7	7.4	7.4	19.6	41.2	41.2
1033	10.5	53.2	52.9	0.6	1.9	1.9	16.2	98.1	98.1
1037	12.2	35.1	34.9	0.9	1.5	0.2	24.9	57.2	55.9
1040	17.1	52.5	52.2	1.8	5.0	5.0	11.3	47.5	47.5
1043	6.7	19.8	19.6	0.7	1.5	0.7	8.8	36.6	35.8
1047	16.1	59.6	58.9	0.9	2.8	2.2	23.9	50.7	50.1
1052	14.0	38.2	38.2	2.4	4.2	4.2	20.3	33.0	33.0
1054	16.4	48.4	48.1	0.2	0.6	0.6	4.6	21.6	21.6
1064	8.7	27.8	27.8	1.6	3.0	3.0	14.3	40.2	40.2
664	11.0	26.5	26.5	4.9	11.4	11.4	13.9	28.8	28.8

757	8.1	28.0	28.0	4.5	10.7	10.2	17.3	38.5	37.9
813	20.0	46.2	46.2	0.9	1.5	1.1	10.9	23.2	22.9
976	0.2	0.9	0.0	0.6	2.6	1.8	3.1	10.5	9.7
1004	10.2	34.3	30.7	2.7	4.9	3.1	20.0	31.4	29.6
1045	14.4	41.3	41.3	0.1	0.1	0.1	4.1	8.0	8.0
1067	23.2	42.1	41.9	1.3	2.1	1.8	19.3	39.3	39.0
1068	13.6	37.9	37.7	1.9	6.0	5.7	12.1	35.2	34.9
1069	15.2	29.9	29.6	0.8	1.6	1.3	11.9	22.7	22.3
1071	14.0	38.4	37.9	1.0	2.8	2.8	7.0	13.2	13.2
1072	8.0	21.4	21.4	3.1	7.0	7.0	9.2	29.0	29.0

Samples with their *T. gondii* infection intensity grade, as assigned in Bajnok *et al* (2019), as well as applying their grading system to readings in this study as well as the adapted grade assigned and utilised within this study (Dataset J). Infection grade analysis can be found in Subsection 3.3.6

Sample	Assigned Infection Grade	Infection Grade as per Bajnok *et al* (2019) guidelines	Infection Grade Assigned in Bajnok *et al* (2019)
812	1	1	2
818	2	3	3
819	1	2	3
821	1	1	1
822	1	1	2
823	1	1	2
827	1	2	2
828	2	3	2
965			1
968	1	1	1
972	1	1	2
973	1	1	1
975	1	1	1
979	1	1	1
985			3
988	1	2	2
989	1	1	1
997	2	3	3
999	3	3	1
1005	1	2	2
1006	1	2	3
1008	2	3	2
1013	2	3	3
1014	2	3	3
1017	2	3	1
1018	2	3	1

1025	3	3	1
1026	3	3	1
1028	3	3	1
1029	3	3	1
1030	2	3	1
1032	3	3	2
1033	3	3	1
1037	2	3	3
1040	1	3	2
1043	3	2	2
1047	3	3	2
1052	3	3	1
1054	3	3	3
1064	2	3	3
664	2	3	3
757	2	3	2
813	3	3	2
976	1	1	1
1004	2	3	3
1045	3	3	1
1067	3	3	2
1068	3	3	2
1069	2	3	3
1071	3	3	2
1072	2	2	2

Grid coordinate data analysis (Dataset E), as analysed in Subsection 3.3.5 and 3.3.7

	T. gondii High	*T. gondii* Low	*T. gondii* Nil	iNOS High	iNOS Low	iNOS Nil
Arginase-1 High	226	34	2	246	2	3
Arginase-1 Low	265	132	11	362	43	8
Arginase-1 Nil	45	20	2	56	9	2
iNOS High	505	171	12			
iNOS Low	28	19	2			
iNOS Nil	10	2	1			

Tissue specific staining data (Dataset F), as analysed in Subsection 3.3.8

	Smooth muscle	**Macrophages**	**Epithelia**	**Endothelia**
T. gondii positive	46 (92%)	483 (79%)	221 (94%)	76 (89%)
T. gondii negative	4 (8%)	125 (21%)	14 (6%)	9 (11%)
Arginase-1 positive	12 (41%)	486 (76%)		
Arginase-1 negative	17 (59%)	151 (24%)		
iNOS positive	55 (50%)	729 (95%)		
iNOS negative	55 (50%)	35 (5%)		

References

Aaltoma, S. H., Lipponen, P. K., & Kosma, V. M. (2001). Inducible nitric oxide synthase (iNOS) expression and its prognostic value in prostate cancer. *Anticancer research*, *21*(4B), 3101–3106.

Abdel Malek, R., Wassef, R., Rizk, E., Sabry, H., Tadros, N., & Boghdady, A. (2018). Toxoplasmosis an Overlooked Disease: Seroprevalence in Cancer Patients. *Asian Pacific journal of cancer prevention : APJCP*, *19*(7), 1987–1991. doi:10.22034/APJCP.2018.19.7.1987

Adams, L. B., Hibbs, J. B., Jr, Taintor, R. R., & Krahenbuhl, J. L. (1990). Microbiostatic effect of murine-activated macrophages for Toxoplasma gondii. Role for synthesis of inorganic nitrogen oxides from L-arginine. *Journal of immunology (Baltimore, Md. : 1950)*, *144*(7), 2725–2729.

Alaganan, A., Fentress S. J., Tang, K., Wang, Q., & Sibley, L. D. (2014). Toxoplasma GRA7 effector increases turnover of immunity-related GTPases and contributes to acute virulence in the mouse. *Proc Natl Acad Sci U S A, 111*, 1126–1131. doi:10.1073/pnas.1313501111

Alberg, A. J., Brock, M. V., Ford, J. G., Samet, J. M., & Spivack, S. D. (2013). Epidemiology of lung cancer: Diagnosis and management of lung cancer, 3rd ed: American College of Chest Physicians evidence-based clinical practice guidelines. *Chest*, *143*(5 Suppl), e1S–e29S. doi:10.1378/chest.12-2345

Alberg, A. J., Brock, M. V., & Samet, J. M. (2005). Epidemiology of lung cancer: looking to the future. *Journal of clinical oncology : official journal of the American Society of Clinical Oncology*, *23*(14), 3175–3185. doi:10.1200/JCO.2005.10.462

Alexander, J., Scharton-Kersten, T. M., Yap, G., Roberts, C. W., Liew, F. Y., & Sher, A. (1997). Mechanisms of innate resistance to Toxoplasma gondii infection. *Philosophical transactions of the Royal Society of London. Series B, Biological sciences*, *352*(1359), 1355–1359. doi:10.1098/rstb.1997.0120

Anvari, D., Sharif, M., Sarvi, S., Aghayan, S, A., Gholami, Shirzad, P., . . . Daryani, A. (2019). Seroprevalence of Toxoplasma gondii infection in cancer patients: A systematic review and meta-analysis. *Microbial Pathogenesis, 129*, 30-42.

Archontogeorgis, K., Steiropoulos, P., Tzouvelekis, A., Nena, E., & Bouros, D. (2012). Lung cancer and interstitial lung diseases: a systematic review. *Pulmonary medicine*, *2012*, 315918. doi:10.1155/2012/315918

Arnold, S. J., Kinney, M. C., McCormick, M. S., Dummer, S., & Scott, M. A. (1997). Disseminated toxoplasmosis. *Archives of Pathology & Laboratory Medicine, 121*(8), 869-73.

Aubry, M. C., Myers, J. L., Douglas, W. W., Tazelaar, H. D., Washington Stephens, T. L., Hartman, T. E., Pankratz, V. S. (2002). Primary pulmonary carcinoma in patients with idiopathic pulmonary fibrosis. *Mayo Clinic proceedings*, *77*(8), 763–770. doi:10.4065/77.8.763

Baba, M., Batanova, T., Kitoh, K., & Takashima, Y. (2017). Adhesion of Toxoplasma gondii tachyzoite-infected vehicle leukocytes to capillary endothelial cells triggers timely parasite egression. *Scientific reports*, *7*(1), 5675. doi:10.1038/s41598-017-05956-z

Baddley, J. W., Winthrop, K. L., Chen, L., Liu, L., Grijalva, C. G., Delzell, E. . . . Curtis, J. R. (2014). Non-viral opportunistic infections in new users of tumour necrosis factor inhibitor therapy: results of the SAfety Assessment of Biologic ThERapy (SABER) study. *Annals of the rheumatic diseases*, *73*(11), 1942–1948. doi:10.1136/annrheumdis-2013-203407

Bagasra, O., Michaels, F. H., Zheng, Y. M., Bobroski, L. E., Spitsin, S. V., Fu, Z. F. . . . Koprowski, H. (1995). Activation of the inducible form of nitric oxide synthase in the brains of patients with multiple sclerosis. *Proceedings of the National Academy of Sciences of the United States of America*, *92*(26), 12041–12045. doi:10.1073/pnas.92.26.12041

Bajnok, J., Tarabulsi, M., Carlin, H., Bown, K., Southworth, T., Dungwa, J. . . . Hide, G. (2019). High frequency of infection of lung cancer patients with the parasite Toxoplasma gondii. *ERJ Open Research, 5*(2). doi:00143-2018-2018.atom.

Bando, H., Lee, Y., Sakaguchi, N., Pradipta, A., Ma, J. S., Tanaka, S. . . . Yamamoto, M. (2018a). Inducible Nitric Oxide Synthase Is a Key Host Factor for *Toxoplasma* GRA15-Dependent Disruption of the Gamma Interferon-Induced Antiparasitic Human Response. *mBio*, *9*(5), e01738-18. doi:10.1128/mBio.01738-18

Bando, H., Sakaguchi, N., Lee, Y., Pradipta, A., Ma, J. S., Tanaka, S. . . . Yamamoto, M. (2018b). *Toxoplasma* Effector TgIST Targets Host IDO1 to Antagonize the IFN-γ-Induced Anti-parasitic Response in Human Cells. *Frontiers in immunology*, *9*, 2073. doi:10.3389/fimmu.2018.02073

Behnke, M. S., Khan, A., Wootton, J. C., Dubey, J. P., Tang, K., & Sibley, L. D. (2011). Virulence differences in Toxoplasma mediated by amplification of a family of polymorphic pseudokinases. *Proceedings of the National Academy of Sciences of the United States of America*, *108*(23), 9631–9636. doi:10.1073/pnas.1015338108

Bekpen, C., Hunn, J. P., Rohde, C., Parvanova, I., Guethlein, L., Dunn, D. M. . . . Howard, J. C. (2005). The interferon-inducible p47 (IRG) GTPases in vertebrates: loss of the cell autonomous resistance mechanism in the human lineage. *Genome biology*, *6*(11), R92. doi:10.1186/gb-2005-6-11-r92

Benedetto, N., Folgore, A., Ferrara, C., & Galdiero, M. (1996). Susceptibility to toxoplasmosis: correlation between macrophage function, brain cyst formation and mortality in rats. *The new microbiologica*, *19*(1), 47–58.

Bierly, A. L., Shufesky, W. J., Sukhumavasi, W., Morelli, A. E., & Denkers, E. Y. (2008). Dendritic cells expressing plasmacytoid marker PDCA-1 are Trojan horses during Toxoplasma gondii

infection. *Journal of immunology (Baltimore, Md. : 1950)*, *181*(12), 8485–8491. doi:10.4049/jimmunol.181.12.8485

Böhme, G. A., Bon, C., Lemaire, M., Reibaud, M., Piot, O., Stutzmann, J. M. . . . Blanchard, J. C. (1993). Altered synaptic plasticity and memory formation in nitric oxide synthase inhibitor-treated rats. *Proceedings of the National Academy of Sciences of the United States of America*, *90*(19), 9191–9194. doi:10.1073/pnas.90.19.9191

Bozzetti, F., Paladini, I., Rabaiotti, E., Franceschini, A., Alfieri, V., Chetta, A. . . . Sverzellati, N. (2016). Are interstitial lung abnormalities associated with COPD? A nested case-control study. *International journal of chronic obstructive pulmonary disease*, *11*, 1087–1096. doi:10.2147/COPD.S103256

Bradley, P. J., Ward, C., Cheng, S. J., Alexander, D. L., Coller, S., Coombs, G. H. . . . Boothroyd, J. C. (2005). Proteomic analysis of rhoptry organelles reveals many novel constituents for host-parasite interactions in Toxoplasma gondii. *The Journal of biological chemistry*, *280*(40), 34245–34258. doi:10.1074/jbc.M504158200

Brüne, B., Weigert, A., & Dehne, N. (2015). Macrophage Polarization In The Tumor Microenvironment. *Redox Biology, 5*, 419.

Burney, P. G., Patel, J., Newson, R., Minelli, C., & Naghavi, M. (2015). Global and regional trends in COPD mortality, 1990-2010. *The European respiratory journal*, *45*(5), 1239–1247. doi:10.1183/09031936.00142414

Bussolati, G., & Leonardo, E. (2008). Technical pitfalls potentially affecting diagnoses in immunohistochemistry. *Journal of clinical pathology*, *61*(11), 1184–1192. doi:10.1136/jcp.2007.047720

Cabral, G., Wang, Z. T., Sibley, L. D., & DaMatta, R. A. (2018). Inhibition of Nitric Oxide Production in Activated Macrophages Caused by *Toxoplasma gondii* Infection Occurs by Distinct Mechanisms in Different Mouse Macrophage Cell Lines. *Frontiers in microbiology*, *9*, 1936. doi:10.3389/fmicb.2018.01936

Cakir M. V. & Allmer J. (2010). Systematic computational analysis of potential rnai regulation in *Toxoplasma Gondii*, in 2010 5th International Symposium on Health Informatics and Bioinformatics (Antalya: IEEE;), 31–38. doi:10.1109/HIBIT.2010.5478909

Calabrese, V., Mancuso, C., Calvani, M., Rizzarelli, E., Butterfield, D. A., & Stella, A. M. (2007). Nitric oxide in the central nervous system: neuroprotection versus neurotoxicity. *Nature reviews. Neuroscience*, *8*(10), 766–775. doi:10.1038/nrn2214

Caldwell, R. W., Rodriguez, P. C., Toque, H. A., Narayanan, S. P., & Caldwell, R. B. (2018). Arginase: A Multifaceted Enzyme Important in Health and Disease. *Physiological reviews*, *98*(2), 641–665. doi:10.1152/physrev.00037.2016

Campbell, A. L., Goldberg, C. L., Magid, M. S., Gondolesi, G., Rumbo, C., & Herold, B. C. (2006). First case of toxoplasmosis following small bowel transplantation and systematic review of

tissue-invasive toxoplasmosis following noncardiac solid organ transplantation. *Transplantation*, *81*(3), 408–417. doi:10.1097/01.tp.0000188183.49025.d5

Cannon, G., Gupta, P., Gomes, F., Kerner, J., Parra, W., Weiderpass, E. . . . ICCC-4 Working Group (2012). Prevention of cancer and non-communicable diseases. *Asian Pacific journal of cancer prevention : APJCP*, *13*(4 Suppl), 3–11.

Carraway, M. S., Piantadosi, C. A., Jenkinson, C. P., & Huang, Y. C. (1998). Differential expression of arginase and iNOS in the lung in sepsis. *Experimental lung research*, *24*(3), 253–268. doi:10.3109/01902149809041533

Carruthers, V. B., Moreno, S. N., & Sibley, L. D. (1999). Ethanol and acetaldehyde elevate intracellular [Ca2+] and stimulate microneme discharge in Toxoplasma gondii. *The Biochemical journal*, *342*(Pt 2), 379–386.

Carruthers, V. B., & Tomley, F. M. (2008). Microneme proteins in apicomplexans. *Sub-cellular biochemistry*, *47*, 33–45. doi:10.1007/978-0-387-78267-6_2

Carey, R. M., Kimball, A. C., Armstrong, D., & Lieberman, P. H. (1973). Toxoplasmosis. Clinical experiences in a cancer hospital. *The American journal of medicine*, *54*(1), 30–38. doi:10.1016/0002-9343(73)90080-6

Chtanova, T., Schaeffer, M., Han, S. J., van Dooren, G. G., Nollmann, M., Herzmark, P. . . . Robey, E. A. (2008). Dynamics of neutrophil migration in lymph nodes during infection. *Immunity*, *29*(3), 487–496. doi:10.1016/j.immuni.2008.07.012

Cong, W., Liu, G., Meng, Q., Dong, W., Qin, S., Zhang, F., . . . Zhu, X. (2015). Toxoplasma gondii infection in cancer patients: Prevalence, risk factors, genotypes and association with clinical diagnosis. *Cancer Letters, 359*(2), 307-313.

Cook, A. J., Gilbert, R. E., Buffolano, W., Zufferey, J., Petersen, E., Jenum, P. A. . . . Dunn, D. T. (2000). Sources of toxoplasma infection in pregnant women: European multicentre case-control study. European Research Network on Congenital Toxoplasmosis. *BMJ (Clinical research ed.)*, *321*(7254), 142–147. doi:10.1136/bmj.321.7254.142

Courret, N., Darche, S., Sonigo, P., Milon, G., Buzoni-Gâtel, D., & Tardieux, I. (2006). CD11c- and CD11b-expressing mouse leukocytes transport single Toxoplasma gondii tachyzoites to the brain. *Blood*, *107*(1), 309–316. doi:10.1182/blood-2005-02-0666

Czystowska-Kuzmicz, M., Sosnowska, A., Nowis, D., Ramji, K., Szajnik, M., Chlebowska-Tuz, J. . . . Golab, J. (2019). Small extracellular vesicles containing arginase-1 suppress T-cell responses and promote tumor growth in ovarian carcinoma. *Nature communications*, *10*(1), 3000. doi:10.1038/s41467-019-10979-3

Daneshtalab, N., Doré, J., & Smeda, J. (2010). Troubleshooting tissue specificity and antibody selection: Procedures in immunohistochemical studies. *Journal of Pharmacological and Toxicological Methods, 61*(2), 127-135.

Darnell, J. E., Jr, Kerr, I. M., & Stark, G. R. (1994). Jak-STAT pathways and transcriptional activation in response to IFNs and other extracellular signaling proteins. *Science (New York, N.Y.)*, *264*(5164), 1415–1421. doi:10.1126/science.8197455

Davis, A. S., Vergne, I., Master, S. S., Kyei, G. B., Chua, J., & Deretic, V. (2007). Mechanism of inducible nitric oxide synthase exclusion from mycobacterial phagosomes. *PLoS pathogens*, *3*(12), e186. doi:10.1371/journal.ppat.0030186

Delair, E., Monnet, D., Grabar, S., Dupouy-Camet, J., Yera, H., & Brézin, A. P. (2008). Respective roles of acquired and congenital infections in presumed ocular toxoplasmosis. *American journal of ophthalmology*, *146*(6), 851–855. Doi:10.1016/j.ajo.2008.06.027

Drakopanagiotakis, F., Xifteri, A., Polychronopoulos, V., & Bouros, D. (2008). Apoptosis in lung injury and fibrosis. *The European respiratory journal*, *32*(6), 1631–1638. doi:10.1183/09031936.00176807

Kobzik, L., Bredt, D. S., Lowenstein, C. J., Drazen, J., Gaston, B., Sugarbaker, D., & Stamler, J. S. (1993). Nitric oxide synthase in human and rat lung: immunocytochemical and histochemical localization. *American journal of respiratory cell and molecular biology*, *9*(4), 371–377. doi:10.1165/ajrcmb/9.4.371

Dubey, J. (1995). Duration of Immunity to Shedding of Toxoplasma gondii Oocysts by Cats. *The Journal of Parasitology, 81*(3), 410-415. doi:10.2307/3283823

Dubey J. P. (1997a). Bradyzoite-induced murine toxoplasmosis: stage conversion, pathogenesis, and tissue cyst formation in mice fed bradyzoites of different strains of Toxoplasma gondii. *The Journal of eukaryotic microbiology*, *44*(6), 592–602. Doi:10.1111/j.1550-7408.1997.tb05965.x

Dubey J. P. (1997b). Distribution of tissue cysts in organs of rats fed Toxoplasma gondii oocysts. *The Journal of parasitology*, *83*(4), 755–757.

Dubey, J. P. (2009). History of the discovery of the life cycle of Toxoplasma gondii. *International Journal for Parasitology*. 39. 877-882. Doi:10.1016/j.ijpara.2009.01.005.

Dubey, J. P. (2010). *Toxoplasmosis of animals and humans* (Second ed.).

Dubey, J. P., & Carpenter, J. L. (1993). Histologically confirmed clinical toxoplasmosis in cats: 100 cases (1952-1990). *Journal of the American Veterinary Medical Association*, *203*(11), 1556–1566.

Dubey, J. P., & Frenkel, J. K. (1972). Cyst-induced toxoplasmosis in cats. *The Journal of protozoology*, *19*(1), 155–177. Doi:10.1111/j.1550-7408.1972.tb03431.x

Duleu, S., Vincendeau, P., Courtois, P., Semballa, S., Lagroye, I., Daulouede, S. . . . Gobert, I. (2004). Mouse strain susceptibility to trypanosome infection: An arginase-dependent effect. *Journal Of Immunology, 172*(10), 6298-6303.

Dumètre, A., Dubey, J. P., Ferguson, D. J., Bongrand, P., Azas, N., & Puech, P. H. (2013). Mechanics of the Toxoplasma gondii oocyst wall. *Proceedings of the National Academy of*

Sciences of the United States of America, *110*(28), 11535–11540. doi:10.1073/pnas.1308425110

Durante W. (2013). Role of arginase in vessel wall remodeling. *Frontiers in immunology*, *4*, 111. doi:10.3389/fimmu.2013.00111

Eizirik, D. L., Delaney, C. A., Green, M. H., Cunningham, J. M., Thorpe, J. R., Pipeleers, D. G. . . . Green, I. C. (1996). Nitric oxide donors decrease the function and survival of human pancreatic islets. *Molecular and cellular endocrinology*, *118*(1-2), 71–83. doi:10.1016/0303-7207(96)03768-9

Ekmekcioglu, S., Grimm, E. A., & Roszik, J. (2017). Targeting iNOS to increase efficacy of immunotherapies. *Human vaccines & immunotherapeutics*, *13*(5), 1105–1108. doi:10.1080/21645515.2016.1276682

El Kasmi, K. C., Qualls, J. E., Pesce, J. T., Smith, A. M., Thompson, R. W., Henao-Tamayo, M. . . . Murray, P. J. (2008). Toll-like receptor-induced arginase 1 in macrophages thwarts effective immunity against intracellular pathogens. *Nature immunology*, *9*(12), 1399–1406. doi:10.1038/ni.1671

Elmore, S. A., Jones, J. L., Conrad, P. A., Patton, S., Lindsay, D. S., & Dubey, J. P. (2010). Toxoplasma gondii: epidemiology, feline clinical aspects, and prevention. *Trends in parasitology*, *26*(4), 190–196. doi:10.1016/j.pt.2010.01.009

Ermert, M., Ruppert, C., Günther, A., Duncker, H. R., Seeger, W., & Ermert, L. (2002). Cell-specific nitric oxide synthase-isoenzyme expression and regulation in response to endotoxin in intact rat lungs. *Laboratory investigation; a journal of technical methods and pathology*, *82*(4), 425–441. doi:10.1038/labinvest.3780436

Etheridge, R. D., Alaganan, A., Tang, K., Lou, H. J., Turk, B. E., & Sibley, L. D. (2014). The Toxoplasma pseudokinase ROP5 forms complexes with ROP18 and ROP17 kinases that synergize to control acute virulence in mice. *Cell host & microbe*, *15*(5), 537–550. doi:10.1016/j.chom.2014.04.002

Evans, A. K., Strassmann, P. S., Lee, I. P., & Sapolsky, R. M. (2014). Patterns of Toxoplasma gondii cyst distribution in the forebrain associate with individual variation in predator odor avoidance and anxiety-related behavior in male Long-Evans rats. *Brain, behavior, and immunity*, *37*, 122–133. doi:10.1016/j.bbi.2013.11.012

Fang F. C. (2004). Antimicrobial reactive oxygen and nitrogen species: concepts and controversies. *Nature reviews. Microbiology*, *2*(10), 820–832. doi:10.1038/nrmicro1004

Fentress, S. J., Behnke, M. S., Dunay, I. R., Mashayekhi, M., Rommereim, L. M., Fox, B. A. . . . Sibley, L. D. (2010). Phosphorylation of immunity-related GTPases by a Toxoplasma gondii-secreted kinase promotes macrophage survival and virulence. *Cell host & microbe*, *8*(6), 484–495. doi:10.1016/j.chom.2010.11.005

Field, R. W., & Withers, B. L. (2012). Occupational and environmental causes of lung cancer. *Clinics in chest medicine*, *33*(4), 681–703. doi:10.1016/j.ccm.2012.07.001

Flatt, A., & Shetty, N. (2013). Seroprevalence and risk factors for toxoplasmosis among antenatal women in London: a re-examination of risk in an ethnically diverse population. *European journal of public health*, *23*(4), 648–652. doi:10.1093/eurpub/cks075

Flegr J. (2007). Effects of toxoplasma on human behavior. *Schizophrenia bulletin*, *33*(3), 757–760. Doi:10.1093/schbul/sbl074

Flegr, J., Prandota, J., Sovičková, M., & Israili, Z. H. (2014). Toxoplasmosis--a global threat. Correlation of latent toxoplasmosis with specific disease burden in a set of 88 countries. *PloS one*, *9*(3), e90203. doi:10.1371/journal.pone.0090203

Förstermann, U., Closs, E. I., Pollock, J. S., Nakane, M., Schwarz, P., Gath, I., & Kleinert, H. (1994). Nitric oxide synthase isozymes. Characterization, purification, molecular cloning, and functions. *Hypertension (Dallas, Tex. : 1979)*, *23*(6 Pt 2), 1121–1131. doi:10.1161/01.hyp.23.6.1121

Förstermann, U., & Sessa, W. C. (2012). Nitric oxide synthases: regulation and function. *European heart journal*, *33*(7), 829–837d. doi:10.1093/eurheartj/ehr304

Fritschy J. M. (2008). Is my antibody-staining specific? How to deal with pitfalls of immunohistochemistry. *The European journal of neuroscience*, *28*(12), 2365–2370. doi:10.1111/j.1460-9568.2008.06552.x

Fritz, H., Barr, B., Packham, A., Melli, A., & Conrad, P. A. (2012a). Methods to produce and safely work with large numbers of Toxoplasma gondii oocysts and bradyzoite cysts. *Journal of microbiological methods*, *88*(1), 47–52. doi:10.1016/j.mimet.2011.10.010

Fritz, H. M., Bowyer, P. W., Bogyo, M., Conrad, P. A., & Boothroyd, J. C. (2012b). Proteomic analysis of fractionated Toxoplasma oocysts reveals clues to their environmental resistance. *PloS one*, *7*(1), e29955. Doi:10.1371/journal.pone.0029955

Fuhrman, S. A., & Joiner, K. A. (1989). Toxoplasma gondii: mechanism of resistance to complement-mediated killing. *Journal of immunology (Baltimore, Md. : 1950)*, *142*(3), 940–947.

Fujii, H., Kamiyama, T., & Hagiwara, T. (1983). Species and strain differences in sensitivity to Toxoplasma infection among laboratory rodents. *Japanese journal of medical science & biology*, *36*(6), 343–346. doi:10.7883/yoken1952.36.343

Gao, J., Yi, S., Wu, M., Geng, G., Shen, J., Lu, F., . . . Lun, Z. (2015). Investigation of infectivity of neonates and adults from different rat strains to toxoplasma gondii prugniaud shows both variation which correlates with iNOS and Arginase-1 activity and increased susceptibility of neonates to infection. *Elsevier, 2015*(02). doi: 10.1016/j.exppara.2014.12.008.

Gay, G., Braun, L., BrenierPinchart, M., Vollaire, J., Josserand, V., Bertini, R.L. . . . Hakimi M-A. (2016). Toxoplasma gondii TgIST co-opts host chromatin repressors dampening STAT1-dependent gene regulation and IFN-gamma-mediated host defenses. *J Exp Med, 213*, 1779–1798. doi:10.1084/jem.20160340

Gov, L., Karimzadeh, A., Ueno, N., & Lodoen, M. B. (2013). Human innate immunity to Toxoplasma gondii is mediated by host caspase-1 and ASC and parasite GRA15. *mBio*, *4*(4), e00255-13. doi:10.1128/mBio.00255-13

Giordano, D., Li, C., Suthar, M. S., Draves, K. E., Ma, D. Y., Gale, M., Jr, & Clark, E. A. (2011). Nitric oxide controls an inflammatory-like Ly6C(hi)PDCA1+ DC subset that regulates Th1 immune responses. *Journal of leukocyte biology*, *89*(3), 443–455. doi:10.1189/jlb.0610329

Grabowski, P. S., Wright, P. K., Van 't Hof, R. J., Helfrich, M. H., Ohshima, H., & Ralston, S. H. (1997). Immunolocalization of inducible nitric oxide synthase in synovium and cartilage in rheumatoid arthritis and osteoarthritis. *British journal of rheumatology*, *36*(6), 651–655. doi:10.1093/rheumatology/36.6.651

Grasemann, H., Tullis, E., & Ratjen, F. (2013). A randomized controlled trial of inhaled L-arginine in patients with cystic fibrosis. *Journal of cystic fibrosis : official journal of the European Cystic Fibrosis Society*, *12*(5), 468–474. doi:10.1016/j.jcf.2012.12.008

Grody, W. W., Dizikes, G. J., & Cederbaum, S. D. (1987). Human arginase isozymes. *Isozymes*, *13*, 181–214.

Guerrouahen, B. S., Maccalli, C., Cugno, C., Rutella, S., & Akporiaye, E. T. (2020). Reverting Immune Suppression to Enhance Cancer Immunotherapy. *Frontiers in oncology*, *9*, 1554. doi:10.3389/fonc.2019.01554

Guo, H. M., Gao, J. M., Luo, Y. L., Wen, Y. Z., Zhang, Y. L., Hide, G. . . . Lun, Z. R. (2015). Infection by Toxoplasma gondii, a severe parasite in neonates and AIDS patients, causes impaired anion secretion in airway epithelia. *Proceedings of the National Academy of Sciences of the United States of America*, *112*(14), 4435–4440. doi:10.1073/pnas.1503474112

Guy, E. C., & Joynson, D. H. (1995). Potential of the polymerase chain reaction in the diagnosis of active Toxoplasma infection by detection of parasite in blood. *The Journal of infectious diseases*, *172*(1), 319–322. doi:10.1093/infdis/172.1.319

Hamad, A. M., Johnson, S. R., & Knox, A. J. (1999). Antiproliferative effects of NO and ANP in cultured human airway smooth muscle. *The American journal of physiology*, *277*(5), L910–L918. doi:10.1152/ajplung.1999.277.5.L910

Hamad, A. M., & Knox, A. J. (2001). Mechanisms mediating the antiproliferative effects of nitric oxide in cultured human airway smooth muscle cells. *FEBS letters*, *506*(2), 91–96. doi:10.1016/s0014-5793(01)02883-6

Hamid, Q., Springall, D. R., Riveros-Moreno, V., Chanez, P., Howarth, P., Redington, A. . . . Polak, J. M. (1993). Induction of nitric oxide synthase in asthma. *Lancet (London, England)*, *342*(8886-8887), 1510–1513. doi:10.1016/s0140-6736(05)80083-2

Heiss, C., Rodriguez-Mateos, A., & Kelm, M. (2015). Central role of eNOS in the maintenance of endothelial homeostasis. *Antioxidants & redox signaling*, *22*(14), 1230–1242. doi:10.1089/ars.2014.6158

Hernandez, C. P., Morrow, K., Lopez-Barcons, L. A., Zabaleta, J., Sierra, R., Velasco, C. . . . Rodriguez, P. C. (2010). Pegylated arginase I: a potential therapeutic approach in T-ALL. *Blood*, *115*(25), 5214–5221. doi:10.1182/blood-2009-12-258822

Hickey M. J. (2001). Role of inducible nitric oxide synthase in the regulation of leucocyte recruitment. *Clinical science (London, England : 1979)*, *100*(1), 1–12.

Hide, G, Morley, E. K, Hughes, J. M, Gerwash, O, Elmahaishi, M. S, Elmahaishi, K. H, . . . Smith, J. E. (2009). Evidence for high levels of vertical transmission in Toxoplasma gondii. *Parasitology, 136*(14), 1877-1885.

Hochstedler, C. M., Leidinger, M. R., Maher-Sturm, M. T., Gibson-Corley, K. N., & Meyerholz, D. K. (2013). Immunohistochemical detection of arginase-I expression in formalin-fixed lung and other tissues. *Journal of histotechnology*, *36*(4), 128–134. doi:10.1179/2046023613Y.0000000032

Holliman R. E. (1988). Toxoplasmosis and the acquired immune deficiency syndrome. The Journal of infection, 16(2), 121–128. doi:10.1016/s0163-4453(88)93847-9

Hölscher, C., & Rose, S. P. (1992). An inhibitor of nitric oxide synthesis prevents memory formation in the chick. *Neuroscience letters*, *145*(2), 165–167. doi:10.1016/0304-3940(92)90012-v

Huang, H. J., Isakow, W., Byers, D. E., Engle, J. T., Griffin, E. A., Kemp, D. . . . Chen, D. L. (2015). Imaging pulmonary inducible nitric oxide synthase expression with PET. *Journal of nuclear medicine : official publication, Society of Nuclear Medicine*, *56*(1), 76–81. doi:10.2967/jnumed.114.146381

Hunter, C. A., & Sibley, L. D. (2012). Modulation of innate immunity by Toxoplasma gondii virulence effectors. *Nature reviews. Microbiology*, *10*(11), 766–778. doi:10.1038/nrmicro2858

Israelski, D. M., & Remington, J. S. (1993). Toxoplasmosis in patients with cancer. *Clinical infectious diseases : an official publication of the Infectious Diseases Society of America*, *17 Suppl 2*, S423–S435. doi:10.1093/clinids/17.supplement_2.s423

Iyer, R., Jenkinson, C. P., Vockley, J. G., Kern, R. M., Grody, W. W., & Cederbaum, S. (1998). The human arginases and arginase deficiency. *Journal of inherited metabolic disease*, *21 Suppl 1*, 86–100. doi:10.1023/a:1005313809037

James S. L. (1995). Role of nitric oxide in parasitic infections. *Microbiological reviews*, *59*(4), 533–547.

Jayaraman, P., Alfarano, M. G., Svider, P. F., Parikh, F., Lu, G., Kidwai, S. . . . Sikora, A. G. (2014). iNOS expression in CD4+ T cells limits Treg induction by repressing TGFβ1: combined iNOS inhibition and Treg depletion unmask endogenous antitumor immunity. *Clinical cancer research : an official journal of the American Association for Cancer Research*, *20*(24), 6439–6451. doi:10.1158/1078-0432.CCR-13-3409

Jemal, A., Tiwari, R. C., Murray, T., Ghafoor, A., Samuels, A., Ward, E. . . . American Cancer Society (2004). Cancer statistics, 2004. *CA: a cancer journal for clinicians*, *54*(1), 8–29. doi:10.3322/canjclin.54.1.8

Jemal, A., Travis, W. D., Tarone, R. E., Travis, L., & Devesa, S. S. (2003). Lung cancer rates convergence in young men and women in the United States: analysis by birth cohort and histologic type. *International journal of cancer*, *105*(1), 101–107. doi:10.1002/ijc.11020

Jensen, K. D., Hu, K., Whitmarsh, R. J., Hassan, M. A., Julien, L., Lu, D. . . . Saeij, J. P. (2013). Toxoplasma gondii rhoptry 16 kinase promotes host resistance to oral infection and intestinal inflammation only in the context of the dense granule protein GRA15. *Infection and immunity*, *81*(6), 2156–2167. doi:10.1128/IAI.01185-12

Jiang, C., Li, Z., Chen, P., & Chen, L. (2015). The Seroprevalence of Toxoplasma gondii in Chinese Population With Cancer: A Systematic Review and Meta-analysis. *Medicine*, *94*(50), e2274. Doi:10.1097/MD.0000000000002274

Jones, J.L., & Dubey, J.P. (2010). Waterborne toxoplasmosis--recent developments. *Experimental parasitology, 124* (1), 10-25.

Kämpfer, H., Pfeilschifter, J., & Frank, S. (2003). Expression and activity of arginase isoenzymes during normal and diabetes-impaired skin repair. *The Journal of investigative dermatology*, *121*(6), 1544–1551. doi:10.1046/j.1523-1747.2003.12610.x

Kempf, M. C., Cesbron-Delauw, M. F., Deslee, D., Gross, U., Herrmann, T., & Sutton, P. (1999). Different manifestations of Toxoplasma gondii infection in F344 and LEW rats. *Medical microbiology and immunology*, *187*(3), 137–142. doi:10.1007/s004300050085

Kizawa, Y., Ohuchi, N., Saito, K., Kusama, T., & Murakami, H. (2001). Effects of endothelin-1 and nitric oxide on proliferation of cultured guinea pig bronchial smooth muscle cells. *Comparative biochemistry and physiology. Toxicology & pharmacology : CBP*, *128*(4), 495–501. doi:10.1016/s1532-0456(01)00172-7

Klasen, S., Hammermann, R., Fuhrmann, M., Lindemann, D., Beck, K. F., Pfeilschifter, J., & Racké, K. (2001). Glucocorticoids inhibit lipopolysaccharide-induced up-regulation of arginase in rat alveolar macrophages. *British journal of pharmacology*, *132*(6), 1349–1357. doi:10.1038/sj.bjp.0703951

Kojima, M., Morisaki, T., Tsukahara, Y., Uchiyama, A., Matsunari, Y., Mibu, R., & Tanaka, M. (1999). Nitric oxide synthase expression and nitric oxide production in human colon carcinoma tissue. *Journal of surgical oncology*, *70*(4), 222–229. doi:10.1002/(sici)1096-9098(199904)70:4<222::aid-jso5>3.0.co;2-g

Koshy, A. A., Dietrich, H. K., Christian, D. A., Melehani, J. H., Shastri, A. J., Hunter, C. A., & Boothroyd, J. C. (2012). Toxoplasma co-opts host cells it does not invade. *PLoS pathogens*, *8*(7), e1002825. doi:10.1371/journal.ppat.1002825

Kröncke, K. D., Kolb-Bachofen, V., Berschick, B., Burkart, V., & Kolb, H. (1991). Activated macrophages kill pancreatic syngeneic islet cells via arginine-dependent nitric oxide

generation. *Biochemical and biophysical research communications*, *175*(3), 752–758. doi:10.1016/0006-291x(91)91630-u

Kung, J. T., Brooks, S. B., Jakway, J. P., Leonard, L. L., & Talmage, D. W. (1977). Suppression of in vitro cytotoxic response by macrophages due to induced arginase. *The Journal of experimental medicine*, *146*(3), 665–672. doi:10.1084/jem.146.3.665

Kuwano, K., Kunitake, R., Kawasaki, M., Nomoto, Y., Hagimoto, N., Nakanishi, Y., & Hara, N. (1996). P21Waf1/Cip1/Sdi1 and p53 expression in association with DNA strand breaks in idiopathic pulmonary fibrosis. *American journal of respiratory and critical care medicine*, *154*(2 Pt 1), 477–483. doi:10.1164/ajrccm.154.2.8756825

Lala, P. K., & Chakraborty, C. (2001). Role of nitric oxide in carcinogenesis and tumour progression. *The Lancet. Oncology*, *2*(3), 149–156. doi:10.1016/S1470-2045(00)00256-4

Lala, P. K., & Orucevic, A. (1998). Role of nitric oxide in tumor progression: lessons from experimental tumors. *Cancer metastasis reviews*, *17*(1), 91–106. doi:10.1023/a:1005960822365

Leal, F. E., Cavazzana, C. L., de Andrade, H. F., Jr, Galisteo, A., Jr, de Mendonça, J. S., & Kallas, E. G. (2007). Toxoplasma gondii pneumonia in immunocompetent subjects: case report and review. *Clinical infectious diseases : an official publication of the Infectious Diseases Society of America*, *44*(6), e62–e66. doi:10.1086/511871

Lelchuk, R., Radomski, M. W., Martin, J. F., & Moncada, S. (1992). Constitutive and inducible nitric oxide synthases in human megakaryoblastic cells. *The Journal of pharmacology and experimental therapeutics*, *262*(3), 1220–1224.

Lewis, W.P., & Markell, E.K. (1958). Acquisition of immunity to toxoplasmosis by the newborn rat. *Experimental Parasitology, 7*(5), 463-467. doi:10.1016/0014-4894(58)90040-7

Li, Y-X., Wei, C-Y., Zhang, X-Y., Duan, Y-H., Zhang, P-N., Guo., M-j., & Niu, H-T. (2020). Toxoplasma gondii infection in patients with lung diseases in Shandong province, eastern China. *Acta Tropica, 211*, 105554.

Li, Z., Zhao, Z. J., Zhu, X. Q., Ren, Q. S., Nie, F. F., Gao, J. M. . . . Lun, Z. R. (2012). Differences in iNOS and arginase expression and activity in the macrophages of rats are responsible for the resistance against T. gondii infection. *PloS one*, *7*(4), e35834. doi:10.1371/journal.pone.0035834

Liu, Q., Singla, L. D., & Zhou, H. (2012). Vaccines against Toxoplasma gondii: status, challenges and future directions. *Human vaccines & immunotherapeutics*, *8*(9), 1305–1308. doi:10.4161/hv.21006

Lu, N., Liu, C., Wang, J., Ding, Y., & Ai, Q. (2015). Toxoplasmosis complicating lung cancer: a case report. *International medical case reports journal*, *8*, 37–40. doi:10.2147/IMCRJ.S76488

Lucas, R., Czikora, I., Sridhar, S., Zemskov, E. A., Oseghale, A., Circo, S. . . . Romero, M. J. (2013). Arginase 1: an unexpected mediator of pulmonary capillary barrier dysfunction in models of acute lung injury. *Frontiers in immunology*, *4*, 228. doi:10.3389/fimmu.2013.00228

Lucas, R., Fulton, D., Caldwell, R. W., & Romero, M. J. (2014). Arginase in the vascular endothelium: friend or foe?. *Frontiers in immunology*, *5*, 589. doi:10.3389/fimmu.2014.00589

Lucas, R., Verin, A. D., Black, S. M., & Catravas, J. D. (2009). Regulators of endothelial and epithelial barrier integrity and function in acute lung injury. *Biochemical pharmacology*, *77*(12), 1763–1772. doi:10.1016/j.bcp.2009.01.014

Lüder, C. G., Algner, M., Lang, C., Bleicher, N., & Gross, U. (2003). Reduced expression of the inducible nitric oxide synthase after infection with Toxoplasma gondii facilitates parasite replication in activated murine macrophages. *International journal for parasitology*, *33*(8), 833–844. doi:10.1016/s0020-7519(03)00092-4

Lundbäck, B., Lindberg, A., Lindström, M., Rönmark, E., Jonsson, A. C., Jönsson, E. . . . Obstructive Lung Disease in Northern Sweden Studies (2003). Not 15 but 50% of smokers develop COPD?--Report from the Obstructive Lung Disease in Northern Sweden Studies. *Respiratory medicine*, *97*(2), 115–122. doi:10.1053/rmed.2003.1446

Ma, J. S., Sasai, M., Ohshima, J., Lee, Y., Bando, H., Takeda, K., & Yamamoto, M. (2014). Selective and strain-specific NFAT4 activation by the Toxoplasma gondii polymorphic dense granule protein GRA6. *The Journal of experimental medicine*, *211*(10), 2013–2032. Doi:10.1084/jem.20131272

Machala, L., Kodym, P., Malý, M., Geleneky, M., Beran, O., & Jilich, D. (2015). Toxoplasmóza u imunokompromitovaných pacientů [Toxoplasmosis in immunocompromised patients]. *Epidemiologie, mikrobiologie, imunologie : casopis Spolecnosti pro epidemiologii a mikrobiologii Ceske lekarske spolecnosti J.E. Purkyne*, *64*(2), 59–65.

Marrogi, A. J., Travis, W. D., Welsh, J. A., Khan, M. A., Rahim, H., Tazelaar, H. . . . Harris, C. C. (2000). Nitric oxide synthase, cyclooxygenase 2, and vascular endothelial growth factor in the angiogenesis of non-small cell lung carcinoma. *Clinical cancer research : an official journal of the American Association for Cancer Research*, *6*(12), 4739–4744.

Martin, T. R., & Frevert, C. W. (2005). Innate immunity in the lungs. *Proceedings of the American Thoracic Society*, *2*(5), 403–411. Doi:10.1513/pats.200508-090JS

Martin, T. R., Mathison, J. C., Tobias, P. S., Letúrcq, D. J., Moriarty, A. M., Maunder, R. J., & Ulevitch, R. J. (1992). Lipopolysaccharide binding protein enhances the responsiveness of alveolar macrophages to bacterial lipopolysaccharide. Implications for cytokine production in normal and injured lungs. *The Journal of clinical investigation*, *90*(6), 2209–2219. doi:10.1172/JCI116106

Martin, T. R., Rubenfeld, G. D., Ruzinski, J. T., Goodman, R. B., Steinberg, K. P., Leturcq, D. J. . . . Hudson, L. D. (1997). Relationship between soluble CD14, lipopolysaccharide binding protein, and the alveolar inflammatory response in patients with acute respiratory distress syndrome. *American journal of respiratory and critical care medicine*, *155*(3), 937–944. doi:10.1164/ajrccm.155.3.9117029

Maubon, D., Ajzenberg, D., Brenier-Pinchart, M. P., Dardé, M. L., & Pelloux, H. (2008). What are the respective host and parasite contributions to toxoplasmosis?. *Trends in parasitology*, *24*(7), 299–303. doi:10.1016/j.pt.2008.03.012

McAdam, E., Haboubi, H. N., Forrester, G., Eltahir, Z., Spencer-Harty, S., Davies, C. . . . Jenkins, G. J. S. (2012). Inducible Nitric Oxide Synthase (iNOS) and Nitric Oxide (NO) are Important Mediators of Reflux-induced Cell Signalling in Esophageal Cells. *Carcinogenesis*, 33(11), 2035–2043. doi:10.1093/carcin/bgs241

McInnes, I. B., Leung, B. P., Field, M., Wei, X. Q., Huang, F. P., Sturrock, R. D. . . . Liew, F. Y. (1996). Production of nitric oxide in the synovial membrane of rheumatoid and osteoarthritis patients. *The Journal of experimental medicine*, *184*(4), 1519–1524. doi:10.1084/jem.184.4.1519

Meireles, P., Mendes, A., Aroeira, R., Mounce, B., Vignuzzi, M., Staines, H., & Prudêncio, M. (2017). Uptake and metabolism of arginine impact Plasmodium development in the liver. *Scientific Reports (Nature Publisher Group), 7*(1), 1-12.

Meyer, D. J., Allan, J. E., & Beaman, M. H. (2000). Distribution of parasite stages in tissues of Toxoplasma gondii infected SCID mice and human peripheral blood lymphocyte-transplanted SCID mice. *Parasite immunology*, *22*(11), 567–579. Doi:10.1046/j.1365-3024.2000.00338.x

Mizushima, Y., & Kobayashi, M. (1995). Clinical characteristics of synchronous multiple lung cancer associated with idiopathic pulmonary fibrosis. A review of Japanese cases. *Chest*, *108*(5), 1272–1277. doi:10.1378/chest.108.5.1272

Mogensen T. H. (2009). Pathogen recognition and inflammatory signaling in innate immune defenses. *Clinical microbiology reviews*, *22*(2), 240–273. doi:10.1128/CMR.00046-08

Mohamadi, F., Shakibapour, M., Sharafi, S.M., Andalib, A.R., Tolouei, S., & Yousofi Darani, H. (2019). Anti-Toxoplasma gondii antibodies attach to mouse cancer cell lines but not normal mouse lymphocytes. Biomedical Reports, 10, 183-188. Doi:10.3892/br.2019.1186

Montoya, J. G., & Liesenfeld, O. (2004). Toxoplasmosis. *Lancet (London, England)*, *363*(9425), 1965–1976. doi:10.1016/S0140-6736(04)16412-X

Morris S. M., Jr (2009). Recent advances in arginine metabolism: roles and regulation of the arginases. *British journal of pharmacology*, *157*(6), 922–930. doi:10.1111/j.1476-5381.2009.00278.x

Munder, M. Eichmann, K., & Modolell, M. (1998). Alternative metabolic states in murine macrophages reflected by the nitric oxide synthase arginase balance: Competitive regulation by CD4( ) T cells correlates with Th1/Th2 phenotype. *Journal Of Immunology, 160*(11), 5347-5354.

Murray, H. W., & Teitelbaum, R. F. (1992). L-arginine-dependent reactive nitrogen intermediates and the antimicrobial effect of activated human mononuclear phagocytes. *The Journal of infectious diseases*, *165*(3), 513–517. doi:10.1093/infdis/165.3.513

Must, K., Hytönen, M. K., Orro, T., Lohi, H., & Jokelainen, P. (2017). Toxoplasma gondii seroprevalence varies by cat breed. *PloS one*, *12*(9), e0184659. Doi:10.1371/journal.pone.0184659

Nakayama, I., & Hoshiai, T., (1960). A preliminary report of a comparison of the survival of high virulent RH strain and cyst-producing Beverley strain of Toxoplasma in rats. *Keio J. Med. 9*, 217-223.

Newton, A. H., Cardani, A., & Braciale, T. J. (2016). The host immune response in respiratory virus infection: balancing virus clearance and immunopathology. *Seminars in immunopathology*, *38*(4), 471–482. Doi:10.1007/s00281-016-0558-0

Obermajer, N., Wong, J. L., Edwards, R. P., Chen, K., Scott, M., Khader, S. . . . Kalinski, P. (2013). Induction and stability of human Th17 cells require endogenous NOS2 and cGMP-dependent NO signaling. *The Journal of experimental medicine*, *210*(7), 1433–1445. doi:10.1084/jem.20121277

Ohshima, J., Lee, Y., Sasai, M., Saitoh, T., Su Ma, J., Kamiyama, N. . . . Yamamoto, M. (2014). Role of mouse and human autophagy proteins in IFN-γ-induced cell-autonomous responses against Toxoplasma gondii. *Journal of immunology (Baltimore, Md. : 1950)*, *192*(7), 3328–3335. doi:10.4049/jimmunol.1302822

Olias, P., Etheridge, R. D., Zhang, Y., Holtzman, M. J., & Sibley, L. D. (2016). Toxoplasma Effector Recruits the Mi-2/NuRD Complex to Repress STAT1 Transcription and Block IFN-γ-Dependent Gene Expression. *Cell host & microbe*, *20*(1), 72–82. doi:10.1016/j.chom.2016.06.006

Park, J., Kim, D. S., Shim, T. S., Lim, C. M., Koh, Y., Lee, S. D. . . . Song, K. S. (2001). Lung cancer in patients with idiopathic pulmonary fibrosis. *The European respiratory journal*, *17*(6), 1216–1219. doi:10.1183/09031936.01.99055301

Patel, H. J., Belvisi, M. G., Donnelly, L. E., Yacoub, M. H., Chung, K. F., & Mitchell, J. A. (1999). Constitutive expressions of type I NOS in human airway smooth muscle cells: evidence for an antiproliferative role. *FASEB journal : official publication of the Federation of American Societies for Experimental Biology*, *13*(13), 1810–1816. doi:10.1096/fasebj.13.13.1810

Pegg A. E. (2014). The function of spermine. *IUBMB life*, *66*(1), 8–18. doi:10.1002/iub.1237

Pfefferkorn, E. R., Rebhun, S., & Eckel, M. (1986a). Characterization of an indoleamine 2,3-dioxygenase induced by gamma-interferon in cultured human fibroblasts. *Journal of interferon research*, *6*(3), 267–279. doi:10.1089/jir.1986.6.267

Pfefferkorn, E. R., Eckel, M., & Rebhun, S. (1986b). Interferon-gamma suppresses the growth of Toxoplasma gondii in human fibroblasts through starvation for tryptophan. *Molecular and biochemical parasitology*, *20*(3), 215–224. doi:10.1016/0166-6851(86)90101-5

Platanias L. C. (2005). Mechanisms of type-I- and type-II-interferon-mediated signalling. *Nature reviews. Immunology*, *5*(5), 375–386. doi:10.1038/nri1604

Popovic, P. J., Zeh, H. J., 3rd, & Ochoa, J. B. (2007). Arginine and immunity. *The Journal of nutrition*, *137*(6 Suppl 2), 1681S–1686S. doi:10.1093/jn/137.6.1681S

Rabaud, C., May, T., Lucet, J. C., Leport, C., Ambroise-Thomas, P., & Canton, P. (1996). Pulmonary toxoplasmosis in patients infected with human immunodeficiency virus: a French National Survey. *Clinical infectious diseases : an official publication of the Infectious Diseases Society of America*, *23*(6), 1249–1254. doi:10.1093/clinids/23.6.1249

Raghu, G., Nyberg, F., & Morgan, G. (2004). The epidemiology of interstitial lung disease and its association with lung cancer. *British journal of cancer*, *91 Suppl 2*(Suppl 2), S3–S10. doi:10.1038/sj.bjc.6602061

Ramos-Vara J. A. (2005). Technical aspects of immunohistochemistry. *Veterinary pathology*, *42*(4), 405–426. doi:10.1354/vp.42-4-405

Ratovitski, E. A., Bao, C., Quick, R. A., McMillan, A., Kozlovsky, C., & Lowenstein, C. J. (1999). An inducible nitric-oxide synthase (NOS)-associated protein inhibits NOS dimerization and activity. *The Journal of biological chemistry*, *274*(42), 30250–30257. doi:10.1074/jbc.274.42.30250

Redente, E. F., Higgins, D. M., Dwyer-Nield, L. D., Orme, I. M., Gonzalez-Juarrero, M., & Malkinson, A. M. (2010). Differential polarization of alveolar macrophages and bone marrow-derived monocytes following chemically and pathogen-induced chronic lung inflammation. *Journal of leukocyte biology*, *88*(1), 159–168. doi:10.1189/jlb.0609378

Reese, M. L., Zeiner, G. M., Saeij, J. P., Boothroyd, J. C., & Boyle, J. P. (2011). Polymorphic family of injected pseudokinases is paramount in Toxoplasma virulence. *Proceedings of the National Academy of Sciences of the United States of America*, *108*(23), 9625–9630. doi:10.1073/pnas.1015980108

Rosowski, E. E., Lu, D., Julien, L., Rodda, L., Gaiser, R. A., Jensen, K. D., & Saeij, J. P. (2011). Strain-specific activation of the NF-kappaB pathway by GRA15, a novel Toxoplasma gondii dense granule protein. *The Journal of experimental medicine*, *208*(1), 195–212. doi:10.1084/jem.20100717

Rosowski, E. E., Nguyen, Q. P., Camejo, A., Spooner, E., & Saeij, J. P. (2014). Toxoplasma gondii inhibits gamma interferon (IFN-gamma)- and IFN-beta-induced host cell STAT1 transcriptional activity by increasing the association of STAT1 with DNA. *Infect Immun*, *82*, 706–719. doi:10.1128/IAI.01291-13.

Rosowski, E. E., & Saeij, J. P. (2012). Toxoplasma gondii clonal strains all inhibit STAT1 transcriptional activity but polymorphic effectors differentially modulate IFNγ induced gene expression and STAT1 phosphorylation. *PloS one*, *7*(12), e51448. doi:10.1371/journal.pone.0051448

Rőszer T. (2015). Understanding the Mysterious M2 Macrophage through Activation Markers and Effector Mechanisms. *Mediators of inflammation*, *2015*, 816460. doi:10.1155/2015/816460

Scerra, S., Coignard-Biehler, H., Lanternier, F., Suarez, F., Charlier-Woerther, C., Bougnoux, M. E. . . . Lortholary, O. (2013). Disseminated toxoplasmosis in non-allografted patients with hematologic malignancies: report of two cases and literature review. *European journal of*

clinical microbiology & infectious diseases : official publication of the European Society of Clinical Microbiology, *32*(10), 1259–1268. doi:10.1007/s10096-013-1879-8

Scharton-Kersten, T. M., Yap, G., Magram, J., & Sher, A. (1997). Inducible nitric oxide is essential for host control of persistent but not acute infection with the intracellular pathogen Toxoplasma gondii. *The Journal of experimental medicine*, *185*(7), 1261–1273. doi:10.1084/jem.185.7.1261

Seabra, S. H., de Souza, W., & DaMatta, R. A. (2002). Toxoplasma gondii partially inhibits nitric oxide production of activated murine macrophages. *Experimental parasitology*, *100*(1), 62–70. doi:10.1006/expr.2001.4675

Shen, C. X., Zhang, G. L., Song, X. L., Xie, S. S., & Wang, C. H. (2015). Toxoplasma gondii Pneumonia in an Immunocompetent Individual. *The American journal of the medical sciences*, *350*(1), 70–71. doi:10.1097/MAJ.0000000000000496

Sher, A., Tosh, K., & Jankovic, D. (2017). Innate recognition of Toxoplasma gondii in humans involves a mechanism distinct from that utilized by rodents. *Cellular & molecular immunology*, *14*(1), 36–42. doi:10.1038/cmi.2016.12

Siegel, R. L., Miller, K. D., & Jemal, A. (2018). Cancer statistics, 2018. *CA: a cancer journal for clinicians*, *68*(1), 7–30. doi:10.3322/caac.21442

Slauch J. M. (2011). How does the oxidative burst of macrophages kill bacteria? Still an open question. *Molecular microbiology*, *80*(3), 580–583. doi:10.1111/j.1365-2958.2011.07612.x

Stadelmann, B., Hanevik, K., Andersson, M., Bruserud, O., & Svard, S. (2013). The role of arginine and arginine-metabolizing enzymes during Giardia - host cell interactions in vitro. *BMC Microbiology, 13*(1), 256.

Steinfeldt, T., Könen-Waisman, S., Tong, L., Pawlowski, N., Lamkemeyer, T., Sibley, L. D. . . . Howard, J. C. (2010). Phosphorylation of mouse immunity-related GTPase (IRG) resistance proteins is an evasion strategy for virulent Toxoplasma gondii. *PLoS biology*, *8*(12), e1000576. doi:10.1371/journal.pbio.1000576

Suzuki, Y., Orellana, M. A., Schreiber, R. D., & Remington, J. S. (1988). Interferon-gamma: the major mediator of resistance against Toxoplasma gondii. *Science (New York, N.Y.)*, *240*(4851), 516–518. doi:10.1126/science.3128869

Takahashi, H., Nukiwa, T., Matsuoka, R., Danbara, T., Natori, H., Arai, T., & Kira, S. (1985). Carcinoembryonic antigen in bronchoalveolar lavage fluid in patients with idiopathic pulmonary fibrosis. *Japanese journal of medicine*, *24*(3), 236–243. doi:10.2169/internalmedicine1962.24.236

Tenter, A. M., Heckeroth, A. R., & Weiss, L. M. (2000). Toxoplasma gondii: from animals to humans. *International journal for parasitology*, *30*(12-13), 1217–1258. Doi:10.1016/s0020-7519(00)00124-7

Thirugnanam, S., Rout, N., & Gnanasekar, M. (2013). Possible role of Toxoplasma gondii in brain cancer through modulation of host microRNAs. *Infectious Agents and Cancer, 8*(1), 8.

Thomas, F., Lafferty, K. D., Brodeur, J., Elguero, E., Gauthier-Clerc, M., & Missé, D. (2012). Incidence of adult brain cancers is higher in countries where the protozoan parasite Toxoplasma gondii is common. *Biology letters*, *8*(1), 101–103. doi:10.1098/rsbl.2011.0588

Thomsen, L. L., Lawton, F. G., Knowles, R. G., Beesley, J. E., Riveros-Moreno, V., & Moncada, S. (1994). Nitric oxide synthase activity in human gynecological cancer. *Cancer research*, *54*(5), 1352–1354.

Thomsen, L. L., Miles, D. W., Happerfield, L., Bobrow, L. G., Knowles, R. G., & Moncada, S. (1995). Nitric oxide synthase activity in human breast cancer. *British journal of cancer*, *72*(1), 41–44. doi:10.1038/bjc.1995.274

Travis, W. D., Brambilla, E., Nicholson, A. G., Yatabe, Y., Austin, J., Beasley, M. B. . . . WHO Panel (2015). The 2015 World Health Organization Classification of Lung Tumors: Impact of Genetic, Clinical and Radiologic Advances Since the 2004 Classification. *Journal of thoracic oncology : official publication of the International Association for the Study of Lung Cancer*, *10*(9), 1243–1260. doi:10.1097/JTO.0000000000000630

Vakkala, M., Kahlos, K., Lakari, E., Pääkkö, P., Kinnula, V., & Soini, Y. (2000). Inducible nitric oxide synthase expression, apoptosis, and angiogenesis in in situ and invasive breast carcinomas. *Clinical cancer research : an official journal of the American Association for Cancer Research*, *6*(6), 2408–2416.

Vannini, F., Kashfi, K., & Nath, N. (2015). The dual role of iNOS in cancer. *Redox biology*, *6*, 334–343. doi:10.1016/j.redox.2015.08.009

Vestbo, J., Hurd, S. S., Agustí, A. G., Jones, P. W., Vogelmeier, C., Anzueto, A. . . . Rodriguez-Roisin, R. (2013). Global strategy for the diagnosis, management, and prevention of chronic obstructive pulmonary disease: GOLD executive summary. *American journal of respiratory and critical care medicine*, *187*(4), 347–365. doi:10.1164/rccm.201204-0596PP

Vietzke, W. M., Gelderman, A. H., Grimley, P. M., & Valsamis, M. P. (1968). Toxoplasmosis complicating malignancy. Experience at the National Cancer Institute. *Cancer*, *21*(5), 816–827. doi:10.1002/1097-0142(196805)21:5<816::aid-cncr2820210506>3.0.co;2-#

Villena, I., Ancelle, T., Delmas, C., Garcia, P., Brezin, A. P., Thulliez, P. . . . Toxosurv network and National Reference Centre for Toxoplasmosis (2010). Congenital toxoplasmosis in France in 2007: first results from a national surveillance system. *Euro surveillance : bulletin Europeen sur les maladies transmissibles = European communicable disease bulletin*, *15*(25), 19600. doi:10.2807/ese.15.25.19600-en

Vockley, J. G., Jenkinson, C. P., Shukla, H., Kern, R. M., Grody, W. W., & Cederbaum, S. D. (1996). Cloning and characterization of the human type II arginase gene. *Genomics*, *38*(2), 118–123. doi:10.1006/geno.1996.0606

Vodovotz, Y., Bogdan, C., Paik, J., Xie, Q. W., & Nathan, C. (1993). Mechanisms of suppression of macrophage nitric oxide release by transforming growth factor beta. *The Journal of experimental medicine*, *178*(2), 605–613. doi:10.1084/jem.178.2.605

von Bargen, K., Wohlmann, J., Taylor, G. A., Utermöhlen, O., & Haas, A. (2011). Nitric oxide-mediated intracellular growth restriction of pathogenic Rhodococcus equi can be prevented by iron. *Infection and immunity*, *79*(5), 2098–2111. doi:10.1128/IAI.00983-10

Wahbah, M., Boroumand, N., Castro, C., El-Zeky, F., & Eltorky, M. (2007). Changing trends in the distribution of the histologic types of lung cancer: a review of 4,439 cases. *Annals of diagnostic pathology*, *11*(2), 89–96. doi:10.1016/j.anndiagpath.2006.04.006

Wang, T., Gao, J. M., Yi, S. Q., Geng, G. Q., Gao, X. J., Shen, J. L. . . . Lun, Z. R. (2014). Toxoplasma gondii infection in the peritoneal macrophages of rats treated with glucocorticoids. *Parasitology research*, *113*(1), 351–358. doi:10.1007/s00436-013-3661-3

Wang, J., Liu, X., Jia, B., Lu, H., Peng, S., Piao, X. . . . Chen, Q. (2012). A comparative study of small RNAs in Toxoplasma gondii of distinct genotypes. *Parasites & vectors*, *5*, 186. doi:10.1186/1756-3305-5-186

Wani, J., Carl, M., Henger, A., Nelson, P. J., & Rupprecht, H. (2007). Nitric oxide modulates expression of extracellular matrix genes linked to fibrosis in kidney mesangial cells. *Biological chemistry*, *388*(5), 497–506. doi:10.1515/BC.2007.056

Weiss, L. M., & Kim, K. (2000). The development and biology of bradyzoites of Toxoplasma gondii. *Frontiers in bioscience : a journal and virtual library*, *5*, D391–D405. doi:10.2741/weiss

Weiss, L. M., & Kim, K. (2014). Chapter 14 - Interactions Between Toxoplasma Effectors and Host Immune Responses. In *Toxoplasma gondii : The model apicomplexan, perspectives and methods* (2nd ed.). doi:10.1016/B978-0-12-396481-6.00014-3

Wink, D. A., Ridnour, L. A., Hussain, S. P., & Harris, C. C. (2008). The reemergence of nitric oxide and cancer. *Nitric oxide : biology and chemistry*, *19*(2), 65–67. doi:10.1016/j.niox.2008.05.003

Wink, D. A., Vodovotz, Y., Cook, J. A., Krishna, M. C., Kim, S., Coffin, D. . . . Mitchell, J. B. (1998a). The role of nitric oxide chemistry in cancer treatment. *Biochemistry. Biokhimiia*, *63*(7), 802–809.

Wink, D. A., Vodovotz, Y., Laval, J., Laval, F., Dewhirst, M. W., & Mitchell, J. B. (1998b). The multifaceted roles of nitric oxide in cancer. *Carcinogenesis*, *19*(5), 711–721. doi:10.1093/carcin/19.5.711

Wong, Z. S., Sokol-Borrelli, S. L., Olias, P., Dubey J. P., Boyle, J. P. (2020). Head-to-head comparisons of *Toxoplasma gondii* and its near relative *Hammondia hammondi* reveal dramatic differences in the host response and effectors with species-specific functions. *PLOS Pathogens,* 16(6), e1008528. doi:10.1371/journal.ppat.1008528

Wu, G., & Morris, S. M., Jr (1998). Arginine metabolism: nitric oxide and beyond. *The Biochemical journal*, *336 (Pt 1)*(Pt 1), 1–17. doi:10.1042/bj3360001

Xie, K., Huang, S., Dong, Z., Juang, S. H., Gutman, M., Xie, Q. W. . . . Fidler, I. J. (1995). Transfection with the inducible nitric oxide synthase gene suppresses tumorigenicity and abrogates metastasis by K-1735 murine melanoma cells. *The Journal of experimental medicine*, *181*(4), 1333–1343. doi:10.1084/jem.181.4.1333

Yang, Z., & Ming, X. F. (2014). Functions of arginase isoforms in macrophage inflammatory responses: impact on cardiovascular diseases and metabolic disorders. *Frontiers in immunology*, *5*, 533. doi:10.3389/fimmu.2014.00533

Yang, J., Zhang, R., Lu, G., Shen, Y., Peng, L., Zhu, C. . . . Xiong, H. (2013). T cell–derived inducible nitric oxide synthase switches off Th17 cell differentiation. *The Journal of experimental medicine*, *210*(7), 1447–1462. doi:10.1084/jem.20122494

Yoon, J., & Ryoo, S. (2013). Arginase inhibition reduces interleukin-1β-stimulated vascular smooth muscle cell proliferation by increasing nitric oxide synthase-dependent nitric oxide production. *Biochemical and Biophysical Research Communications, 435*(3), 428-433.

Young, R. P., Duan, F., Chiles, C., Hopkins, R. J., Gamble, G. D., Greco, E. M. . . . Aberle, D. (2015). Airflow Limitation and Histology Shift in the National Lung Screening Trial. The NLST-ACRIN Cohort Substudy. *American journal of respiratory and critical care medicine*, *192*(9), 1060–1067. doi:10.1164/rccm.201505-0894OC

Young, R. P., & Hopkins, R. J. (2010). Link between COPD and lung cancer. *Respiratory medicine*, *104*(5), 758–759. doi:10.1016/j.rmed.2009.11.025

Zhang, Y-B., Cong, W., Li, Z-T., Bi, X-G., Xian, Y., Wang, Y-H., . . . Zhang, K-X. (2015). Seroprevalence of Toxoplasma gondii Infection in Patients of Intensive Care Unit in China: A Hospital Based Study. *BioMed Research International, 2015*(908217).

Zhang, R., Ma, A., Urbanski, S. J., & McCafferty, D. M. (2007). Induction of inducible nitric oxide synthase: a protective mechanism in colitis-induced adenocarcinoma. *Carcinogenesis*, *28*(5), 1122–1130. doi:10.1093/carcin/bgl224

Zhao, Z. J., Zhang, J., Wei, J., Li, Z., Wang, T., Yi, S. Q. . . . Lun, Z. R. (2013). Lower expression of inducible nitric oxide synthase and higher expression of arginase in rat alveolar macrophages are linked to their susceptibility to Toxoplasma gondii infection. *PloS one*, *8*(5), e63650. doi:10.1371/journal.pone.0063650

Zhou, P., Chen, Z., Li, H. L., Zheng, H., He, S., Lin, R. Q., & Zhu, X. Q. (2011). Toxoplasma gondii infection in humans in China. *Parasites & vectors*, *4*, 165. doi:10.1186/1756-3305-4-165

Zhou, L., & Zhu, D. Y. (2009). Neuronal nitric oxide synthase: structure, subcellular localization, regulation, and clinical implications. *Nitric oxide : biology and chemistry*, *20*(4), 223–230. doi:10.1016/j.niox.2009.03.001